Solar Coronal Plasmas

Jörg Büchner
Max-Planck-Institute for Solar System Research & Georg-August-University both in Göttingen & (from Winter semester 2018-19 also at Technical University Berlin), all in Germany
Max-Planck-Princeton Center for Plasma Physics

With many thanks to the collaborating members and students of the TSSSP group (P. Munoz, N. Jain, P. Kilian, F. Widmer, X. Zhou …)

MPI Solar System Research (MPS): New building, Göttingen 2014

MPS: buildings for scientists, laboratories, workshops

Left (glass) building: for scientists; Right: administration & facilities like clean rooms, balloon hall, coelostat/ heliostat…

Thermal-Vacuum Chamber and Clean Room

Research

Planets and Comets

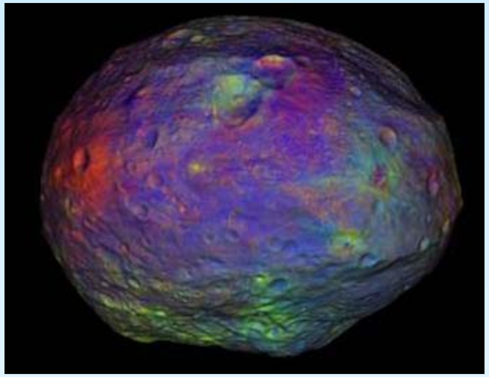

Planetary Atmospheres

Planetary Interiors

Small Bodies

Comets

Planetary Surfaces

Planetary Plasma

Environments

Solar and Stellar Interiors

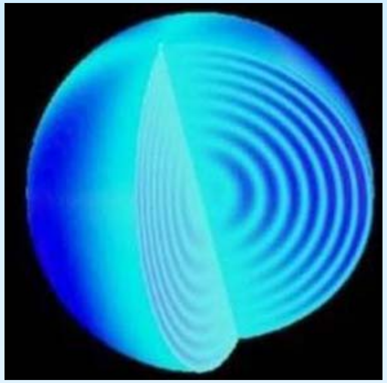

Helioseismology

Asteroseismology

The TSSSP-(Theory and Simulation of Solar System Plasmas) moves to the TU Berlin in winter semester 2018-2019

Sun and Heliosphere

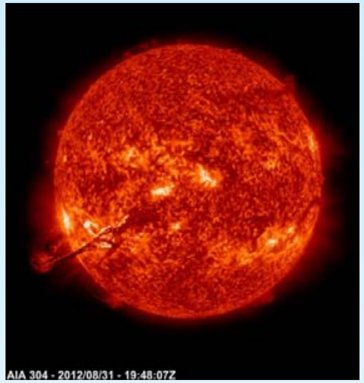

Coronal Spectroscopy and Imaging; Solar Lower Atmosphere and Magnetism

Solar and Stellar MHD

Plasma instabilities, waves, turbulence; reconnection; Numerical simulations: kinetic (PIC & Vlasov), hybrid & MHD models

Contents

- Coronal plasmas & fields
- Eruptions & reconnection
- Turbulence and dissipation
- Electron acceleration

Contents

- Coronal plasmas & fields
- Eruptions & reconnection
- Turbulence and dissipation
- Electron acceleration

Solar corona in the plasma Universe

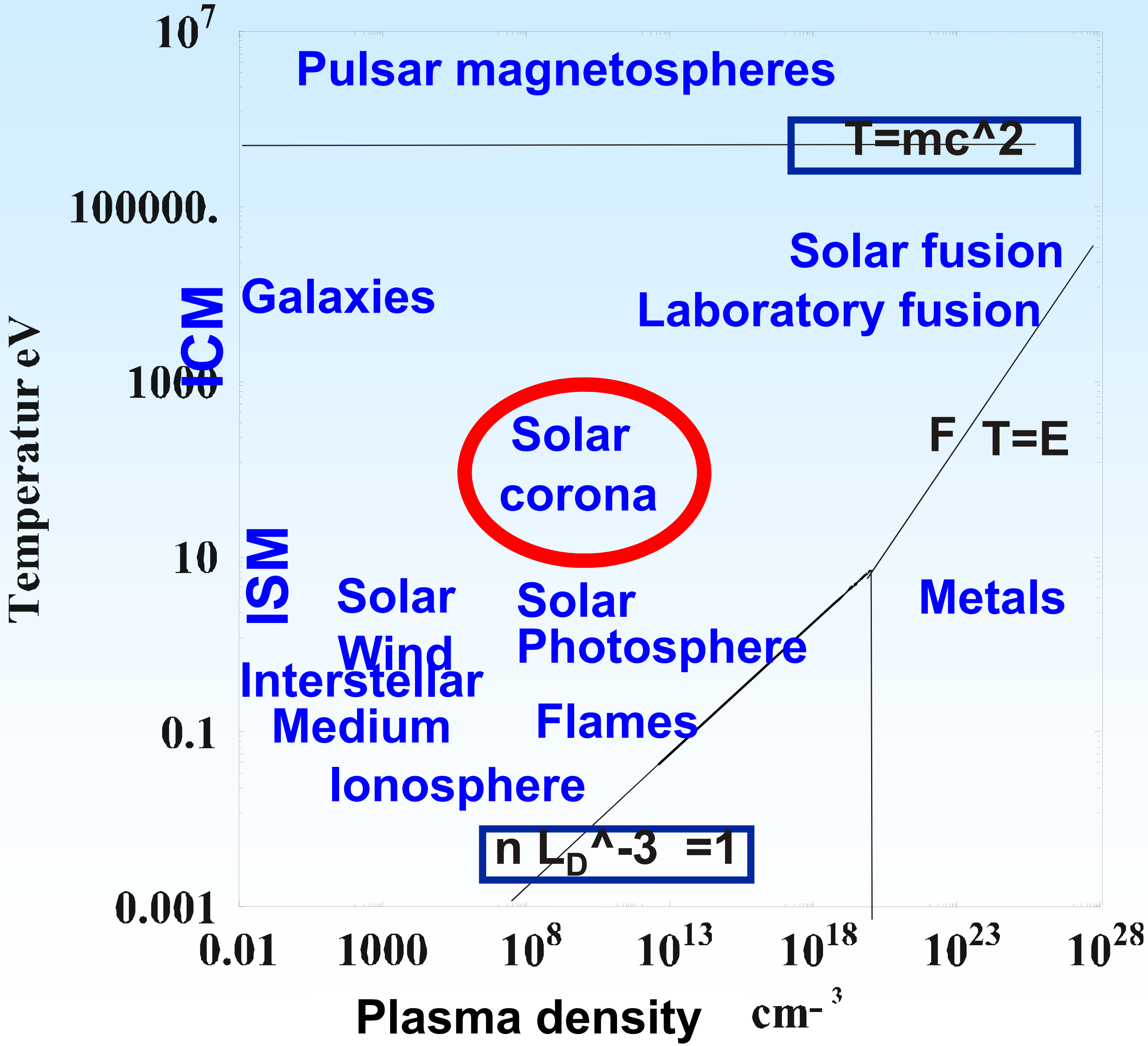

The coronal plasma temperature exceeds 1 Million K (100 eV)

It consists mainly of protons

It is diluted plasma. Its density is much smaller than that of the fusion plasmas!

Typical plasma parameters

Parameter	Unit	Corona	ISM	ICM
T_e (temperature)	eV	**100**	1-100	10^3-10^4
n_e (number density)	cm^-3	**10^9**	10^-3-10^-1	10^-4-10^-2
P-thermal pressure	dyne/cm^2	**0.3**	10^-14-10^-13	10^-13-10^-10
omega_pe/ 2 pi	Hz	**2 10^9**	15-250	0.25-25
V_te / V_sound	km/s	**4 10^3**	10-100	500-1500
lambda_Debye	cm	**0.2**	2 10^3-2 10^9	2 -100 10^5
N_D= lambda_D^3	1	**10^7**	10^9-10^13	10^13-10^15
nu_e (e-e collisions)	Hz	**30**	10^-5-10^-10	10^-14-10^-10
lamba_mfp	km	**100**	10^8-3 10^13	6.(10^13-10^14)
R=nu_e/omega_pe („collisionality“)	1	**1.5 10^-9**	10^-13 – 10^-9	10^-13

-> the solar coronal plasma is still mainly collisioness,

-> kinetic effects might be crucial

Magnetoplasma parameters

Parameter	Unit	Corona	ISM	ICM
T-temperature	eV	100	1-100	10^3-10^4
N - density	cm^-3	10^9	10^-3-10^-1	10^-4-10^-2
P-thermal pressure	dyne/cm^2	0.3	10^-14-10^-13	10^-13-10^-10
B-magnetic field	G	**10**	(1-10) 10^-6	(0.1-10) 10^-6
Thermal plasma beta	1	**0.1**	1-10	50-1000
Rho_e	cm	**2**	10^7	10^8
Rho_p	cm	**80**	4 10^8	4 10^9
omega_pe/ 2 pi	Hz	**2 10^9**	15-250	0.25-25
Omega_ce / 2 pi	Hz	**2.5 10^8**	3-30	1-30
V_A	km/s	**800**	10-100	20-100

-> the magnetic pressure dominates the solar corona

-> force free B fields can be extrapolated

Ideal <-> nonideal solar magnetoplasma

The coronal magnetic fields can grow or become annihilated according to the induction equation:

$$\frac{\partial \mathbf{B}}{\partial t} = \nabla \times (\mathbf{v} \times \mathbf{B}) + \eta \nabla^2 \mathbf{B}$$

Convection >>> Diffusion

Magnetic Reynolds- and Lundquist numbers

$$R_m = \frac{\mu_0 \; l \; v}{\eta} \qquad S \equiv \frac{\mu_0 L_{CS} V_A}{\eta}$$

Reynolds- / Lundquist numbers of (Spitzer-) collisional plasmas are huge ~$10^{6\text{-}12}$ for large scales (L) and typical *V* !

At smaller scales: two-fluid Ohms law

Two-fluid electron equation of motion: -> "Ohm's law":

$$\frac{4\pi}{\omega_{pe}^2}\frac{d\vec{J}}{dt} = \boxed{\vec{E} + \vec{v}_i \times \vec{B}} - \frac{1}{ne}\vec{J}\times\vec{B} + \frac{1}{ne}\nabla p_e - \eta\vec{J}$$

In case of strong guide fields -> to the lowest order one-dimensional balance equation for Epar

$$E_{||} = -\frac{m_e}{ne}\frac{d(nv_e)}{dt} - \frac{1}{ne}\frac{dp_e}{dx_{||}} + \frac{1}{ne}f_{eff}$$

Electric field ⇔ Electron inertia + Pressure gradient + f_{eff} = "drag force" due to collective wave-particle interaction

Plasma phenomena in the Solar corona

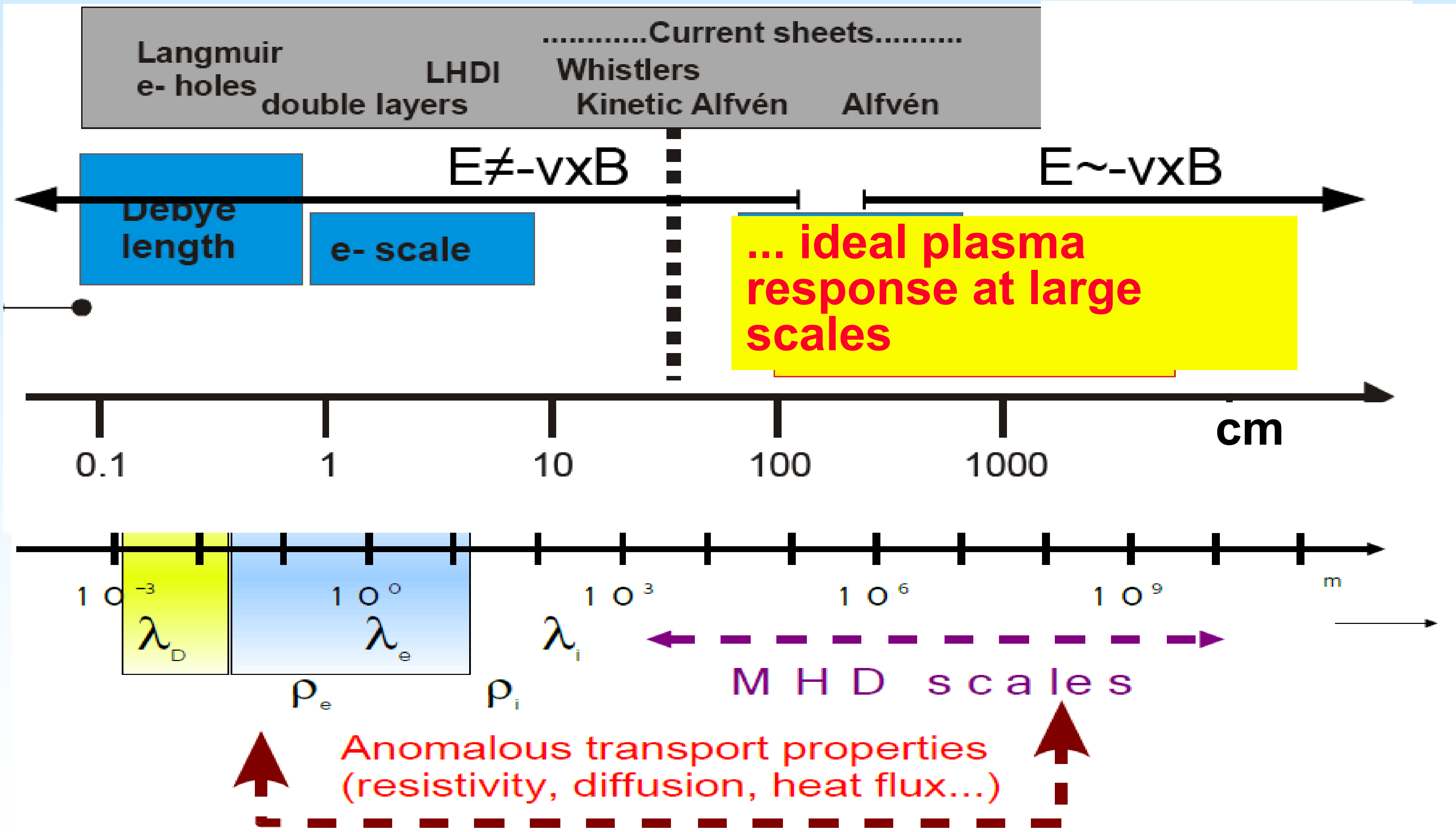

Contents

- Coronal plasmas & fields
- Eruptions & reconnection
- Turbulence and dissipation
- Electron acceleration

Typical evolution

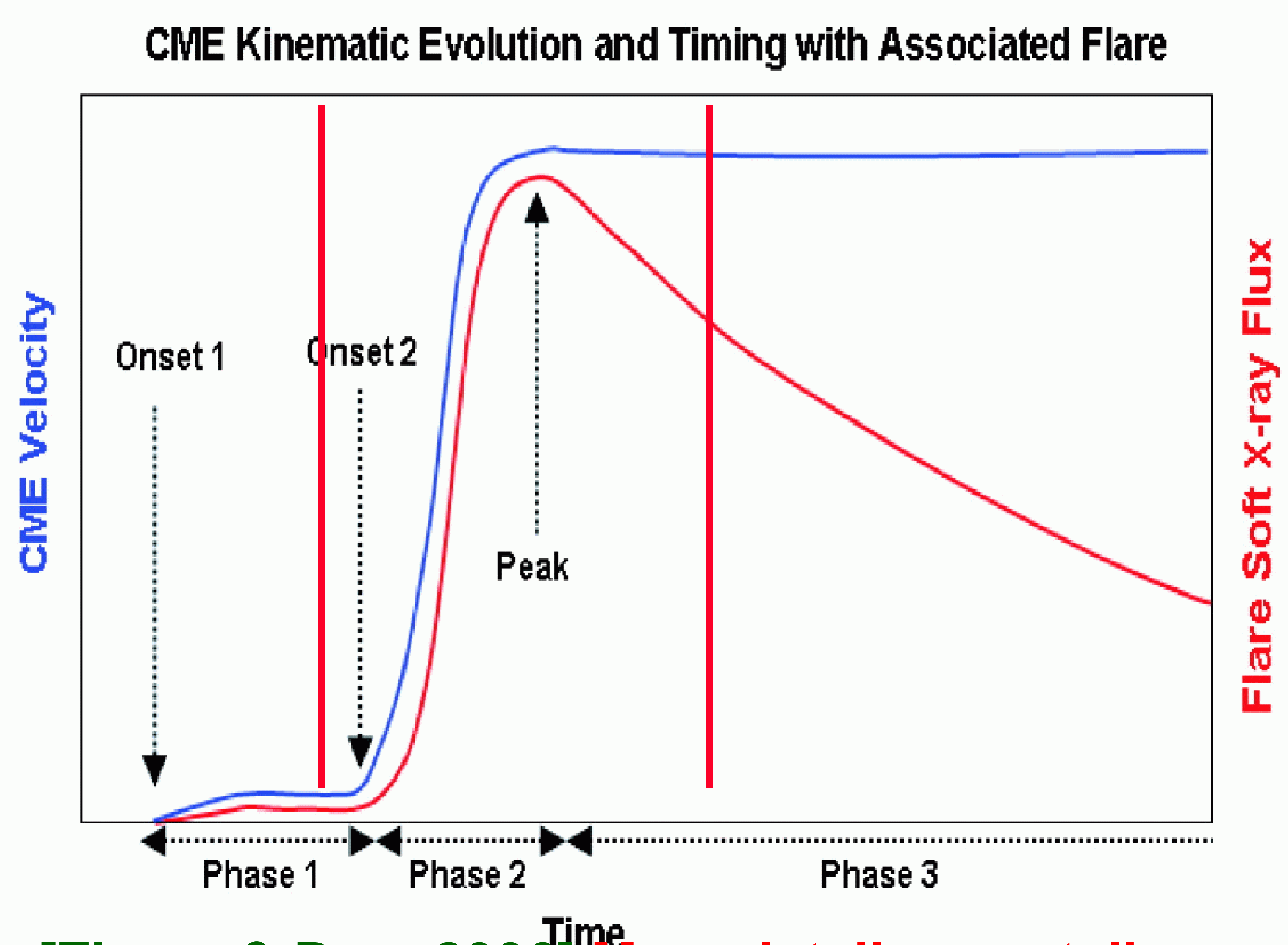

[Zhang & Dere 2006] More details: see talks by Yao Chen and Jeongwu Lee this morning

Three phases (in outward velocities and soft X-ray fluxes):

-> 1: slow rise of the prominence, magnetic energy accumulation

-> 2: fast rise of flare emissions and CME acceleration

-> 3: CME propagation / decreasing X-ray flare activity

e.g. B-field line-tied equilibria

- Primary magnetic field components:
  - Internal poloidal field B_{Pi} (plasma)
  - External "strapping" field B_s (vacuum)
  - Internal toroidal field B_{Ti} (plasma)
  - External "guide" field B_g (vacuum)

- At low-β, **J**×**B** forces dominate:
  - Poloidal hoop force: $f_h = +J_T \times B_{Pi}$
  - Strapping field force: $f_s = -J_T \times B_s$
  - Toroidal field forces: $f_T = -J_P \times (B_g + B_{Ti})$

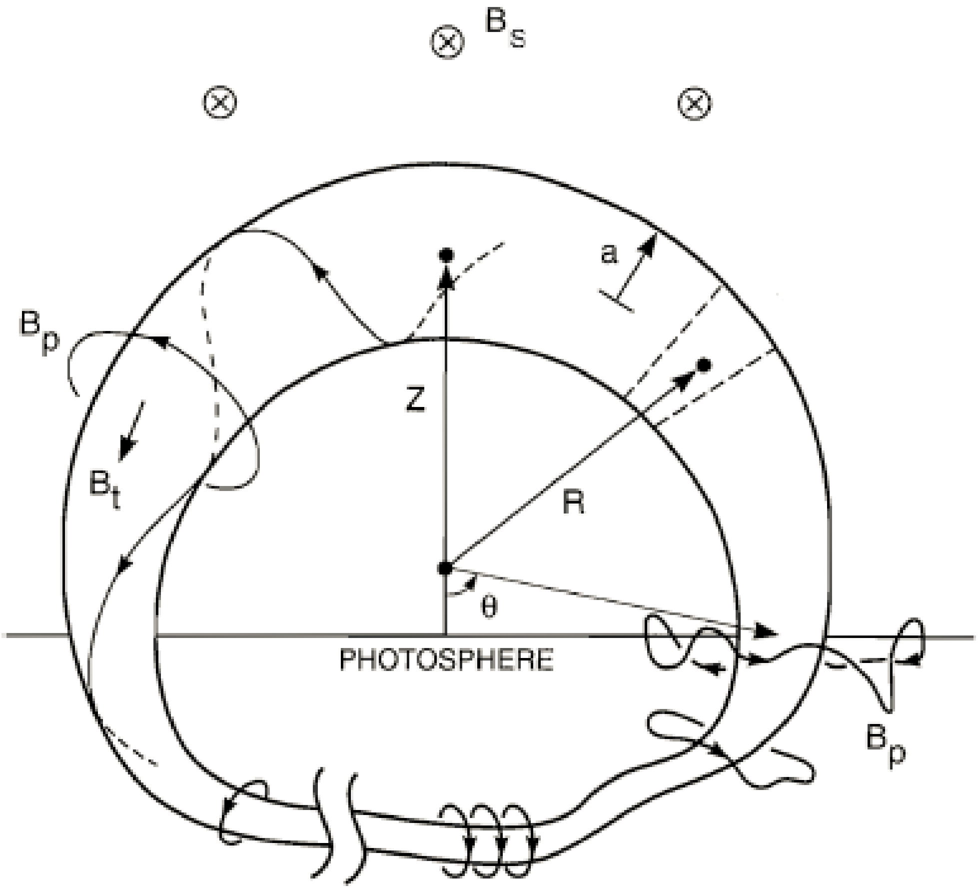

J. Chen, *ApJ*, 1989

Are eruptions due to ideal instabilities?

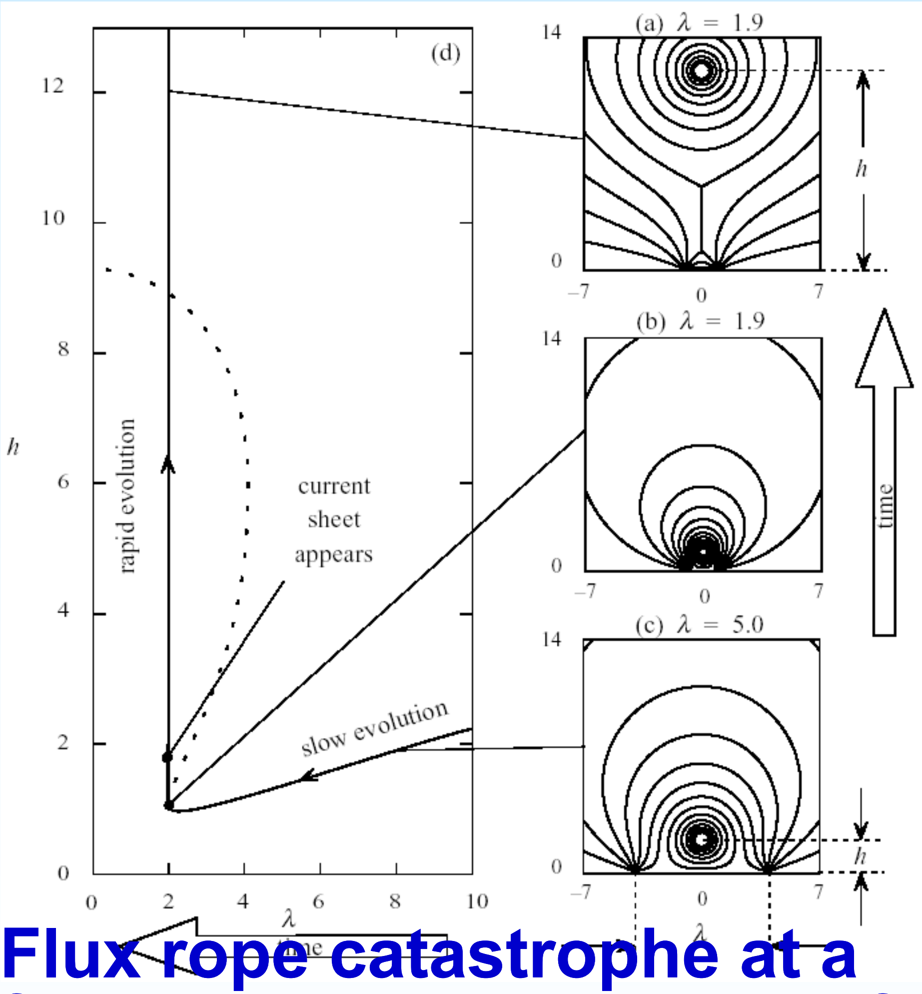

Flux rope catastrophe at a final point in a sequence of equilibria; here: 2D case [see, e.g., Forbes & Isenberg 1991]

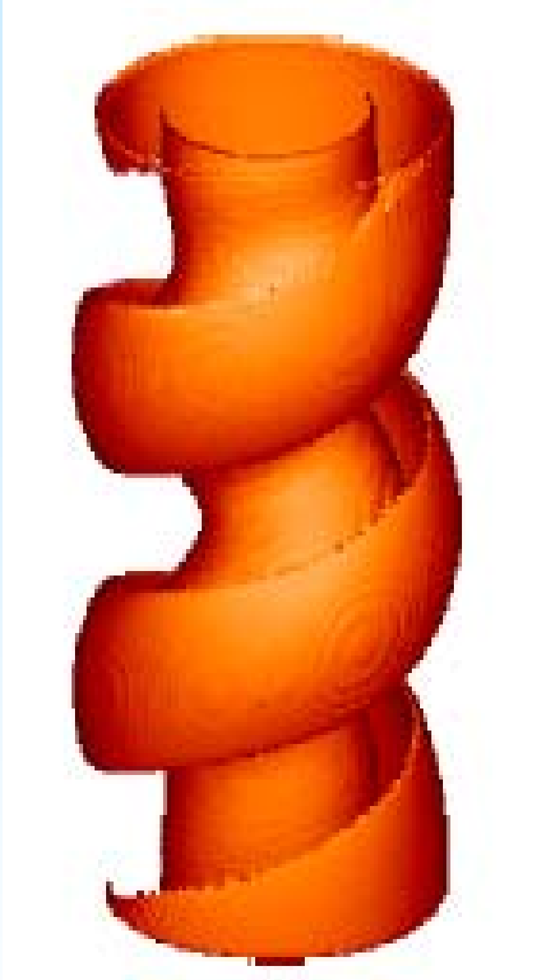

Helical kink (KI) instability m=1, [see, e.g., Gerrard et al. 2001]

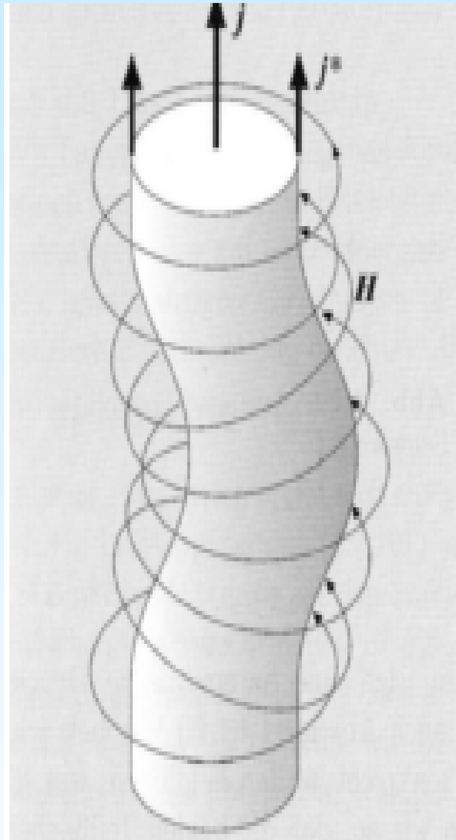

Lateral kink or torus-instability

$$n > n_{cr} \sim 3/2$$

[see, e.g. [Kliem & Török, 2006]

Ideal instability criteria

Winding due to footpoint motion -> flux rope kink?

1.) Windings cause a kink instability

[Kruskal & Schwarzschild, 1954] Instability criterion: „Edge safety factor“ (inverse winding number) :

$$q_a = \frac{2\pi a}{L} \frac{B_{Ta}}{B_{Pa}} < 1,$$

2.) Quickly decaying magnetic fields -> „torus“ instability ?

[Kliem & Török, 2006] Instability criterion: quick decrease of the magnetic downward directed „strapping“ Lorentz force

$$n(z) = \frac{z}{|\mathbf{B}_{pot}|} \frac{\partial |\mathbf{B}_{pot}|}{\partial z} > \frac{3}{2}$$

Saturation of lateral kink instability

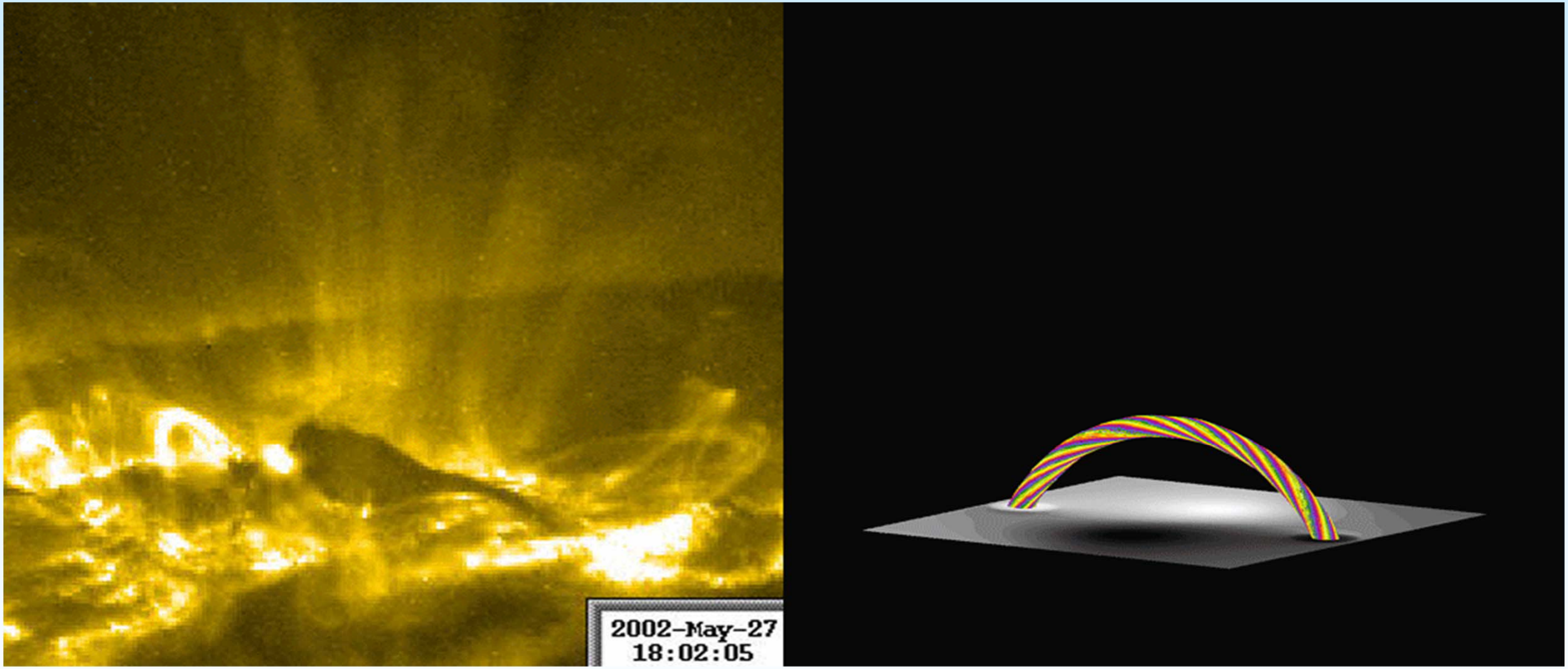

Above: A [Török and Kliem, 2005]-result. However: the ideal instabilities saturate quickly -> failed eruptions [Aulanier et al., 2010]. It still may be behind confined ("failed") eruptions.

MRX experiment of a coronal loop

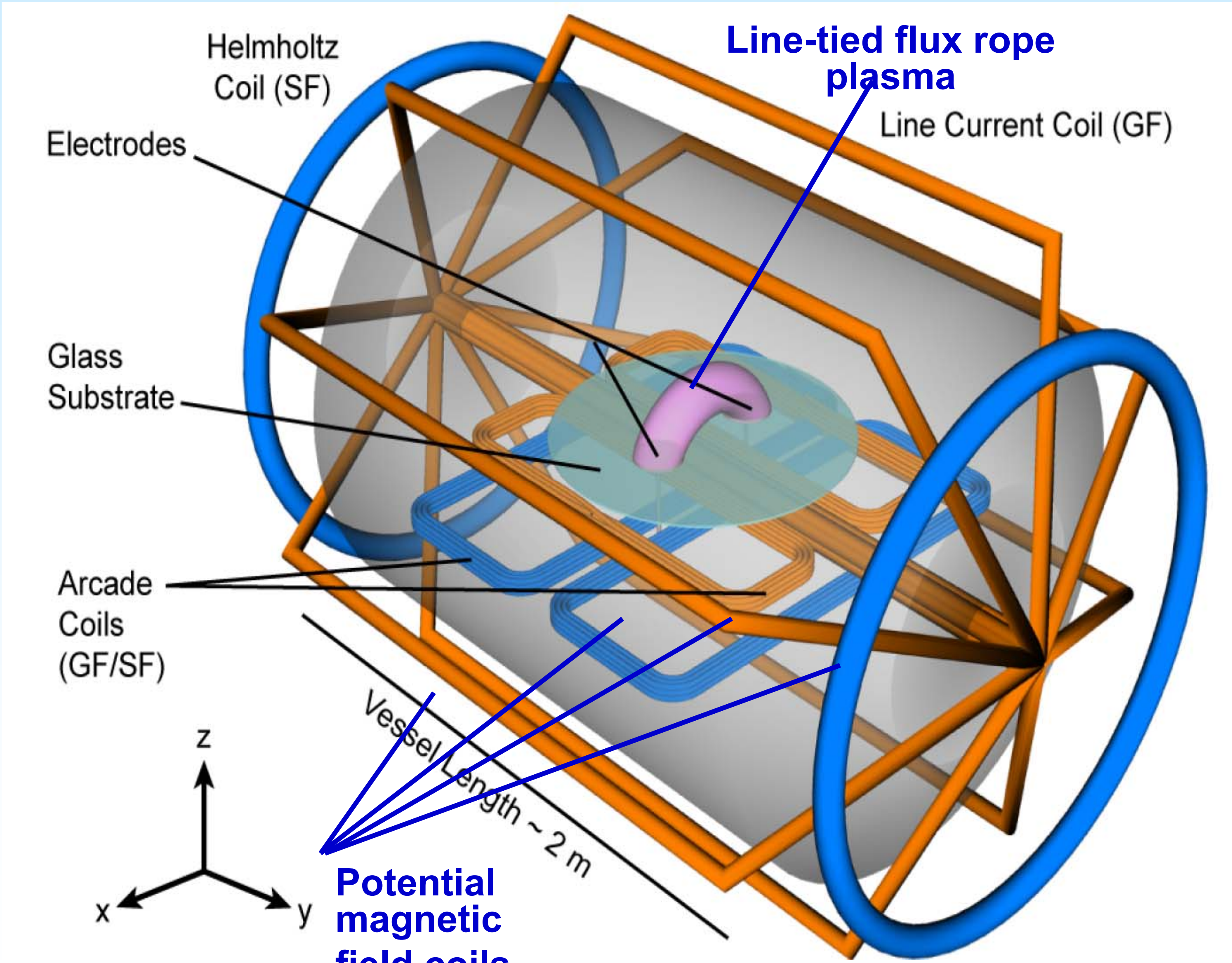

Goals:

Formation of quasi-static flux ropes in a static potential field arcade

Study of the force balance and transition between equilibria, toward loss-of-equilibrium and a kink instability

In a sheared arcade, both strapping and tension forces confine the flux rope

Laboratory experiment to better understand the role of the tension force.

MRX laboratory experimental results

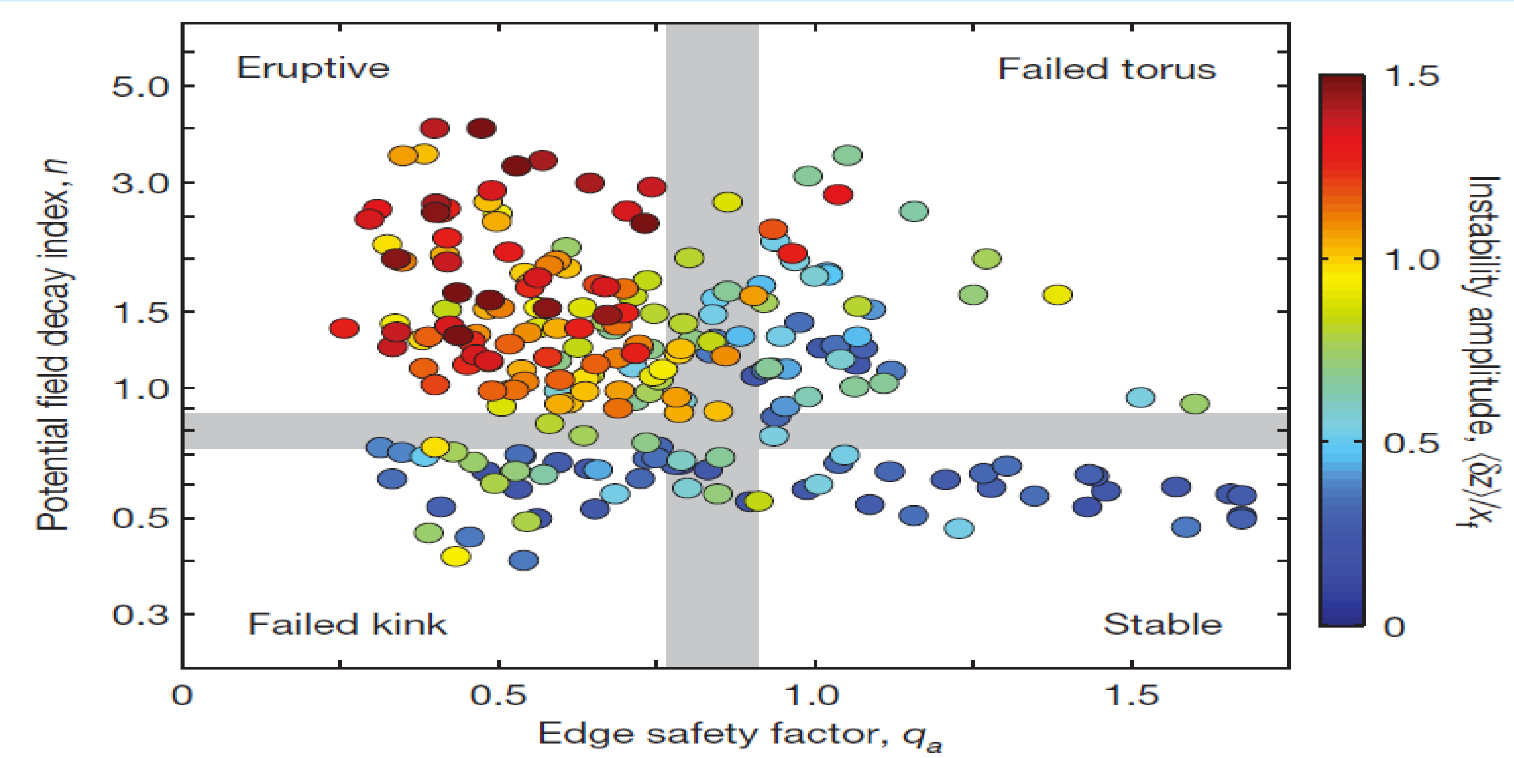

From:

[Myers et al., Nature, Dec. 2015]

I.e. it seems that both instability conditions - for kink and torus instability have to be fulfilled necessarily - but they what is sufficient? E.g. they do not to take into account, e.g. the distance between the footpoints, which was observed to play a role, the current distribution over the small radius et c. Which criterion is sufficient? Role of footpoint distance?

Equilibrium flux ropes -> stability ?

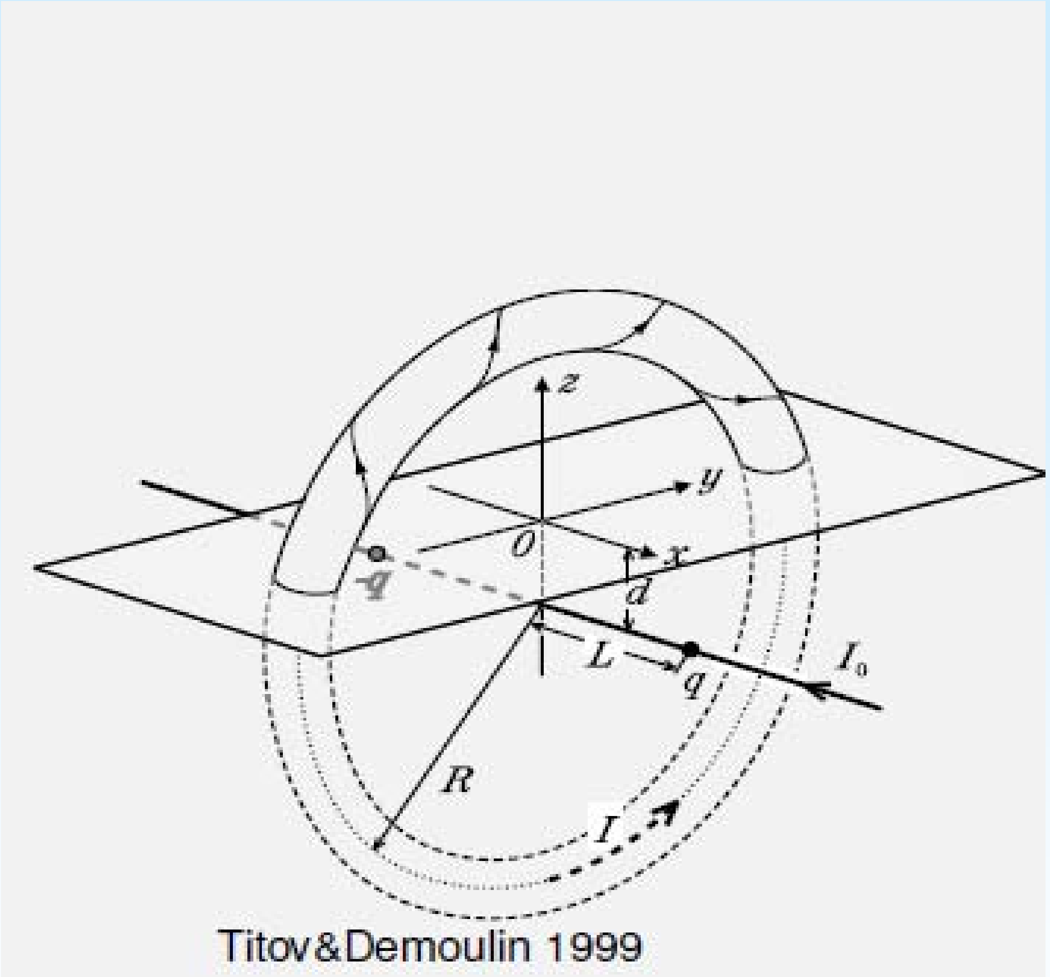

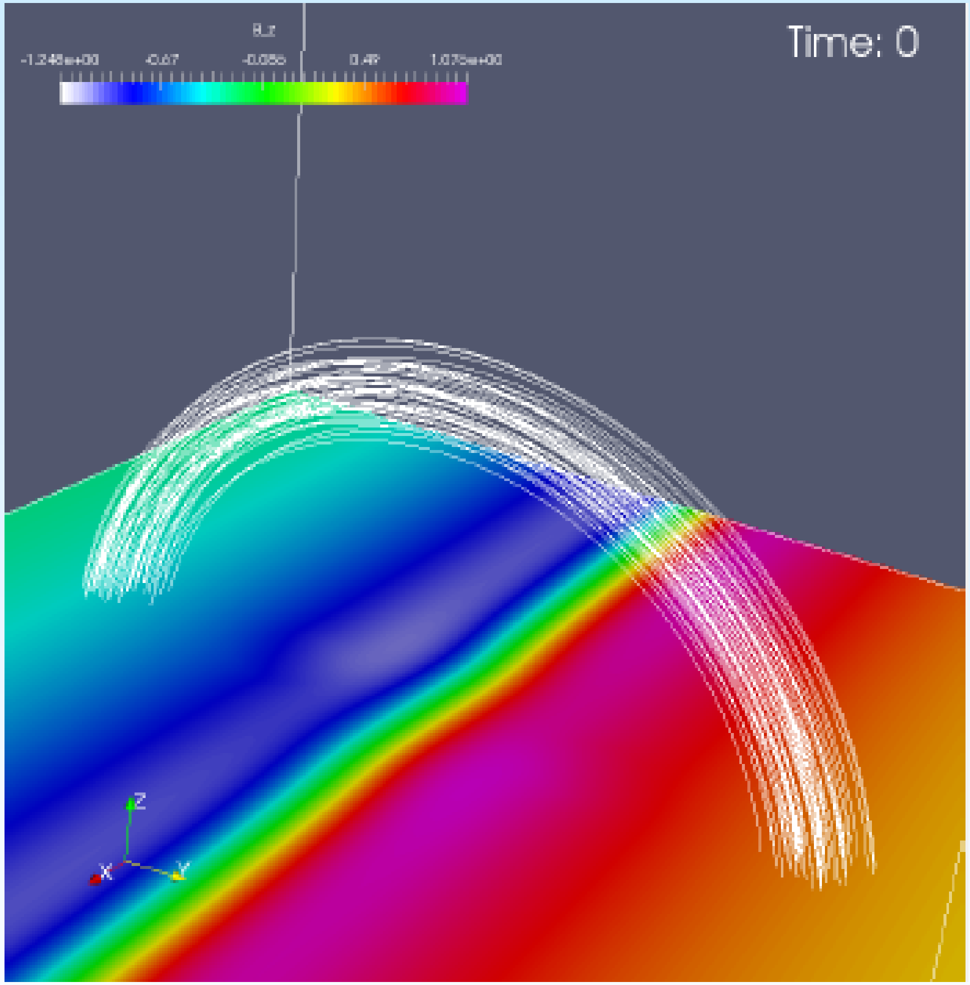

Stability of equilibrium flux ropes [Titov & Demoulin, 1999] (Plasma beta (<< 1); height-stratified density and pressure, the footpoint distance and rope inclination (R,d), ratio of radii.

Rising flux rope due to twisting

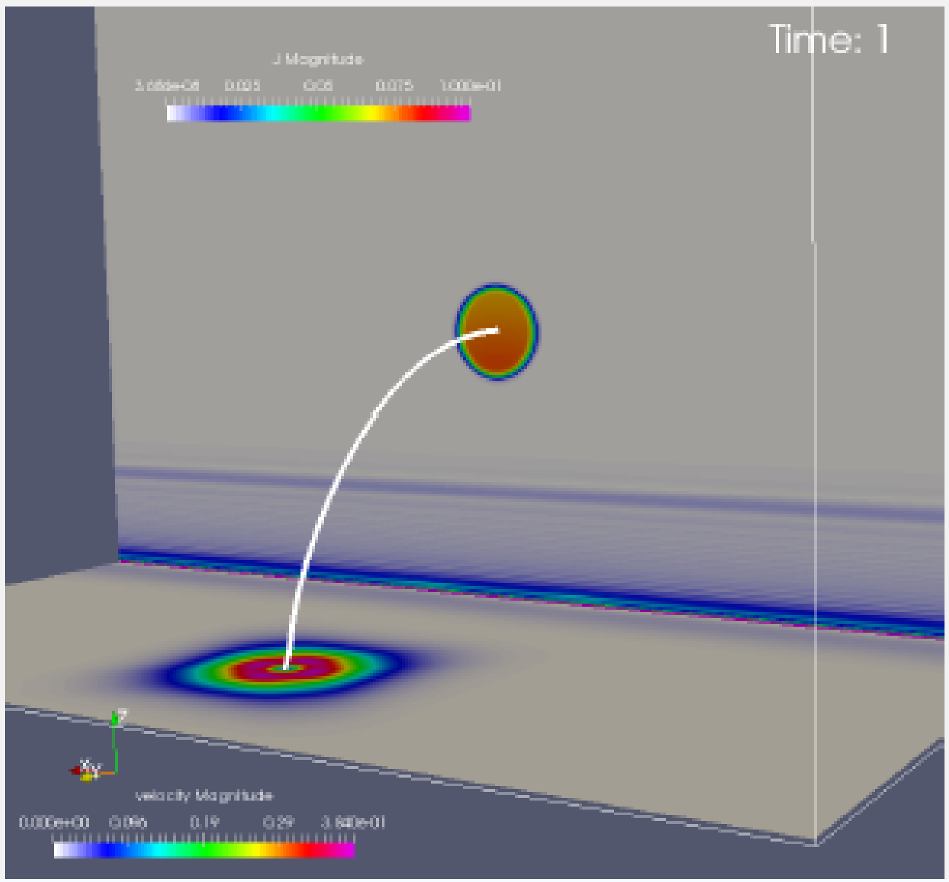

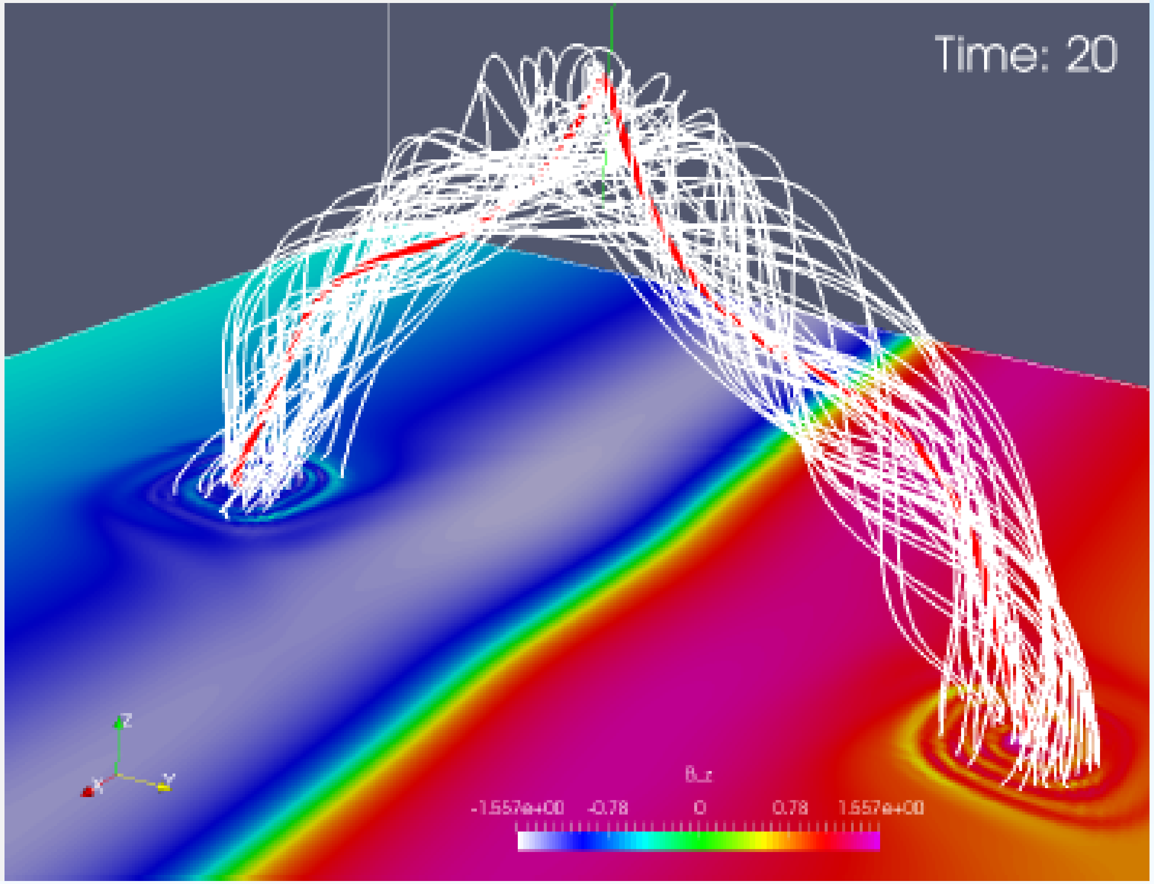

Helicity is injected from below -> The flux rope rises and twists

Stabilitiy investigations for R = 4; 6; 8 and t_{rot} = 0.5; 5; 10; 15; 20 t_{Alfven} when the Alfvenic perturbation reaches the flux rope apex)

R=4 footpoints distance as in MRX

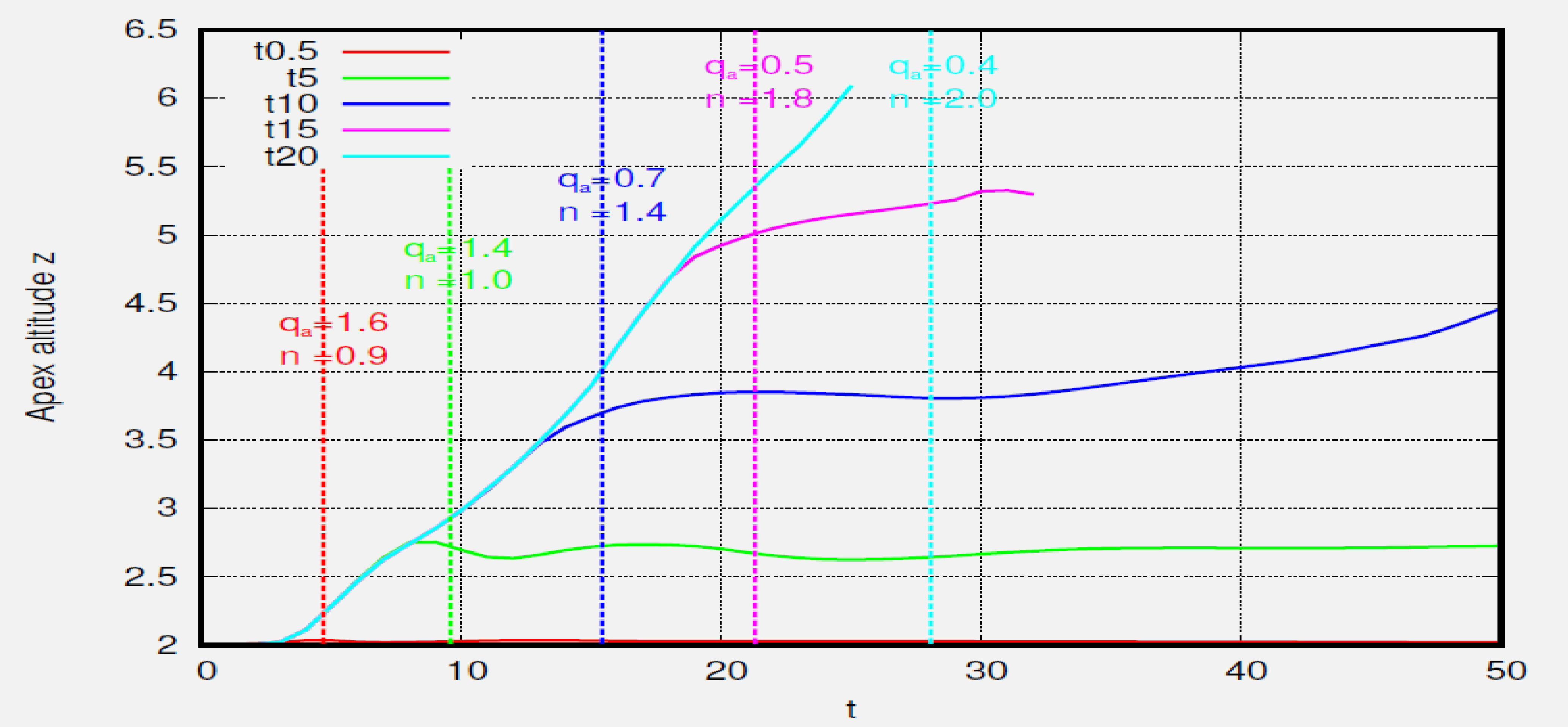

Shown is the rising height of the flux-rope apex driven during different times t_{rot}. The trailing Alvenic perturbation reaches the apex at t_e (dashed lines); Instability for q < 0.7 and N(z) ~ 1.0… 1.4 at the apex

R=6 –> medium footpoint distance

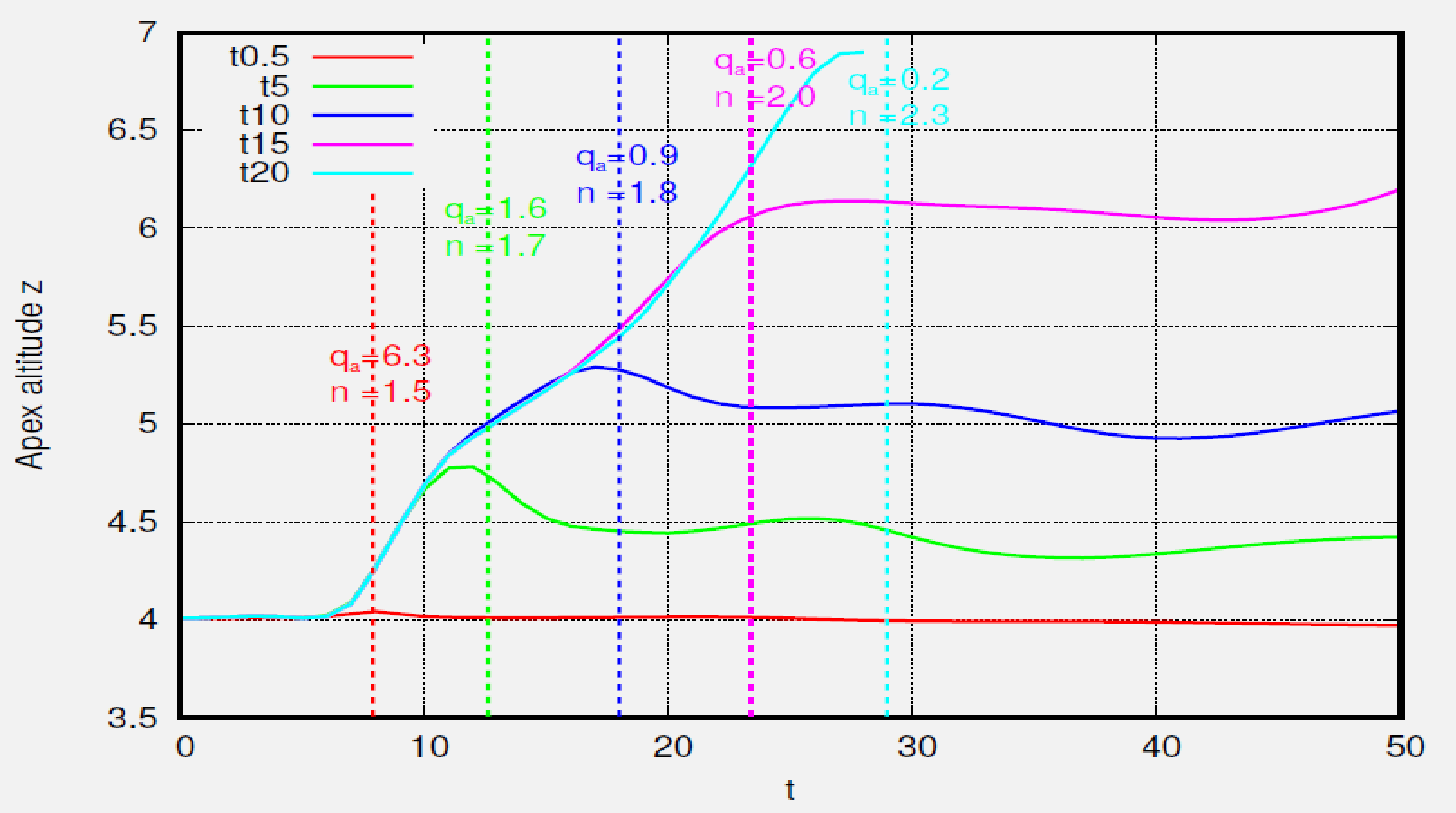

Shown is again the apex height evolution for different driving times t_{rot};

Instability if q < 0.6 but larger N(z) > 2.0 at the apex position required

R=8 –> large footpoint distance

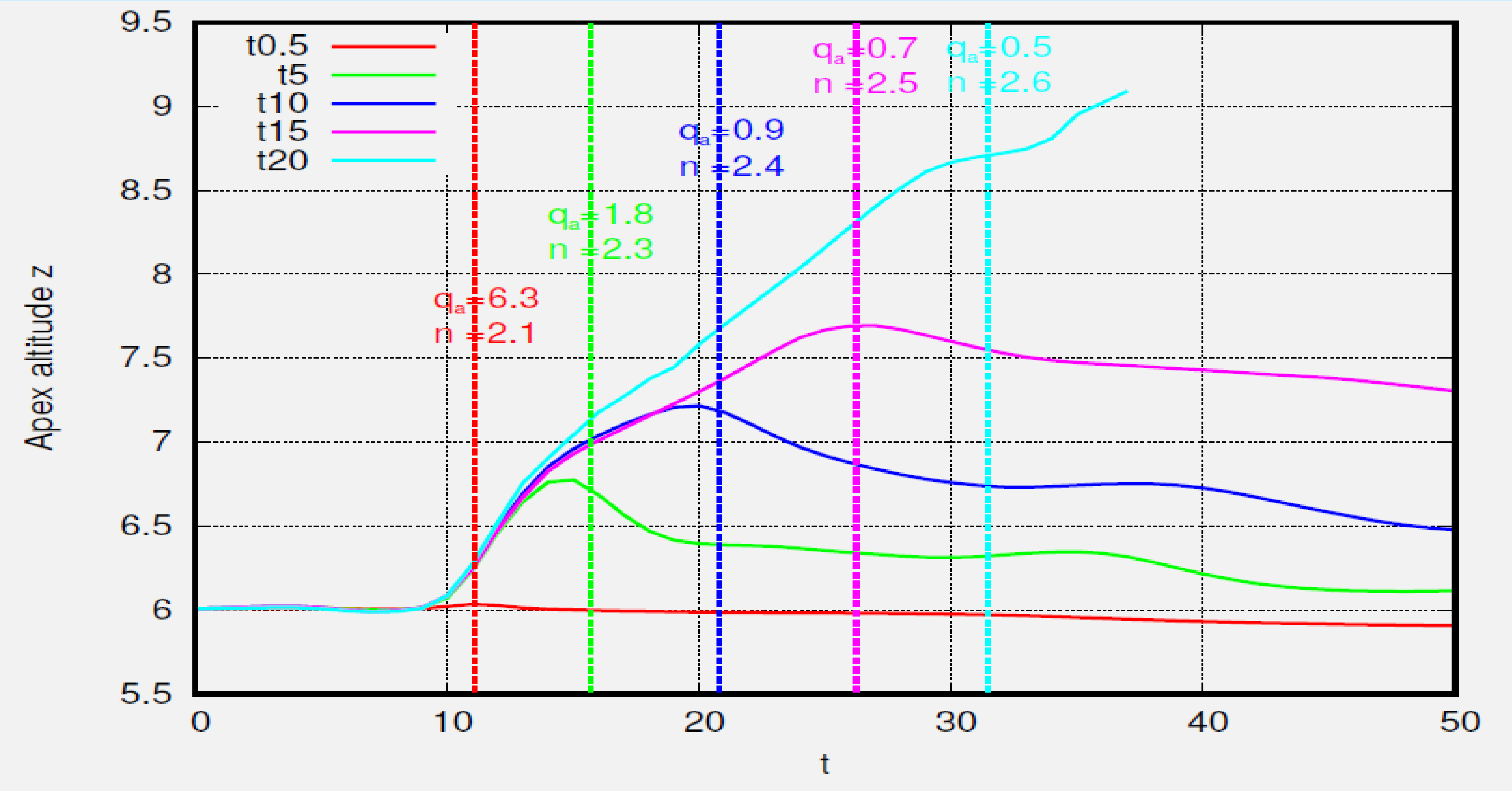

Shown is the apex-height evolution for different driving times t_{rot};
Instability still for q < 0.7 but now only after N(z) > 2.6 at the apex ->
Larger distance between footpoints -> flux ropes are more stable!

-> Lorentz forces due to return currents inhibit eruptions!

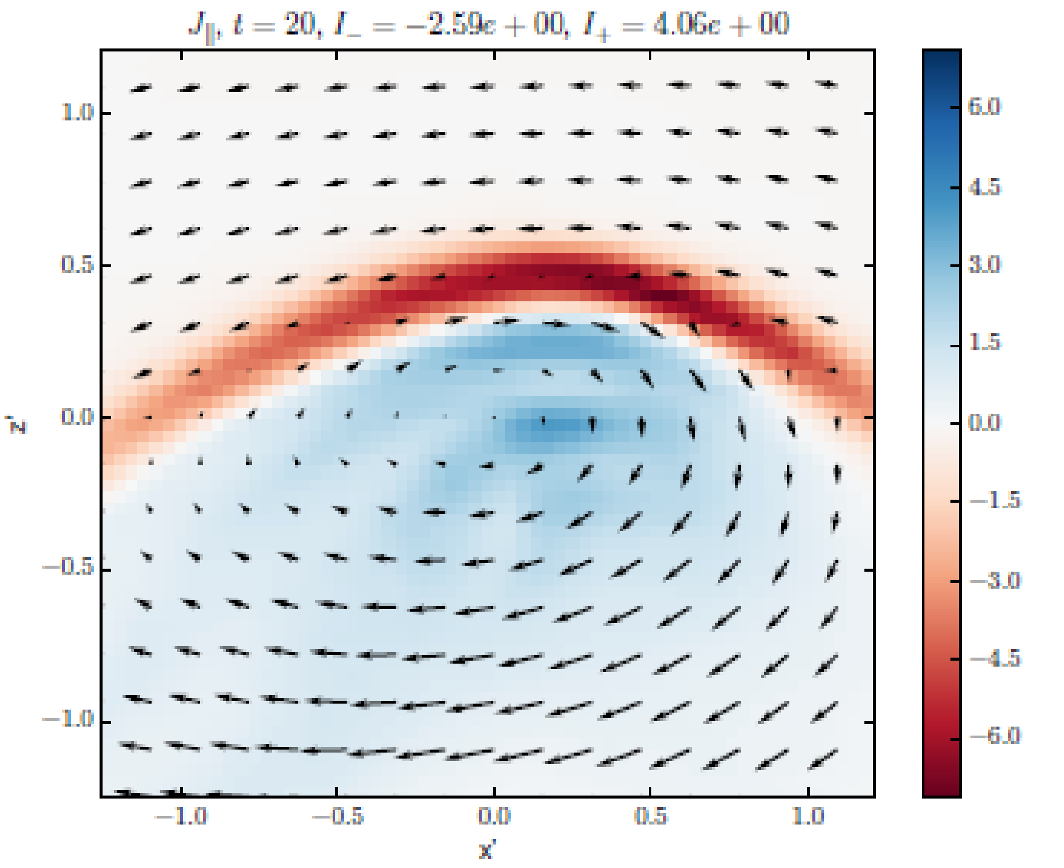

Parallel current $J.B$

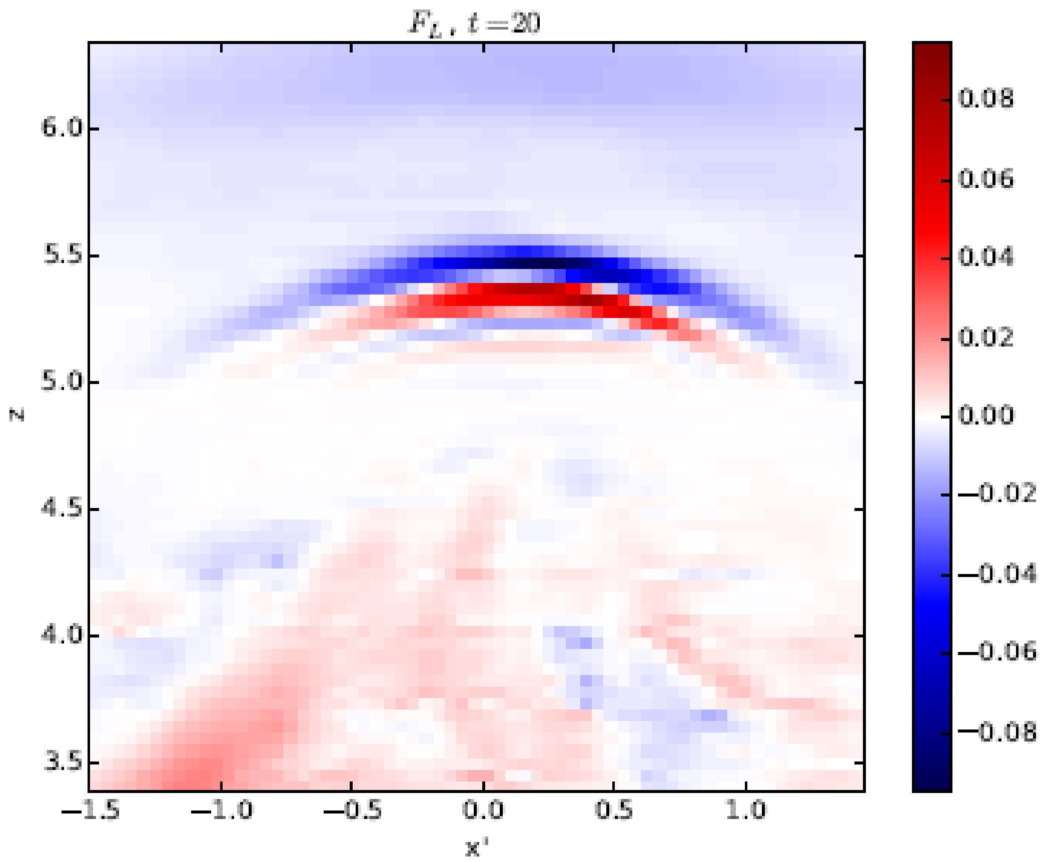

Lorentz force $F_{L,z}$

In almost ideal plasma conditions (here eta=10^-8 Rm=10^8) return currents around the flux rope and the strapping field result in downward directed Lorentz forces -> eruptive instability inhibited!

Eruption only if the return current is dissipated, e.g. by reconnection !

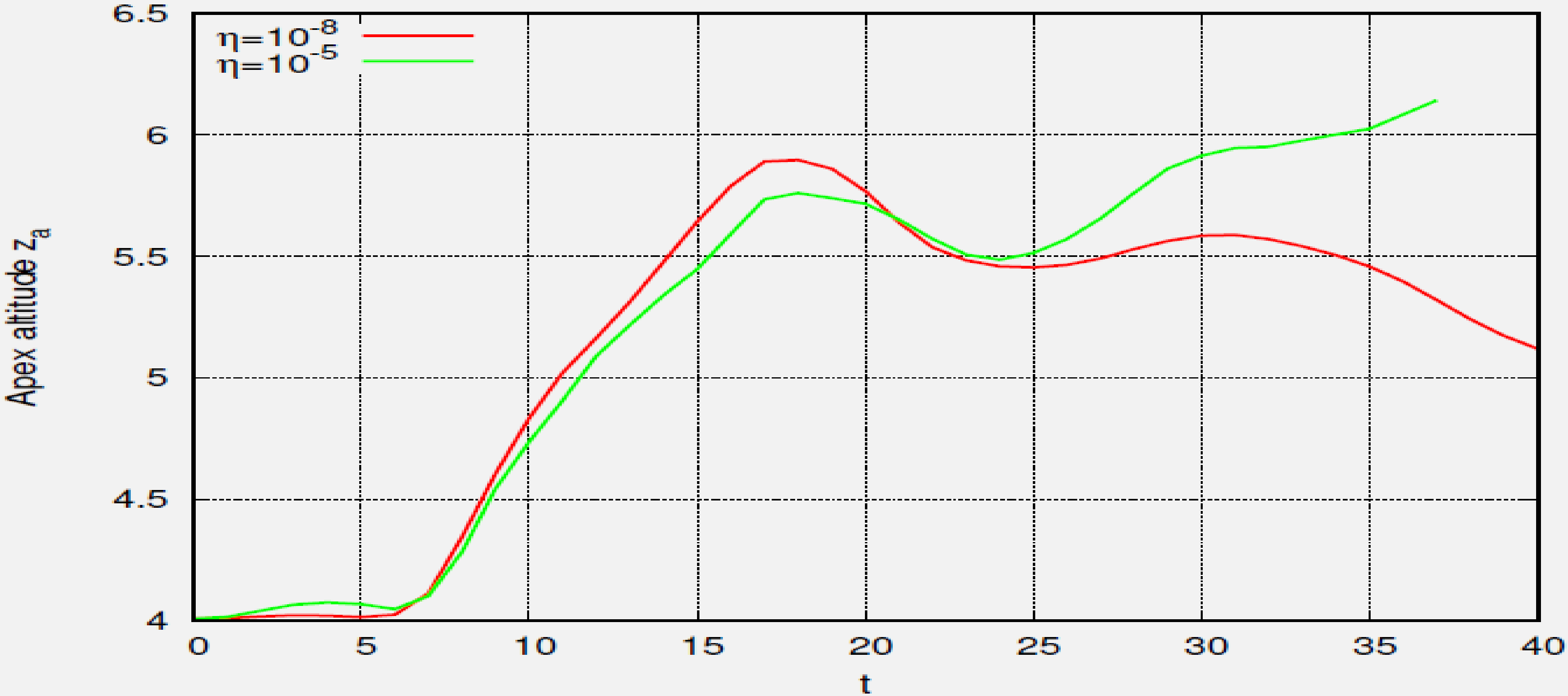

Apex altitude evolution for $R = 6$, $t_{rot} = 10$ and resistivity $\eta = 10^{-8}$ and $\eta = 10^{-5}$

Red line: results for eta ~ 10^{-8} (Rm=10^{8}-ideal plasma).
Green line: eta ~ 10^{-5}:enhanced resitivity->Rm=10^{5} reconnection.
(compare: MRX experiment: eta ~ 10^{-3}, Rm=10^{3})

Similar in Lab. Experiment of Madison Wisconsin

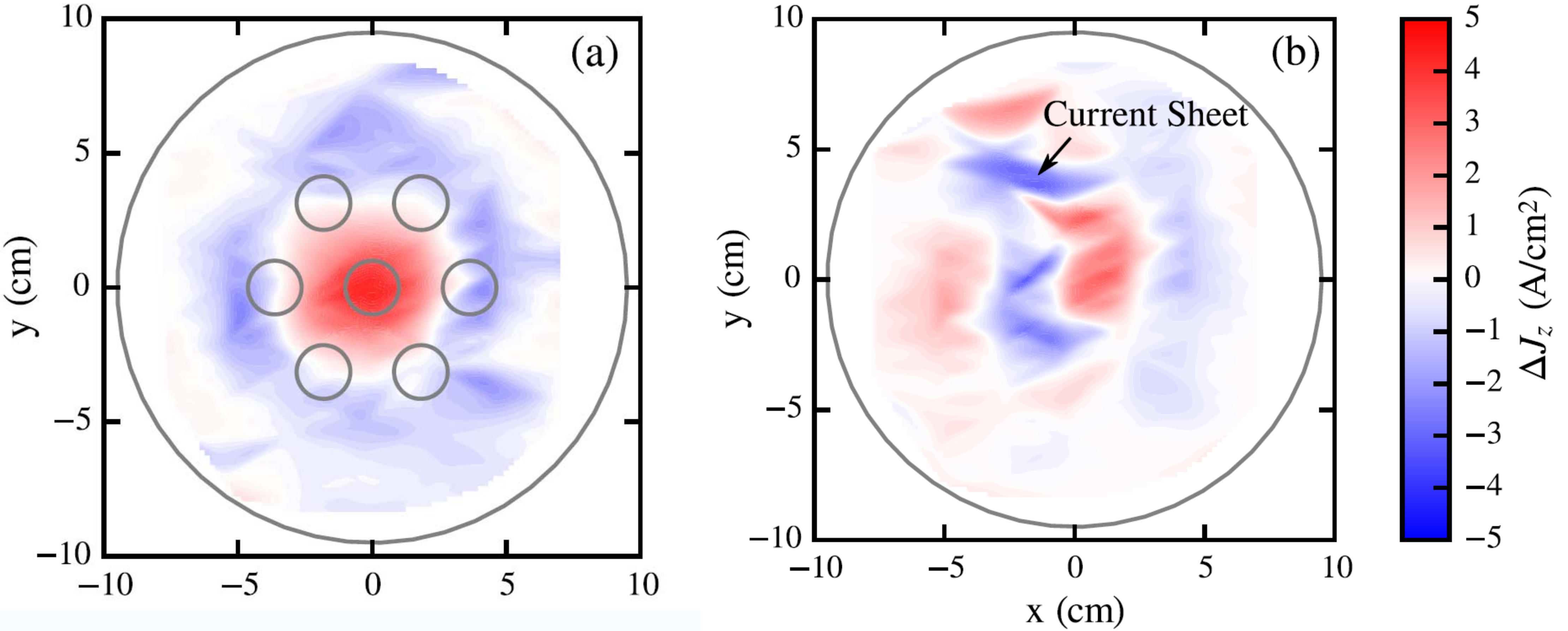

Line-tied University of Wisconsin-Madison pinch experiment: currents cpmpensate via return currents -> Instability only after small CS formation&turbulence [from Brookhart et al., PRL, 2015]

Data driven Simulations of CME cases, e.g. of 24.4.12 ideal and non-ideal 6.-7.3.12

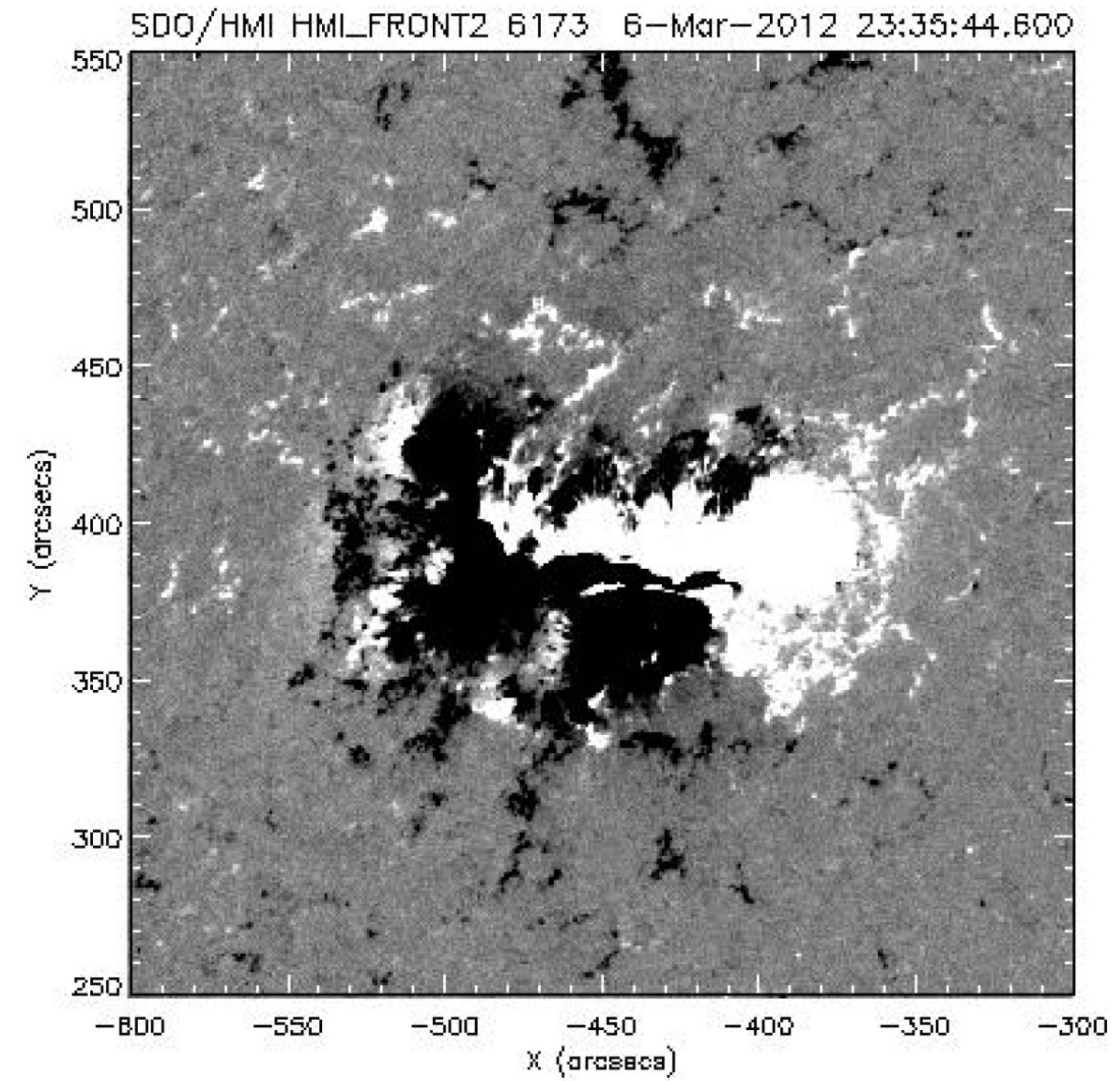

The following simulations are based on observations of the SDO s/c
Left: original B-field (magnetogram), obtained March 6, 2012 at 23:35 UT (AR 11429).
About 60 minutes later a strong X5.4-class Flare took place in this AR area and a CME was launched.
The photospheric plasma velocity for the simulation is also derived using SDO observations.

Preparation of observed B-field data

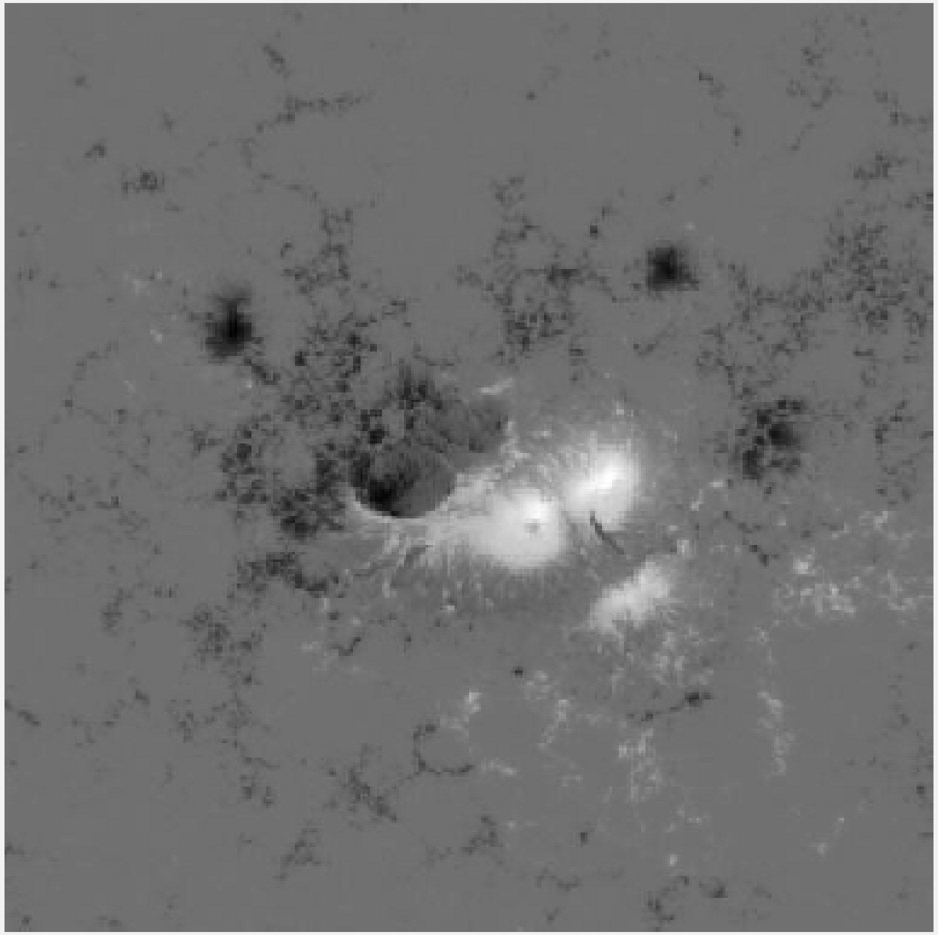
Original magnetogram.

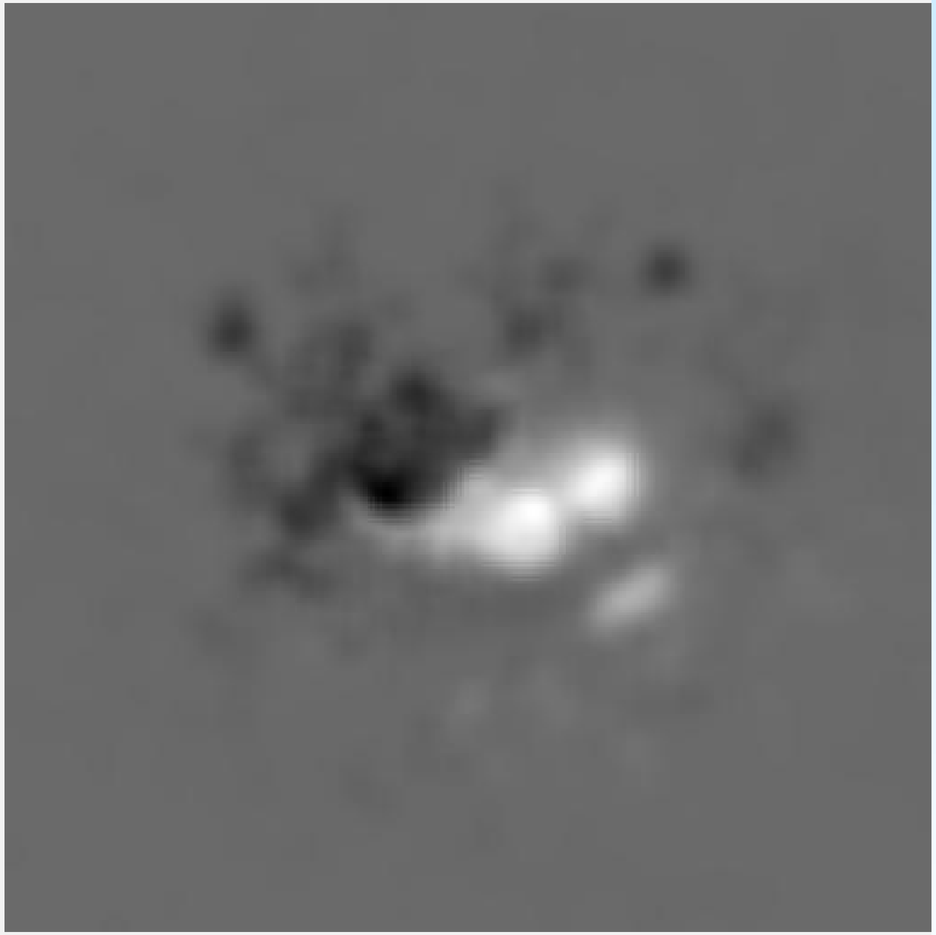
Preprocessed magnetogram.

Preparation of real magnetograms (this example is for AR 11520 on July 7, 2012) by filtering away small scale structures, B fields near the boundaries and balancing the B flux in accordance with the MHD boundary conditions.

Preparation of initial conditions & grid

SDO-observation based extrapolated coronal B-field

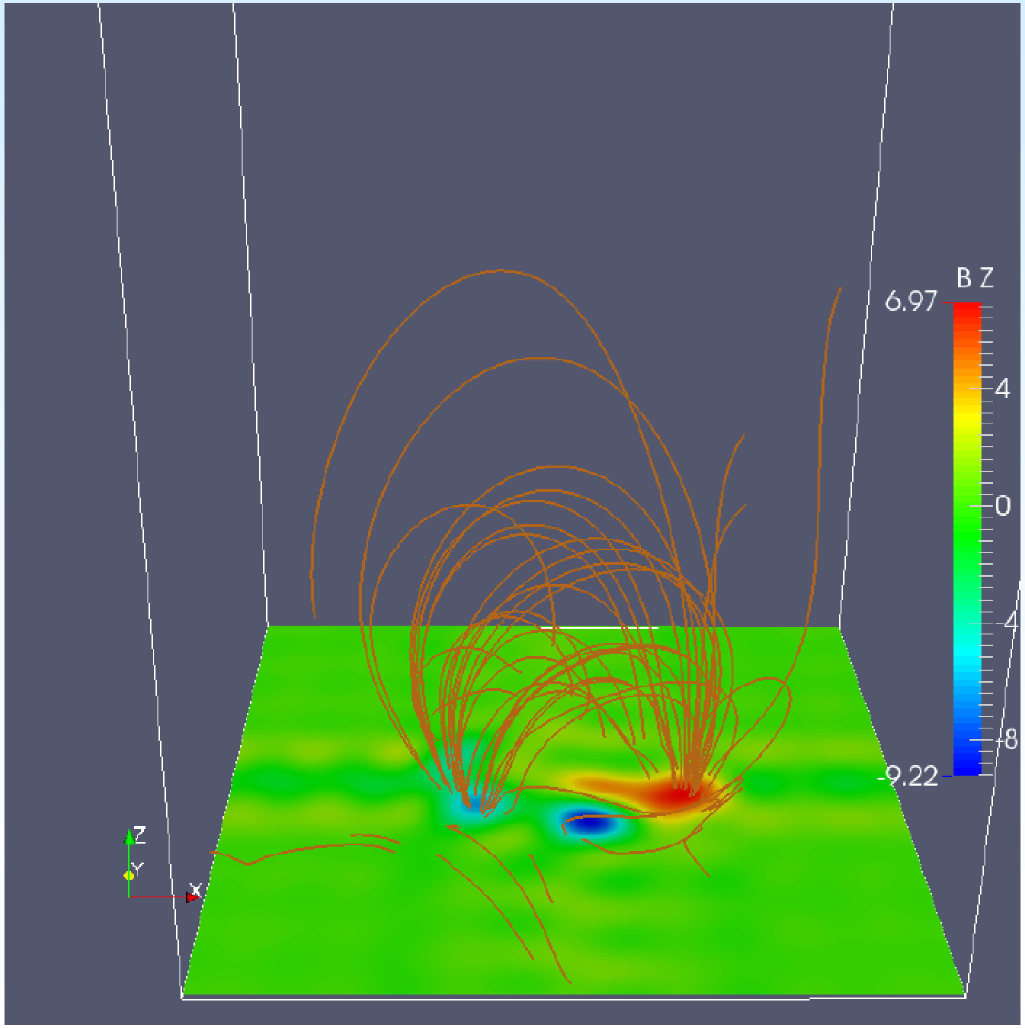

Initial density and temperature distribution photosphere -> corona

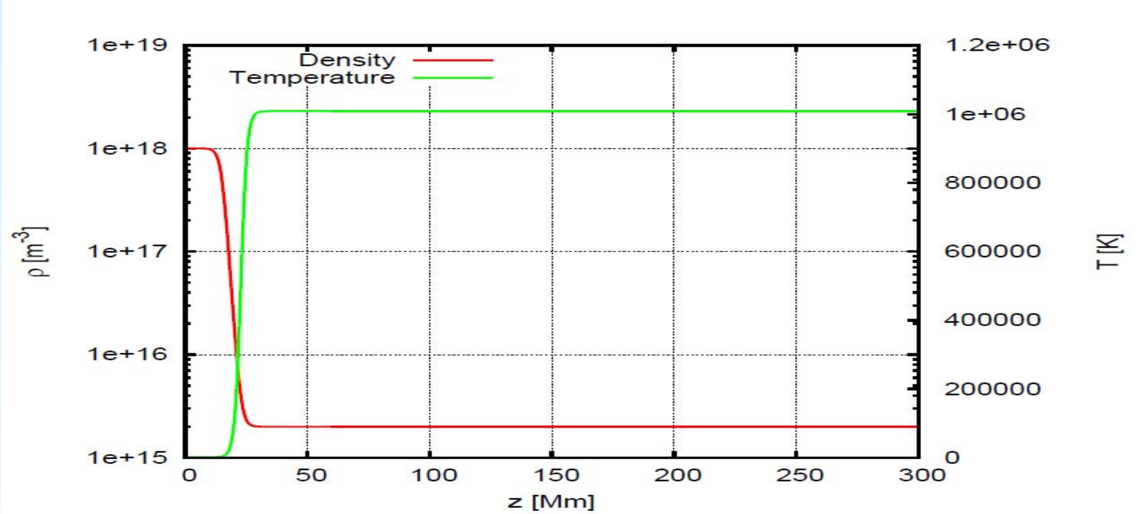

Height-variation of grid spacing:

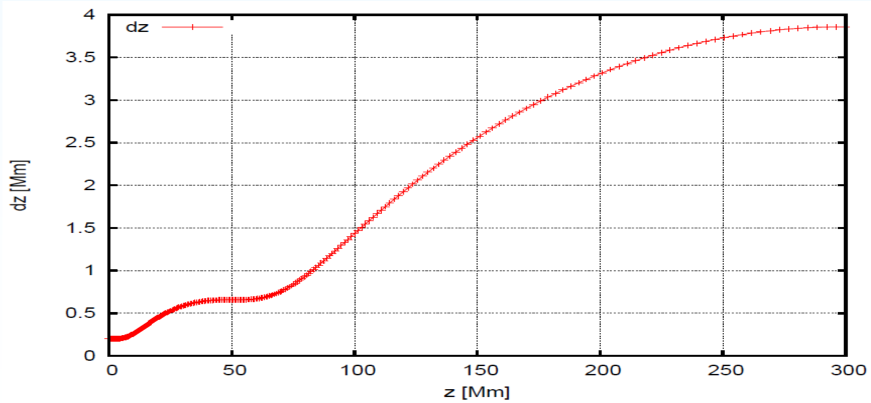

Ideal plasma instability simulation

A torus instability can be reached only after long time or for 4 times too fast winding speed at the footpoints is assumed!

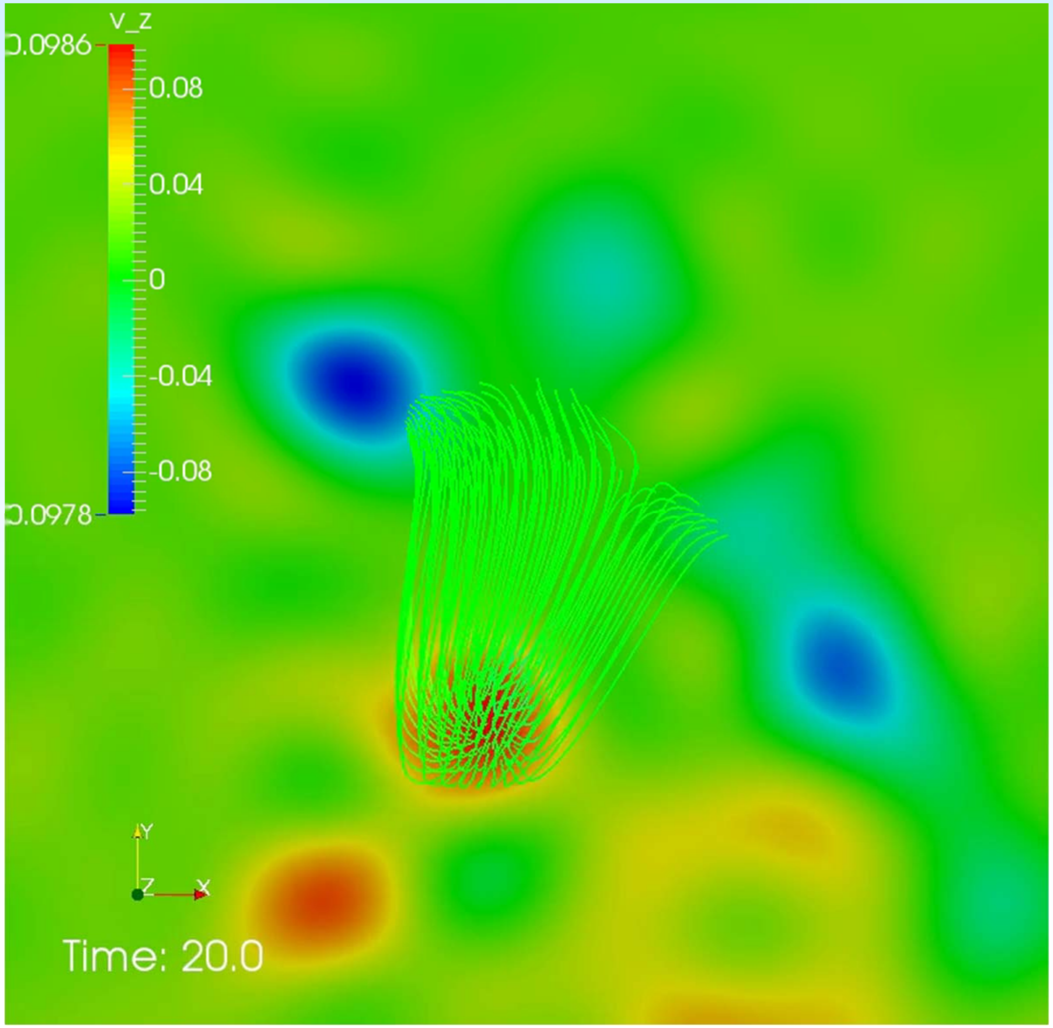

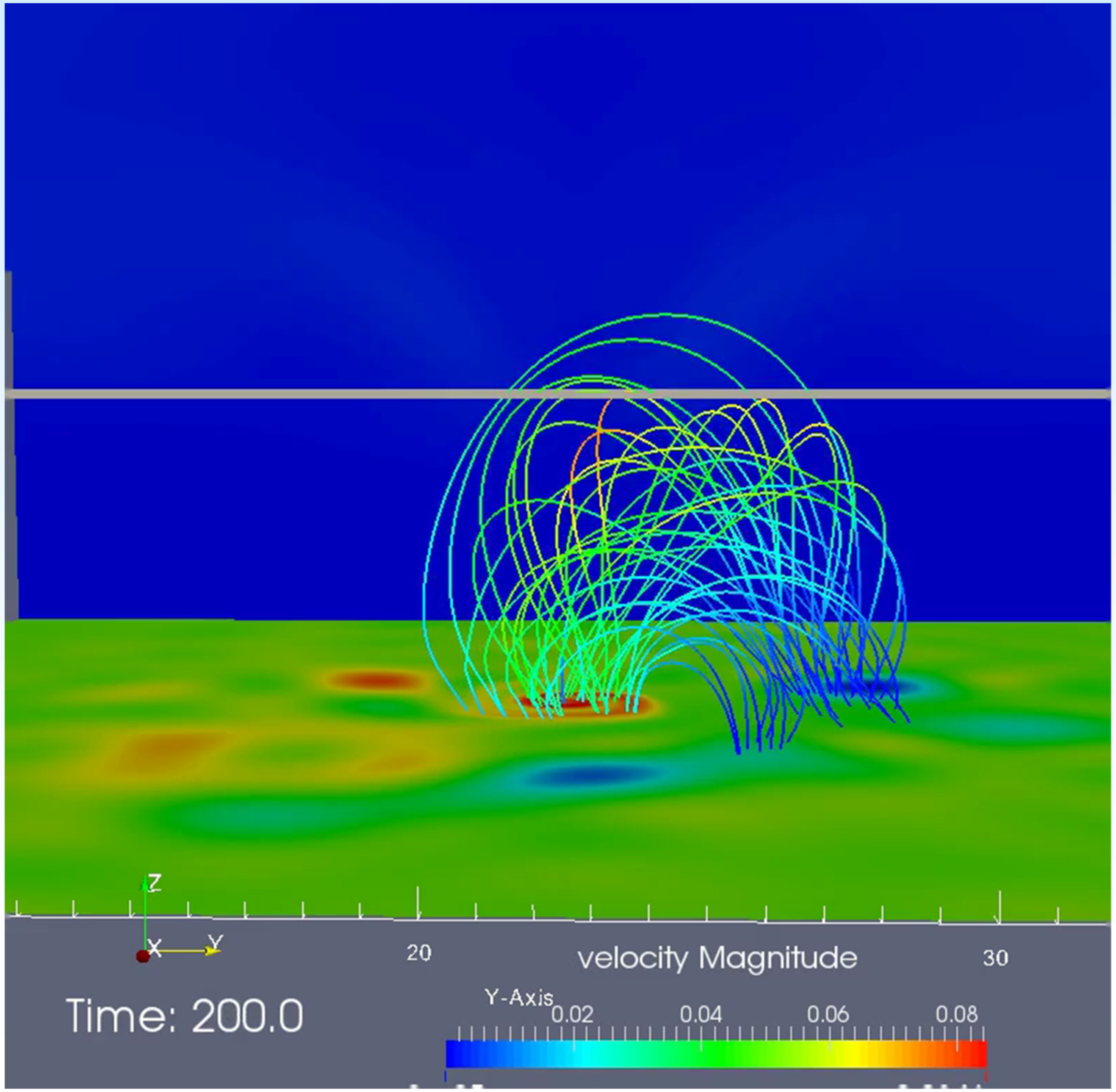

Non-ideal MHD simulation

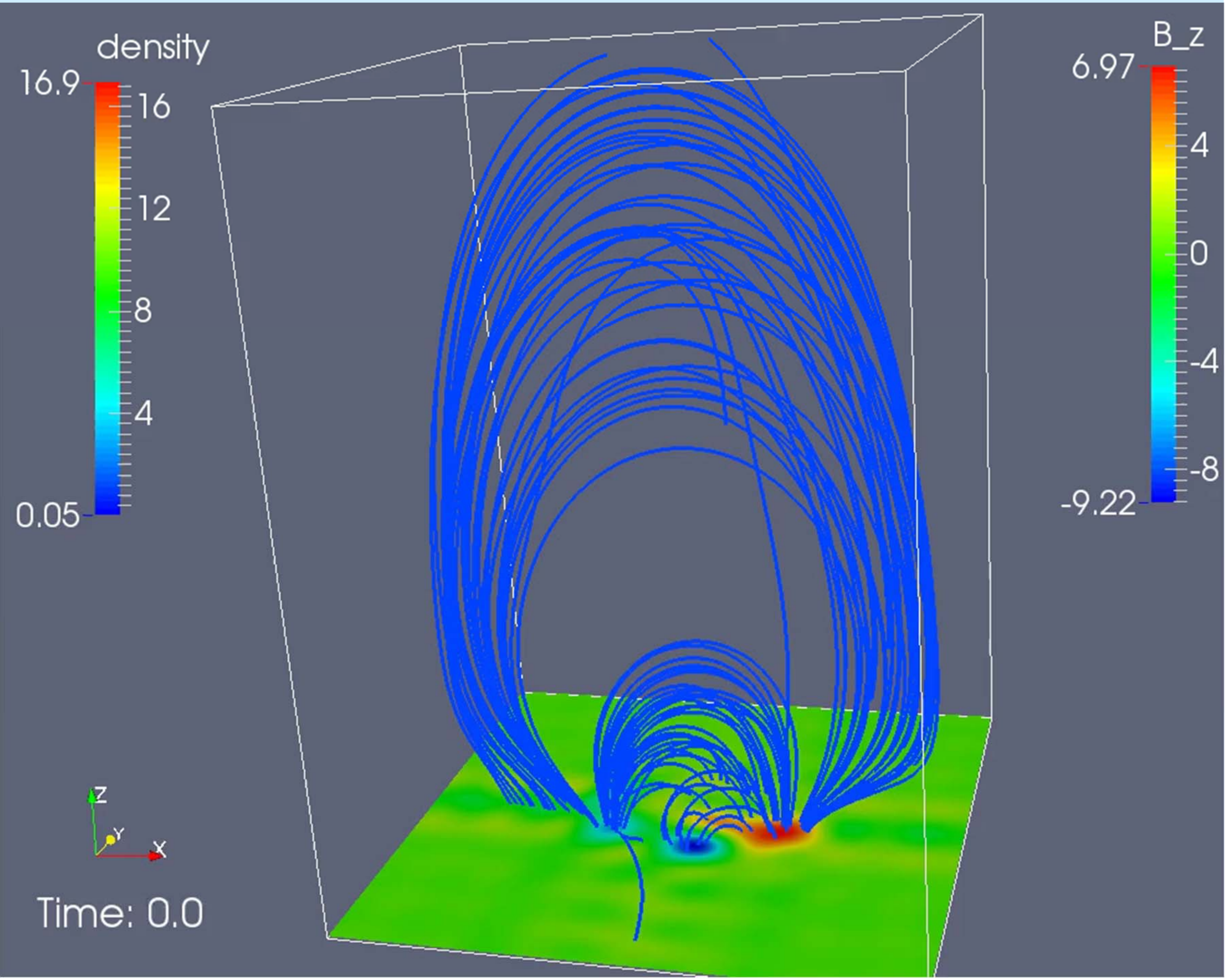

Non-ideal run with a realistic (smaller) winding speed on March 7, 2012. Epar isosurfaces 0.5 mV/m indicate that after 3740 s and after only 0.7 windings, fast reconnection has begun. Indeed, at 00:30 UT AR 11429 released a strong X5.4-class flare (SDO observation).

Evolution of the energies

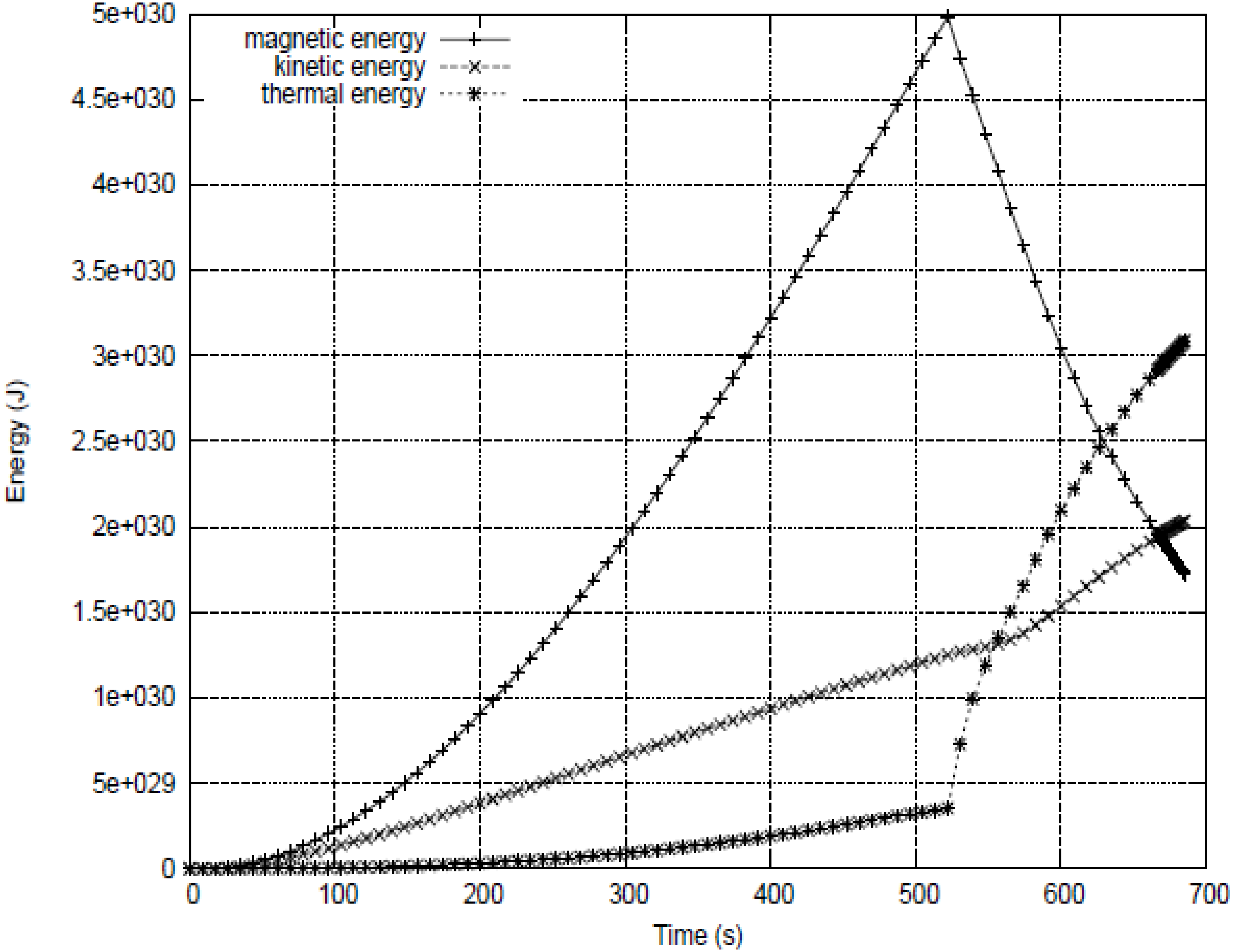

Fast reconnection starts at t=500 s
-> accumulated magnetic energy is released and
-> thermal energy is enhanced.
-> Then the kinetic energy takes over which carries most of the energy away
[Santos, Büchner, Otto, 2011]

Evolution of magnetic helicity

$$\frac{\mathrm{d}H_\mathrm{R}}{\mathrm{d}t} = -2\int_V (\mathbf{E}\cdot\mathbf{B})\mathrm{d}V - 2\int_S \big((\mathbf{A}_\mathrm{p}\cdot\mathbf{V})\mathbf{B} - (\mathbf{A}_\mathrm{p}\cdot\mathbf{B})\mathbf{V}\big)\cdot\mathbf{n}\,\mathrm{d}S.$$

derived by [Berger and Field, 1984]

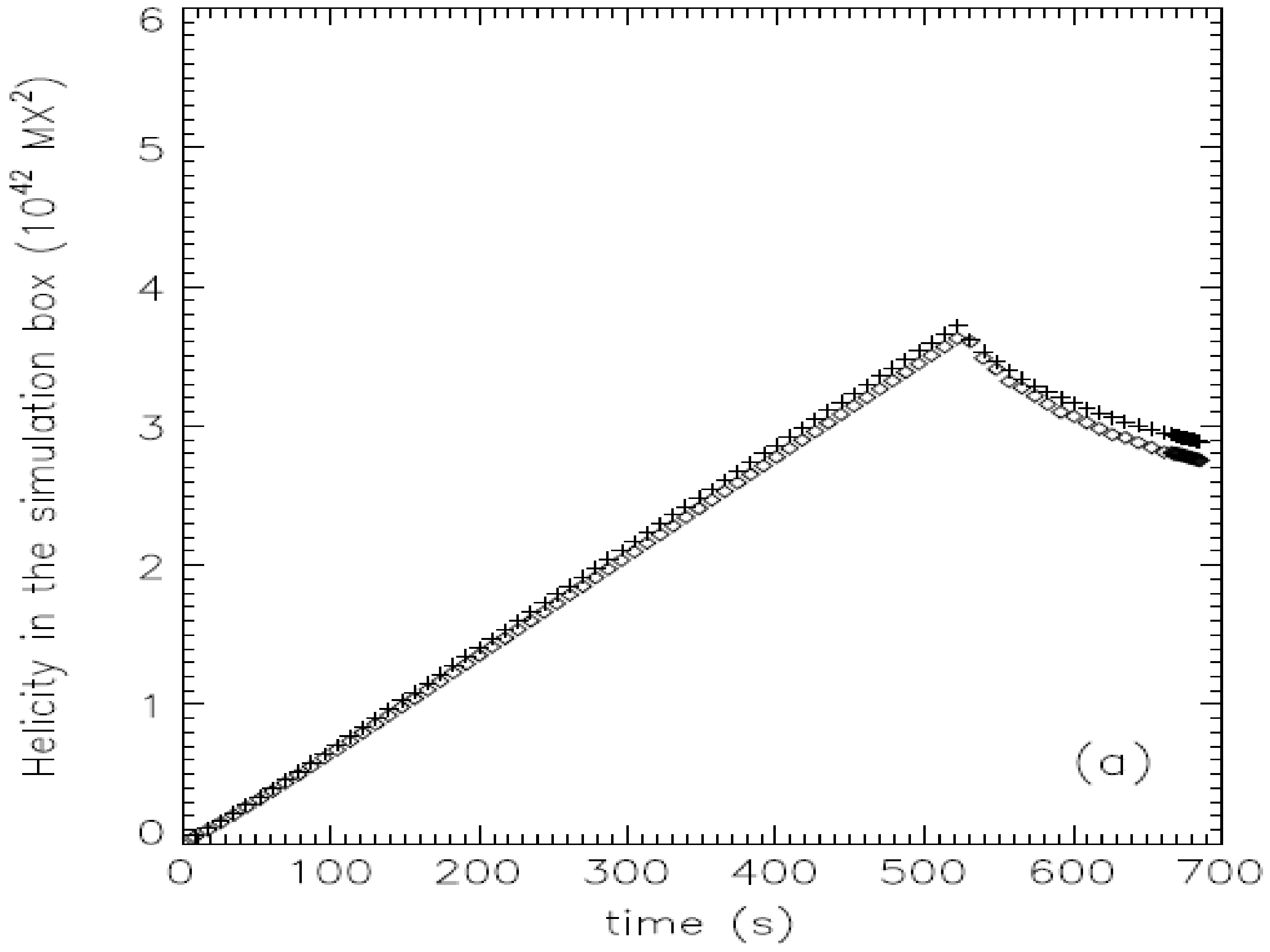

Crosses: Temporal evolution of the relative magnetic helicity H_R in the simulation box according to the time-integrated [Berger and Field, 1984] formula

Diamonds: Relative magnetic helicity H_R obtained from simulation [Yang, Büchner, Santos and Zhang 2013]

New data driven CME eruption simulation confirmed: reconnection required to erupt

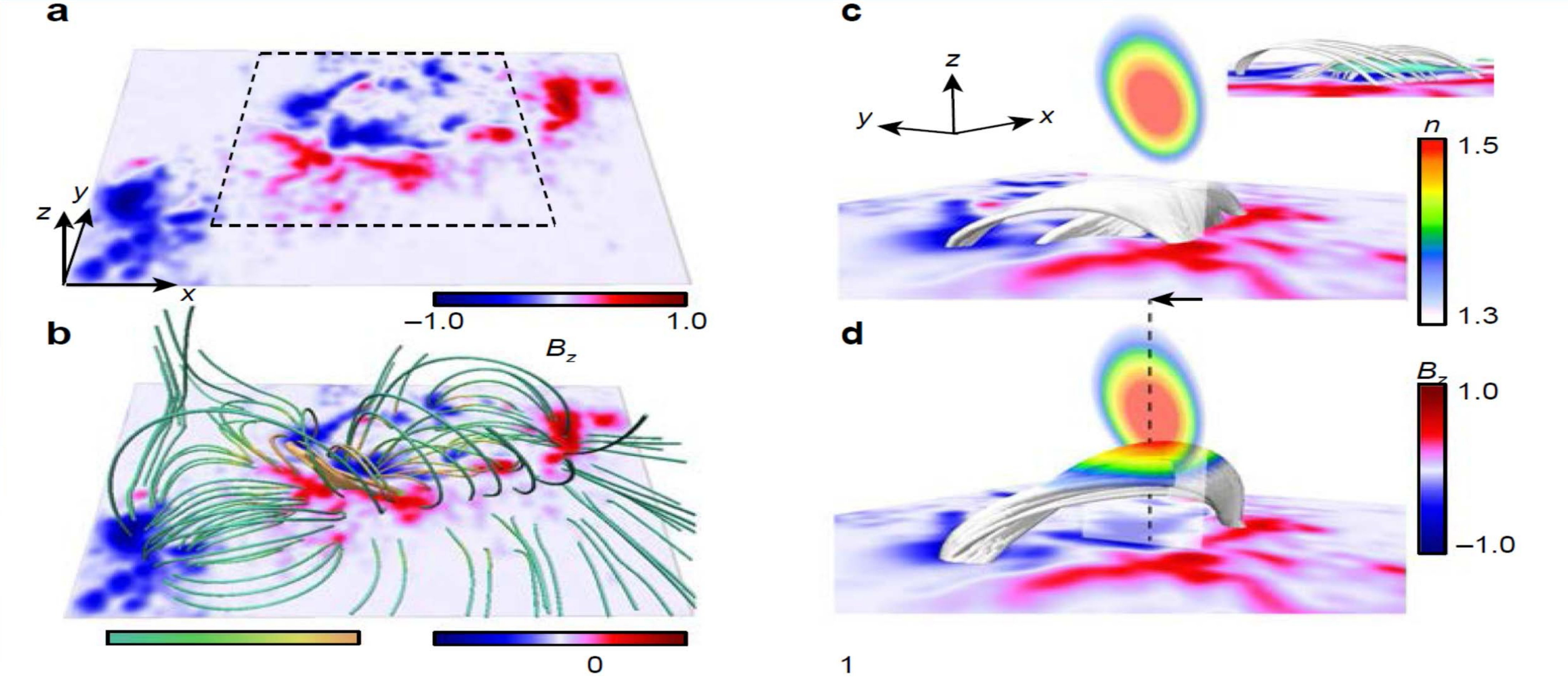

[from Inoue, Kusanao, JB, Skala, 2018 Nature Comm].

More tomorrow by Kusanao-san towards possibilities of prediction for space weather applications

Summary

Ideal plasma instabilities alone do not cause flux rope eruptions, in addition dissipation / reconnection is needed. After that even helicity is dissipated!

Contents

- Coronal plasmas & fields
- Eruptions & reconnection
- Turbulence and dissipation
- Electron acceleration

Unstably self-generated plasma waves change the 3D velocity space distributions

Ion distribution function **Electron distribution function**

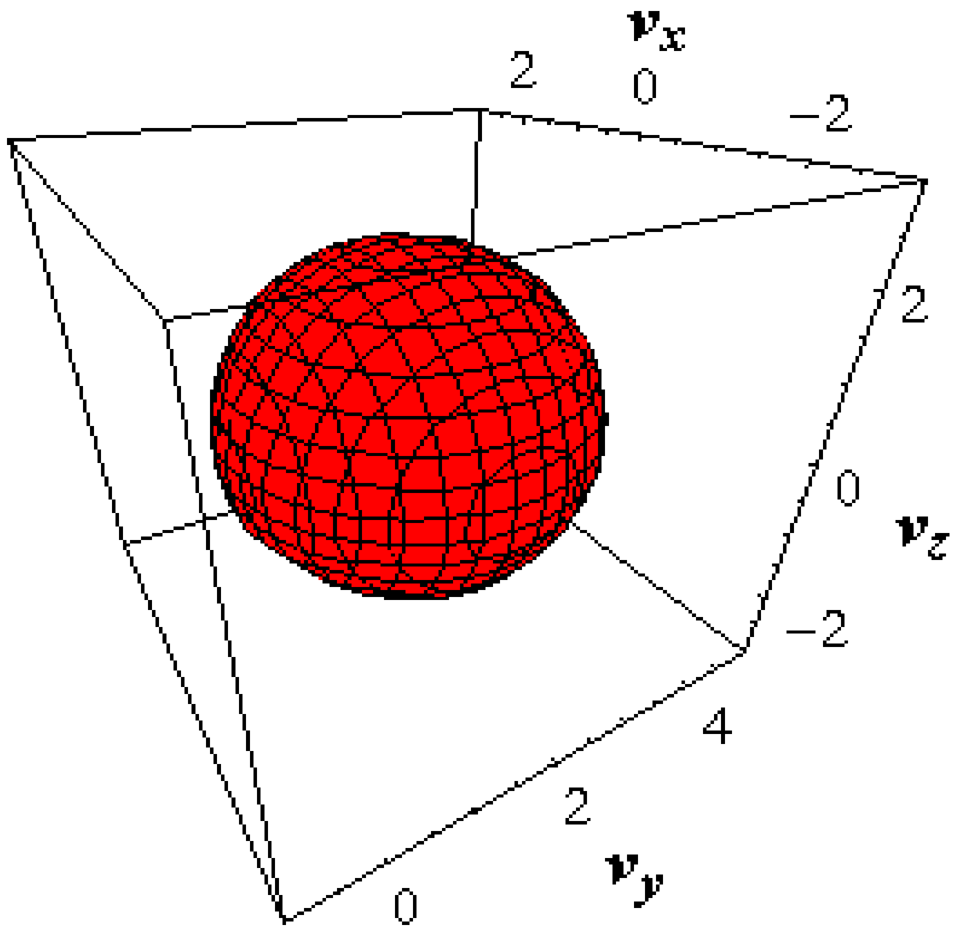

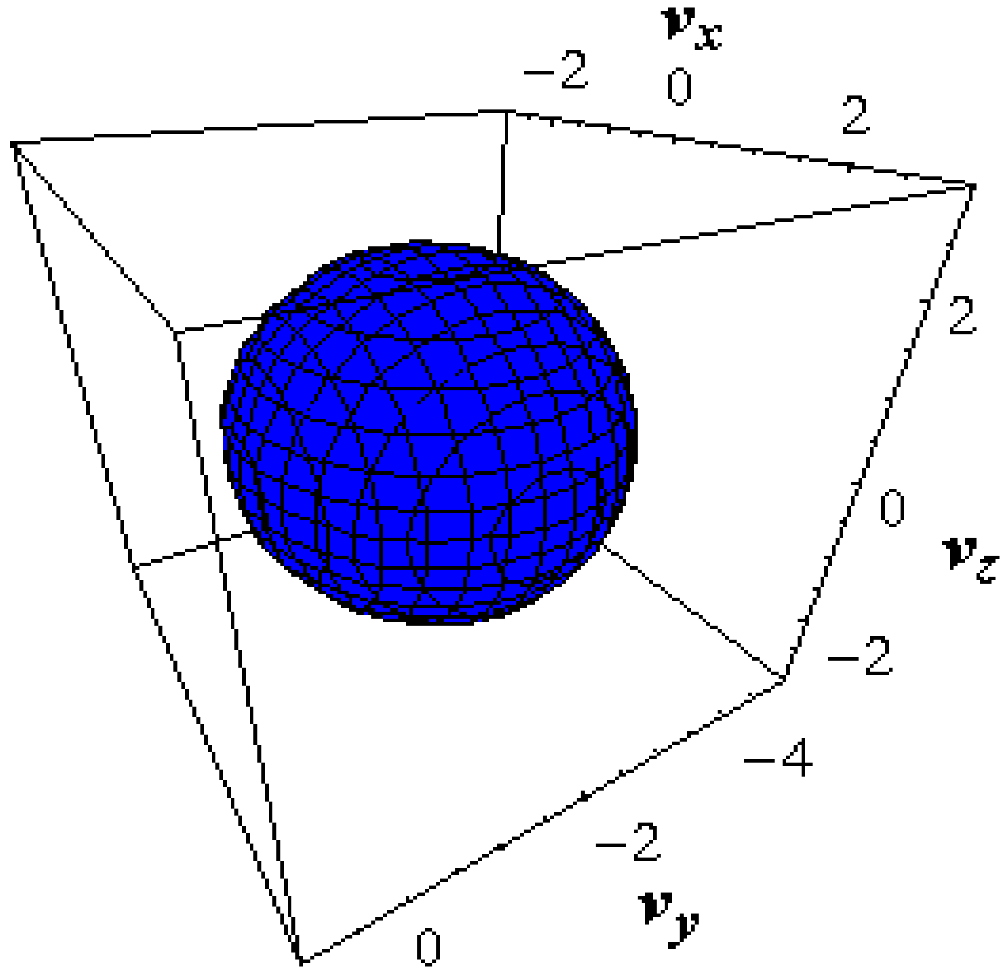

The slowing of the current carriers is often called "anomalous resistivity"

1D electron distribution in the current direction

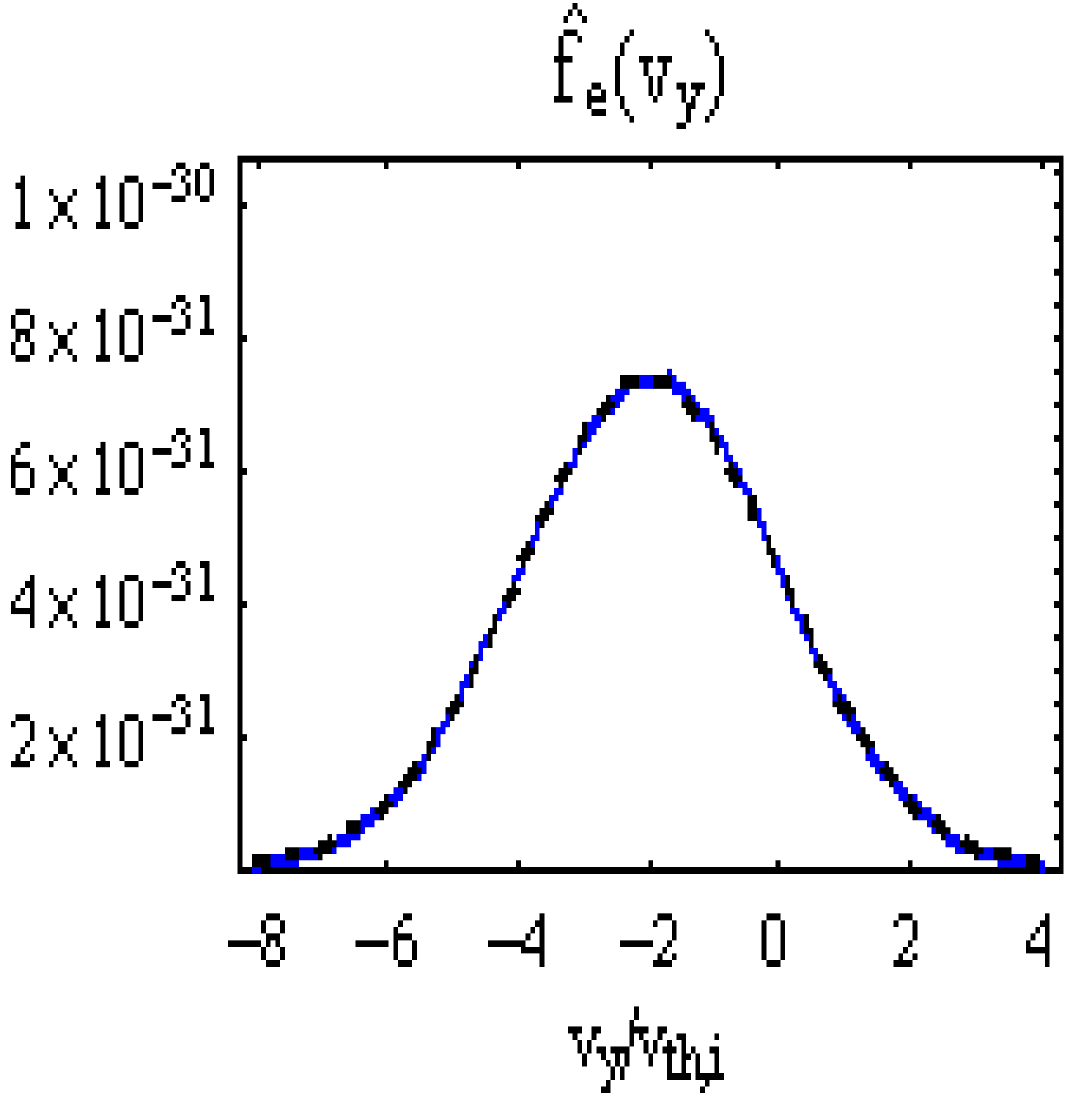

<- electrons; the movie illustrate:

-plateau-formation in the distribution function near the resonant velocity,

- breaking of the bulk electron motion and

- electron heating

Nature of „anomalous resistivity“

Representing $f_j = f_{0j} + \delta f_j \quad E_{\|} = \left\langle E_{\|} \right\rangle + \delta E_{\|} \quad \vec{B} = \delta \vec{B}$

for an appropriate averaging $\langle \delta f_j \rangle = \left\langle \delta \vec{E} \right\rangle = \left\langle \delta \vec{B} \right\rangle = 0.$

-> the Vlasov equation reveals:

$$\frac{\partial f_{0e}}{\partial t} + \vec{v} \cdot \frac{\partial f_{0e}}{\partial \vec{r}} + \frac{e}{m_e} \vec{E} \cdot \frac{\partial f_{0e}}{\partial \vec{v}} = -\frac{e}{m_e} \left\langle \left(\delta \vec{E} + \vec{v} \times \delta \vec{B} \right) \cdot \frac{\partial \delta f_e}{\partial \vec{v}} \right\rangle$$

after velocity-space integration, the momentum exchange rate is

$$\left(\frac{d}{dt} n m_e v_{y,e} \right)_{eff} = \langle \delta E_y \delta \rho_e + \delta j_{z,e} \delta B_x - \delta j_{x,e} \delta B_z \rangle$$

-> What fluctuations / turbulence is generated in the corona?

-> The correlations above have to be determined by kinetic numerical simulations!

Quantification of collisionless dissipation by effective collision rate

Ensemble averaged Vlasov equation for

$$f_j = f_{0j} + \delta f_j .$$

reveals

$$\langle \delta f_j \rangle = \left\langle \delta \vec{E} \right\rangle = \left\langle \delta \vec{B} \right\rangle = 0.$$

$$\frac{\partial f_{0j}}{\partial t} + \vec{v} \cdot \frac{\partial f_{0j}}{\partial \vec{r}} + \frac{e_j}{c m_j} \left(\vec{v} \times \vec{B} \right) \cdot \frac{\partial f_{0j}}{\partial \vec{v}} = \left(\frac{\partial f_j}{\partial t} \right)_{an}$$

$$= - \frac{e_j}{m_j} \left\langle \left(\delta \vec{E} + \frac{\vec{v} \times \delta \vec{B}}{c} \right) \cdot \frac{\partial \delta f_j}{\partial \vec{v}} \right\rangle .$$

$$\left(\frac{\partial}{\partial t} n_j m_j v_{y,j} \right)_{an} = \left\langle \delta E_y \delta \rho_j + \frac{\delta j_{z,j} \delta B_x - \delta j_{x,j} \delta B_z}{c} \right\rangle .$$

$$\nu_{eff,j} = \frac{1}{\langle n_j m_j v_{y,j} \rangle} \left(\frac{\partial}{\partial t} n_j m_j v_{y,j} \right)_{an} .$$

Often used theoretical estimate of the anomalous collision frequency based on waves and their dispersion (quasilinear approximation):

$$\nu = \sum_k \frac{\Delta k |\delta E(k)|^2 \omega_{pe}}{k v_{te}^2 m_e n v_d} Im \xi_e Z(\xi_e)$$

In a simulation one can directly determine the momentum exchange rate

$$\nu(t + \delta t/2) = \frac{2}{\delta t} \frac{p(t + \delta t) - p(t)}{p(t + \delta t) + p(t)}$$

Current sheet „quasi-collisions"

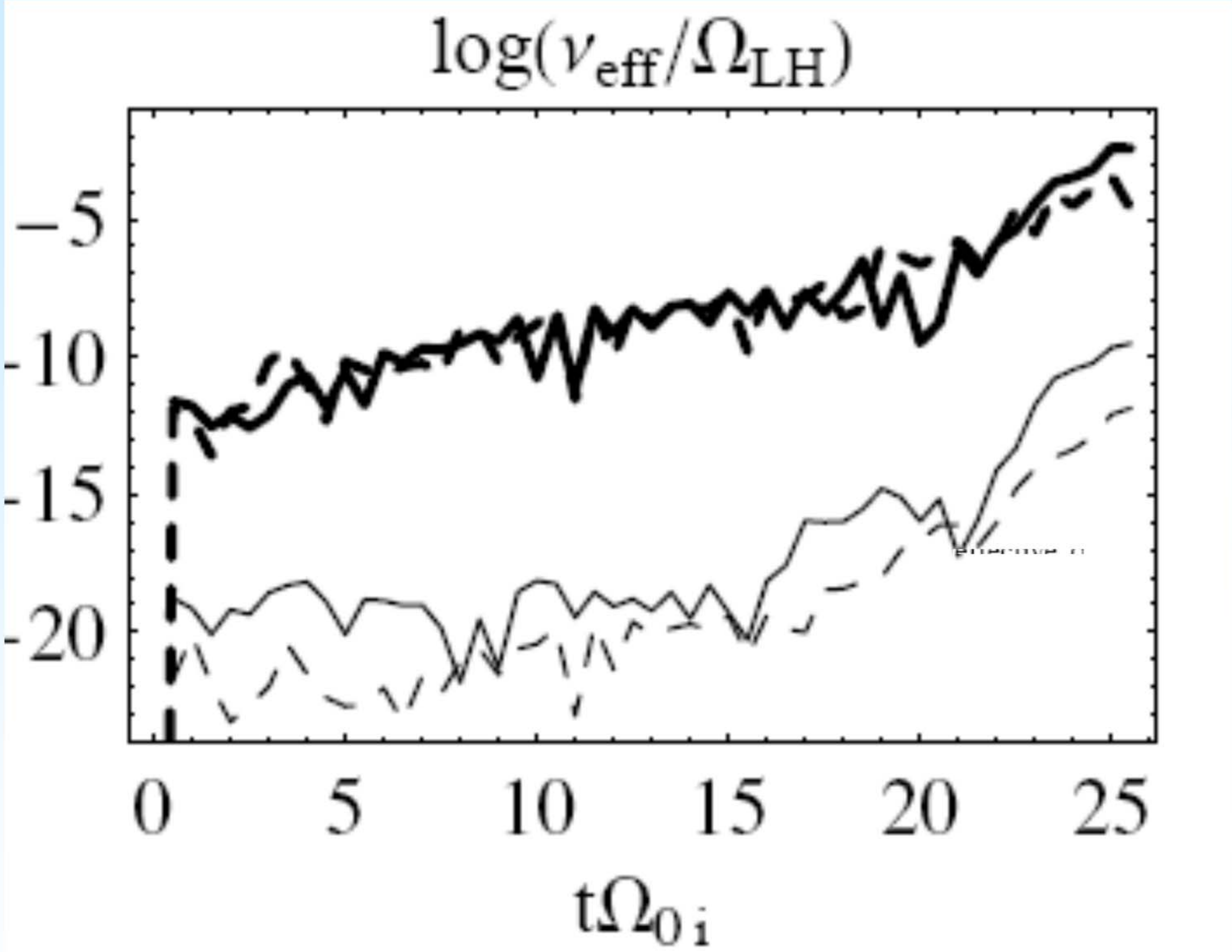

In the solar coronal plasma these rates exceed those of the 1D instability by a factor of about 6
[Silin & JB, 2007]

Effective „collision rates": Solid (electric) $\delta\rho\delta E_{\parallel}$ and dashed (magnetic fluctuations) $\delta j \times \delta B$ lines;
(Upper - thicker lines: electrons; Lower - thinner lines: ions

Summary „Anomalous resistivity“

Magnetic diffusivity expressed via an effective „collision frequency“:

$$\eta = \frac{\nu}{\ldots}$$

Neglible: binary particle collision [Spitzer 56, Härm–Braginski 63]

$$\nu_{coll} \simeq \frac{\omega_{pe}}{n\lambda_D^3}$$

There is no indication for the estimate of [Bunemann 1958] in the solar corona

$$\nu_{eff} \simeq \omega_{pe}/2\pi$$

PIC and Vlasov code simulations revealed for the solar corona: [Büchner, Kuska, Silin, Elkina, 99-08]

– 1D small beta: IA / double layers

$$\nu_c \approx \omega_{pi}/2\pi$$

– 2D higher beta – LH turbulence

$$\nu_c \sim \omega_{LH}$$

- 3D highest beta: LH/kink sausage

$$\nu_c \approx \omega_{pi}$$

But, use „anomalous resistivity“: with care!

Better would be an "SGS" description, as demonstrated for MHD turbulence models

$$\mathbf{E}_\mathrm{M} = -\beta \mathbf{J} + \gamma \mathbf{\Omega} + \alpha \mathbf{B}$$

Reynolds averaging
Mean field approximation
[e.g. Yokoi et al, 2010]

where

$$\beta = \frac{5}{7}\nu_\mathrm{K} = C_\beta \tau K,$$

$$\gamma = \frac{5}{7}\nu_\mathrm{M} = C_\gamma \tau W,$$

$$\alpha = C_\alpha \tau H,$$

with the turbulent energy

$$K (\equiv \langle \mathbf{u}'^2 + \mathbf{b}'^2 \rangle / 2)$$

the turbulent cross-helicity and

$$W (\equiv \langle \mathbf{u}' \cdot \mathbf{b}' \rangle)$$

the turbulent residual helicity

$$H (\equiv \langle -\mathbf{u}' \cdot \boldsymbol{\omega}' + \mathbf{b}' \cdot \mathbf{j}' \rangle)$$

Modified MHD equations (MFM)

$$\frac{\partial \rho}{\partial t} = -\boldsymbol{\nabla}\cdot(\rho \boldsymbol{U}) + \chi \nabla^2 \rho$$

$$\frac{\partial \rho \boldsymbol{U}}{\partial t} = -\nabla \cdot \left[\rho \boldsymbol{U} \otimes \boldsymbol{U} + \frac{1}{2}(p + B^2)\boldsymbol{I} - \boldsymbol{B} \otimes \boldsymbol{B}\right] + \chi \nabla^2 (\rho \boldsymbol{U})$$

$$\frac{\partial \boldsymbol{B}}{\partial t} = \nabla \times (\boldsymbol{U} \times \boldsymbol{B}) - (\nabla(\eta + \beta)) \times \boldsymbol{J} + (\eta + \beta)\nabla^2 \boldsymbol{B} + \nabla \times (\gamma \sqrt{\rho}\Omega)$$

$$\frac{\partial h}{\partial t} = -\nabla \cdot (h\boldsymbol{U}) + \frac{\gamma - 1}{\gamma h^{\gamma - 1}}(\eta \boldsymbol{J}^2 - \frac{\rho K}{\tau_t}) + \chi \nabla^2 h$$

$$\frac{\partial K}{\partial t} = -\boldsymbol{U} \cdot \nabla K + C_\beta \tau_t K \frac{\boldsymbol{J}^2}{\rho} - C_\gamma \tau_t W \frac{\boldsymbol{\Omega} \cdot \boldsymbol{J}}{\sqrt{\rho}} + \frac{\boldsymbol{B}}{\rho} \cdot \nabla W - \frac{K}{\tau_t}$$

$$\frac{\partial W}{\partial t} = -\boldsymbol{U} \cdot \nabla W + C_\beta \tau_t K \frac{\boldsymbol{\Omega} \cdot \boldsymbol{J}}{\sqrt{\rho}} - C_\gamma \tau_t W \boldsymbol{\Omega}^2 + \frac{\boldsymbol{B}}{\sqrt{\rho}} \cdot \nabla K - C_W \frac{W}{\tau_t}$$

(… according to a mean field turbulence model, e.g. of Yoshikava and Yokoi)

MHD turbulence reveals fast reconnection

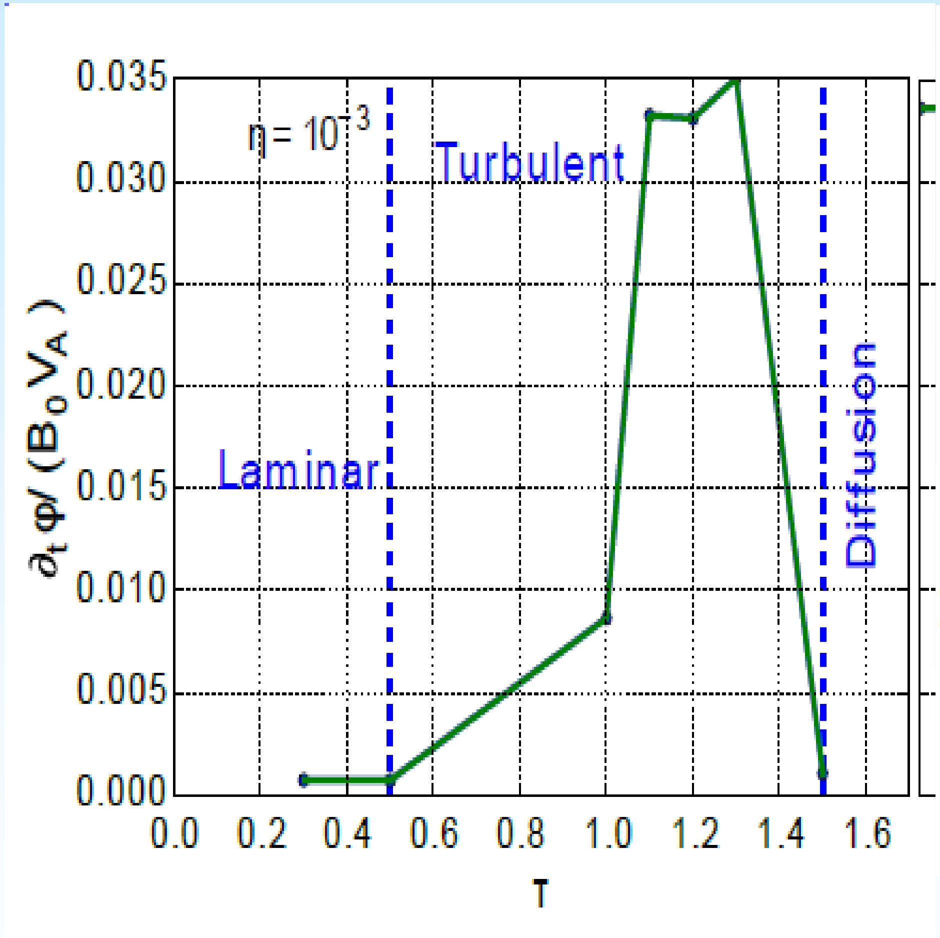

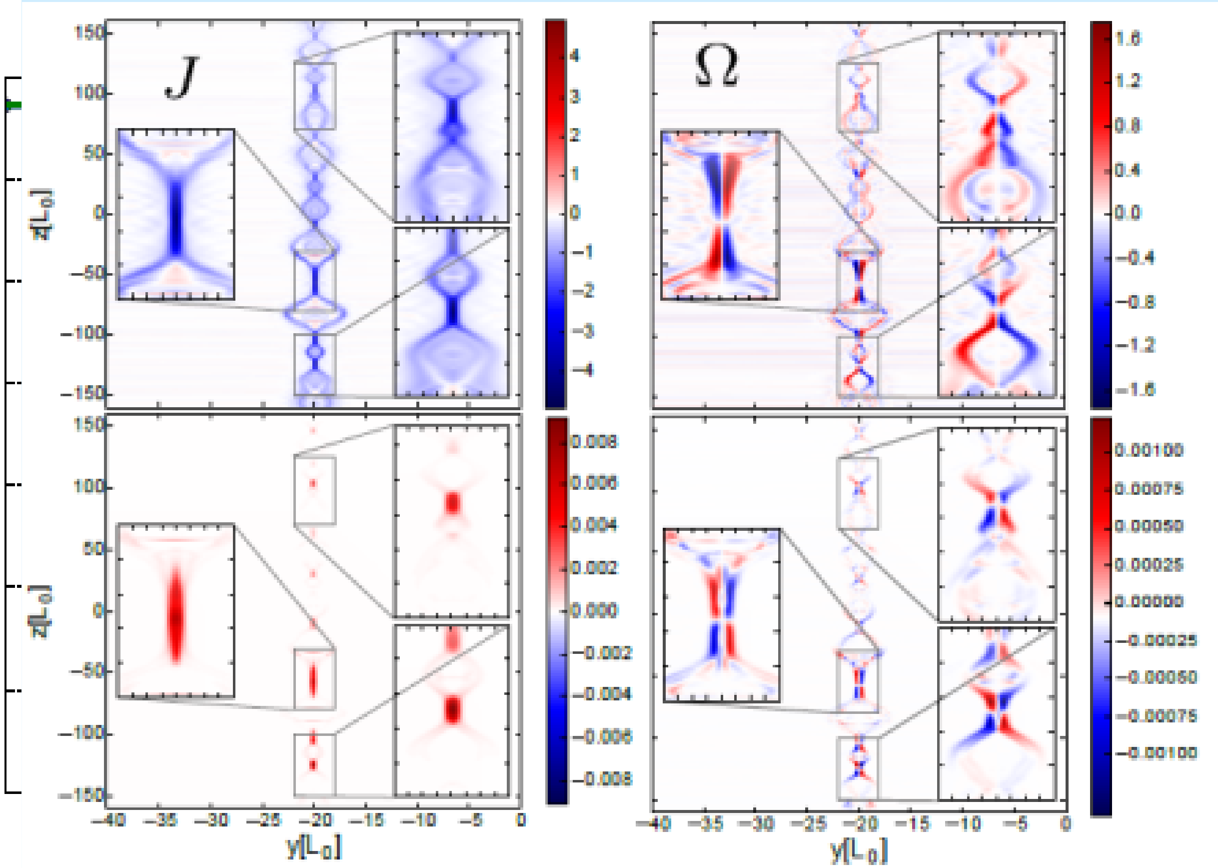

[from Widmer, JB, Yokoi, Hoshino 2016]

But: No model for kinetic scale „SGS“ turbulence, yet!

Summary

Dissipation (as needed for non-ideal coronal instabilities - eruptions) can be provided by collisioness plasma mechanisms. However, their description via anomalous resistivity is of limited use.

Way out: mean field turbulence models. They already reproduce high reconnection rates for MHD.

But no good model for kinetic turbulence, yet.

Contents

- Coronal plasmas & fields
- Eruptions & reconnection
- Turbulence and dissipation
- Electron acceleration

X-ray flare ribbon observations

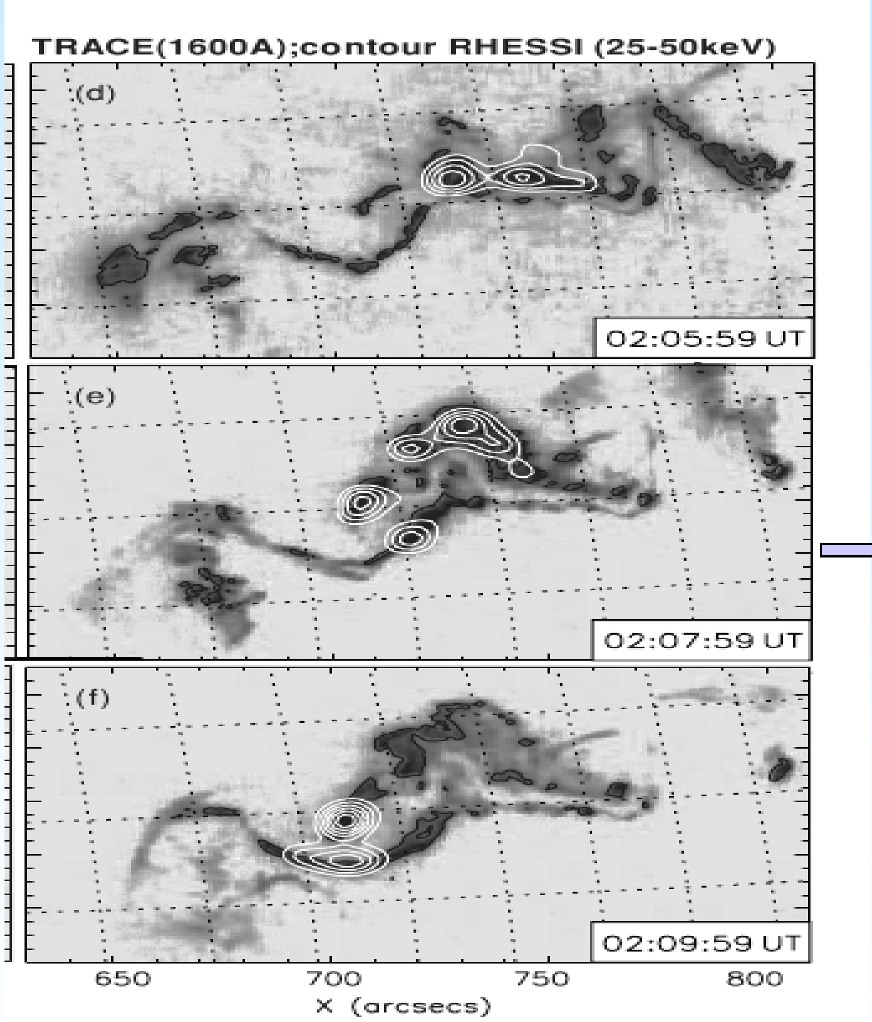

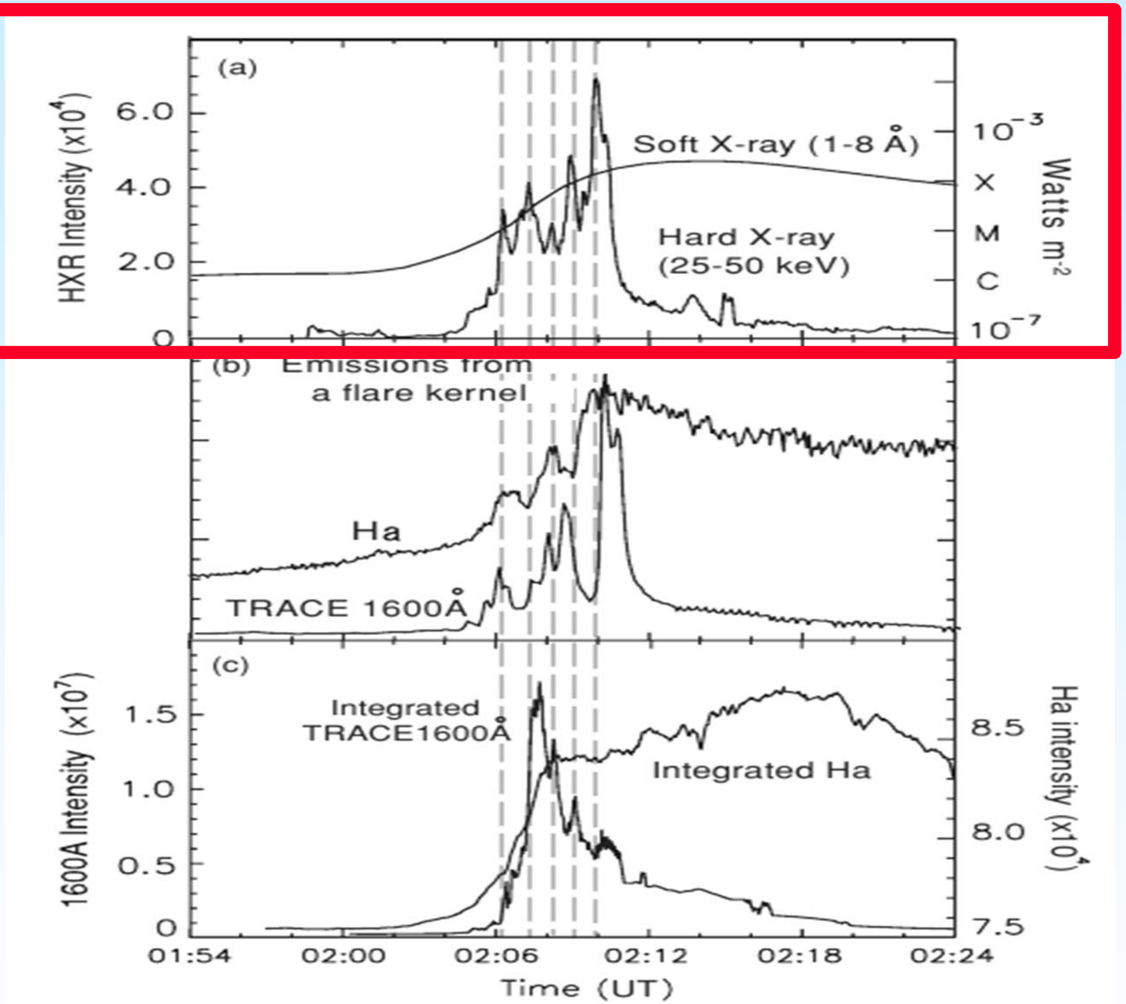

TRACE and RHESSI-observations of flare-ribbons of X-rays due to energetic electron precipitation [Nishizuka et al., 2009, 2014]

Radio observations of Flares

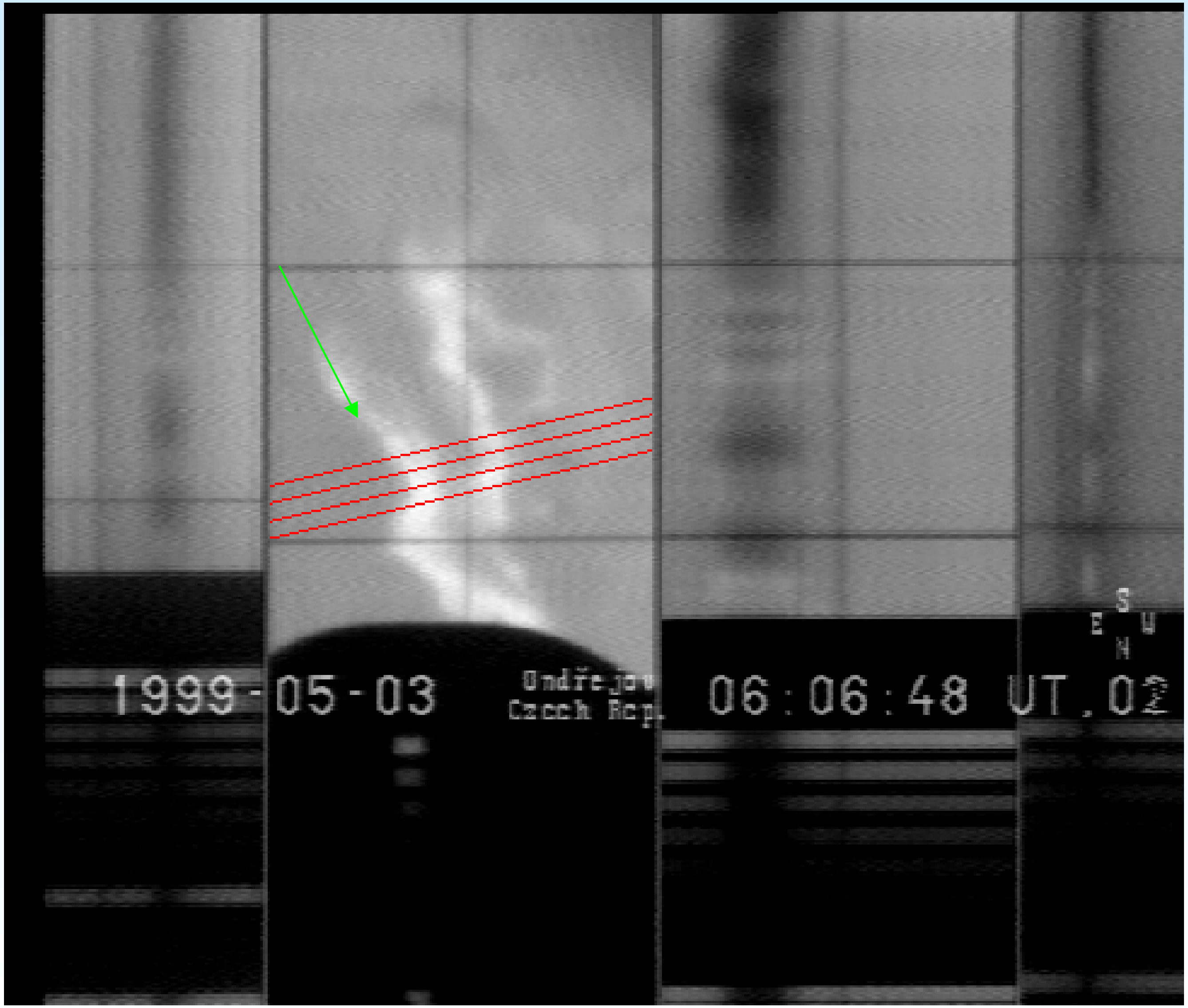

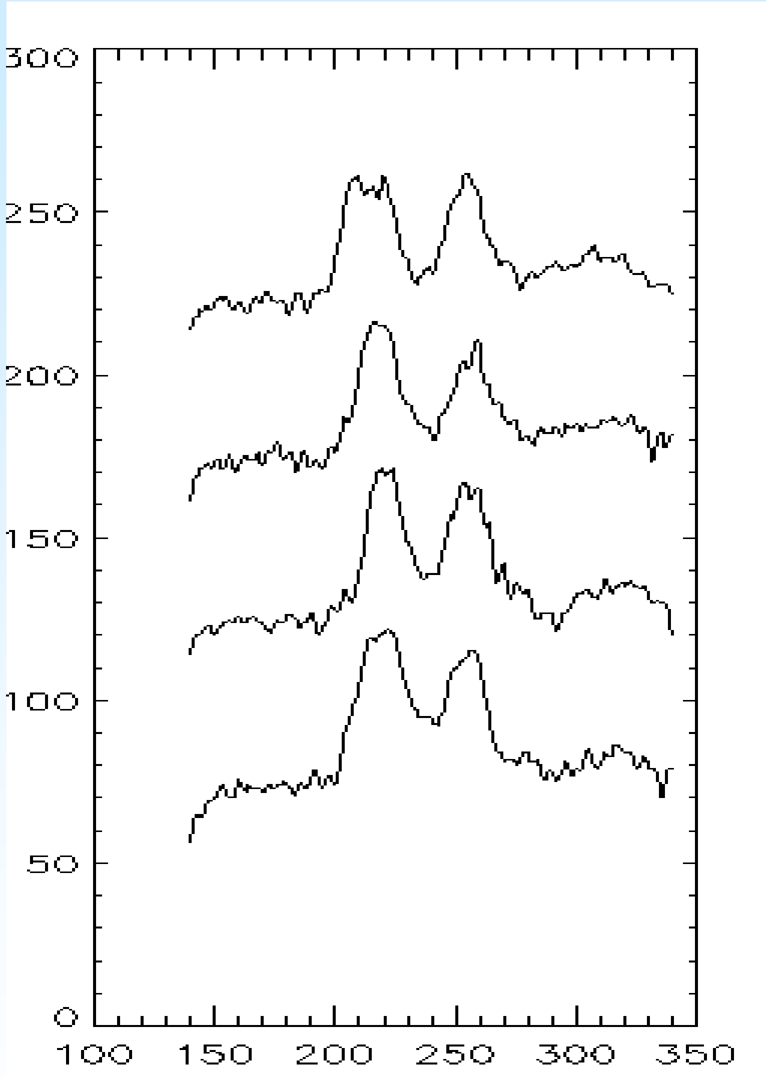

Moving flare-ribbons structures – solar radio observations by the Ondrejov Radio Spectrograph [Kotrč et al. 2009, 2015]

Conditions for reconnection in the corona

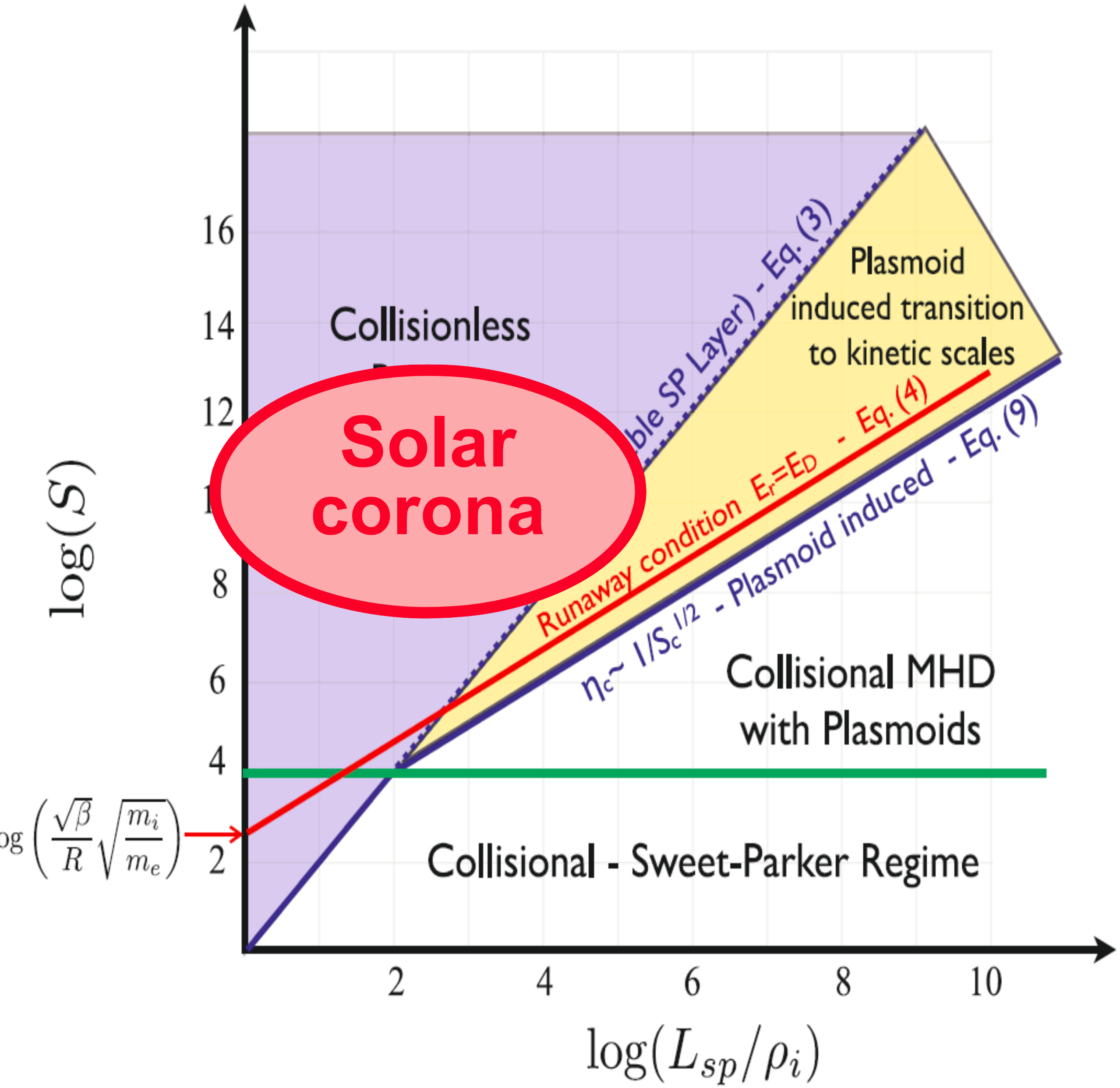

Lsp is the system size,

RHOi the ion Larmor radius,

S the Lundquist number

$$S \equiv \frac{\mu_0 L_{CS} V_A}{\eta}$$

(Obtained for a H+-plasma

$$\beta = 0.2$$

)

[Ji, Daughton, Roytershteyn, Space Sci. Rev., 2012]

-> Collisionless, kinetic reconnection

Cascading reconnection -> plasmoid rec.

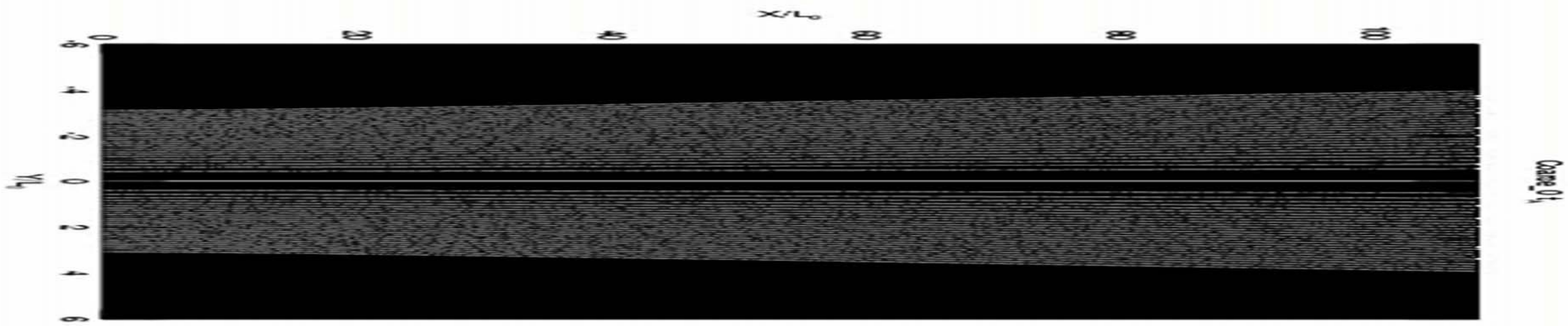

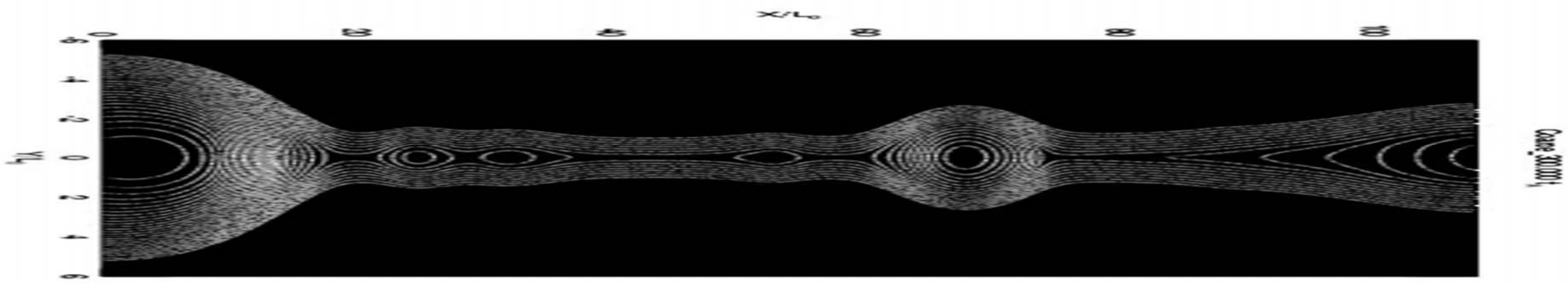

Upper movie: Evolution over 500 t_A of the CME-trailing current sheet: plasmoid instability

Lower movie: higher resolved current sheets (300 to 400 t_A),

[Barta, JB, Karlicky, 2011]

Cascading reconnection->plasmoids

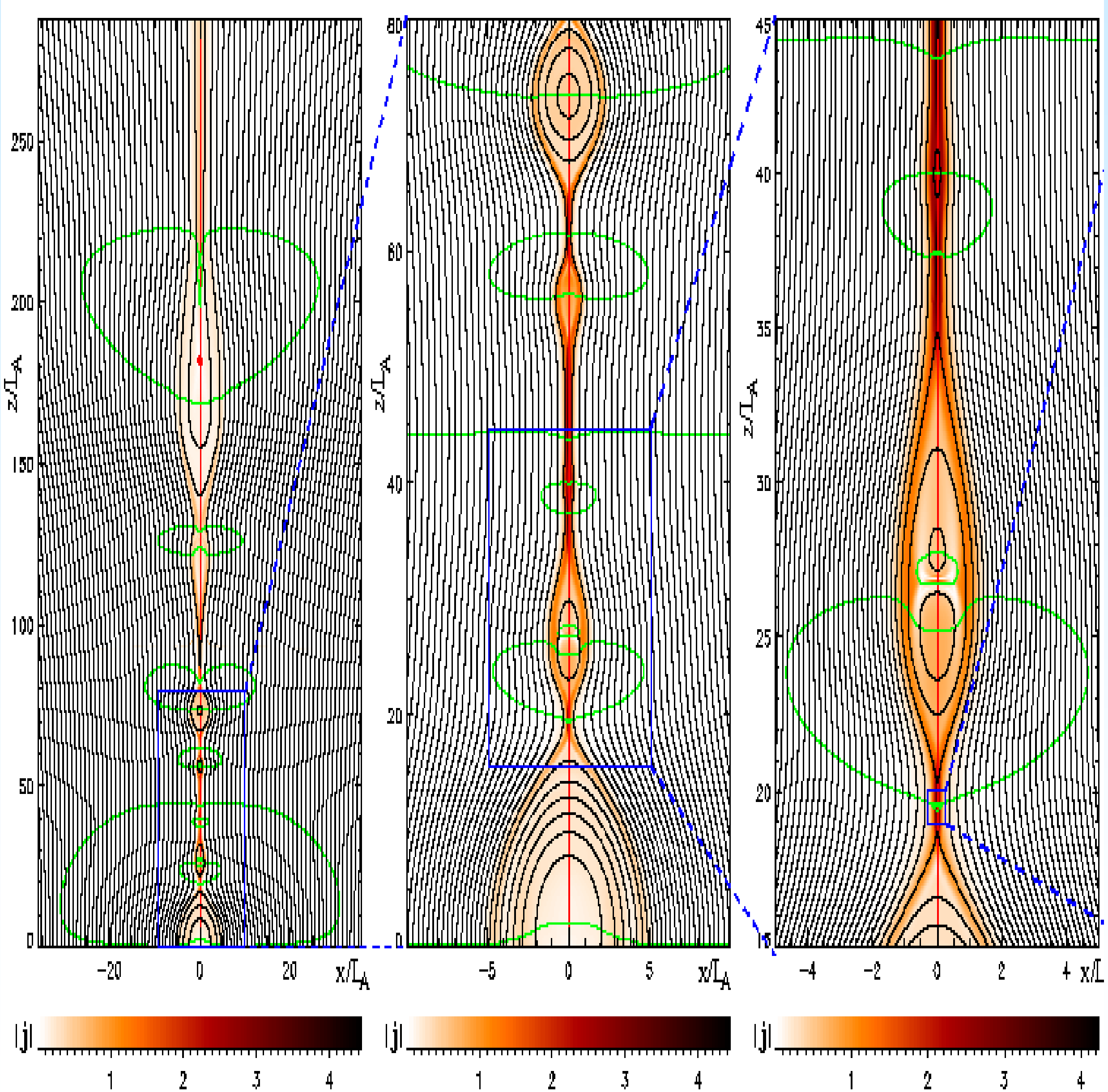

Current sheet breakup into plasmoids by cascading reconnection: adaptive mesh MHD simulation by [Bárta, JB, Karlicky, Skala, 2011] -> high reconnection rates with transitions to turbulent reconnection

-> possible in (observed) wide trailing current sheets

-> corresponds well to radio burst fine structures [Nishizuka et al., 2012]

Plasmoid rec. -> electron acceleration

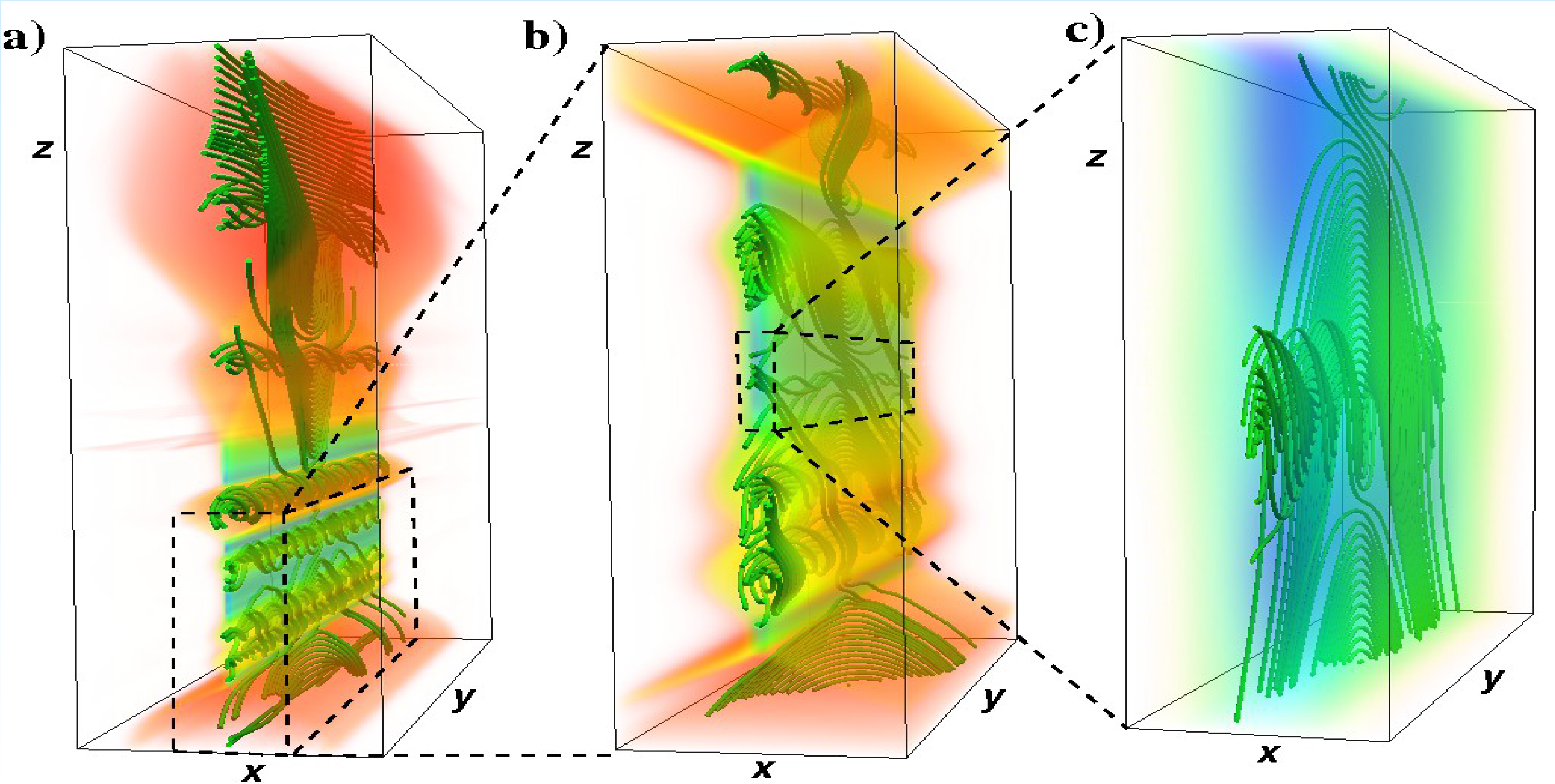

Electrons are accelerated in the plasmoids, ejected out of the islands parallel to B, precipitate down to the chromosphere.

e^- spectrum at reconnection site

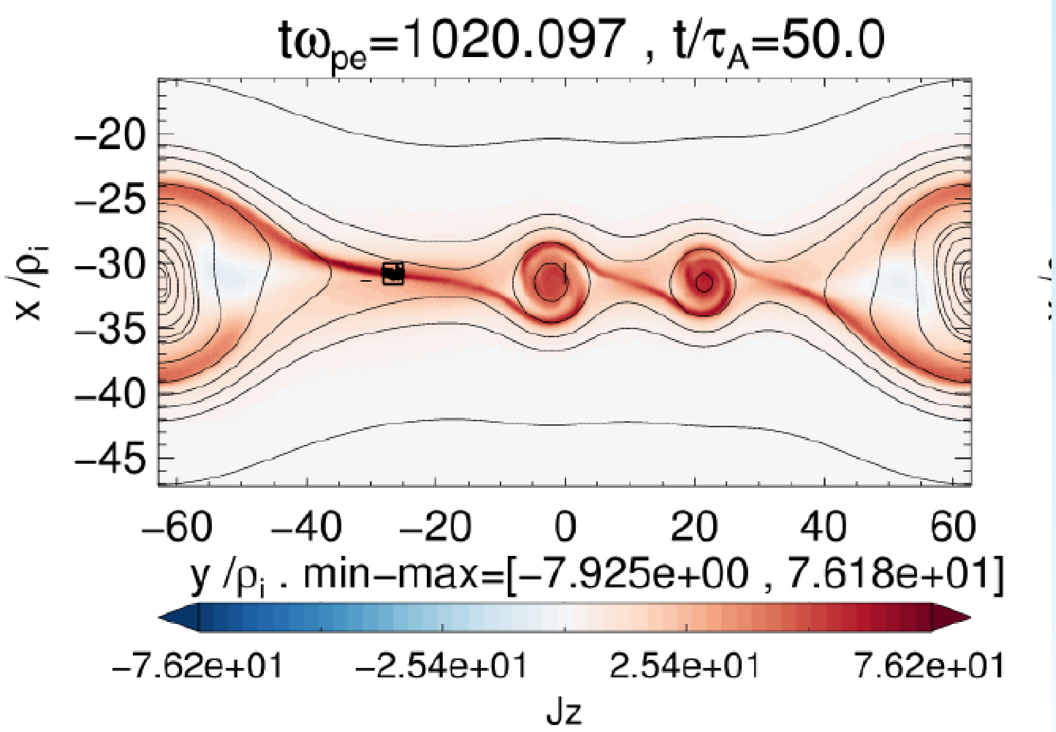

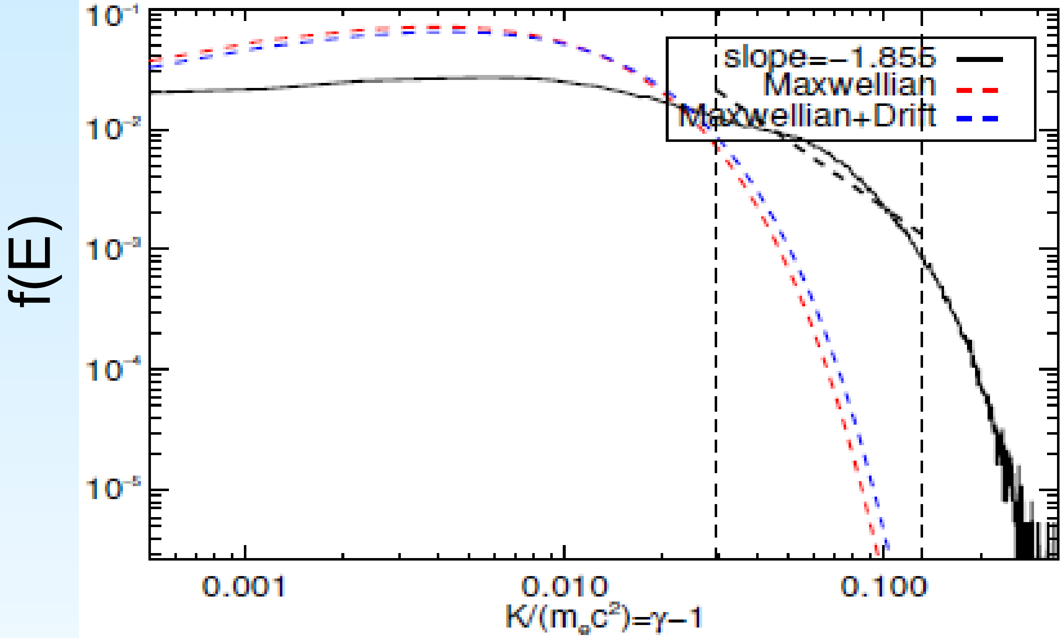

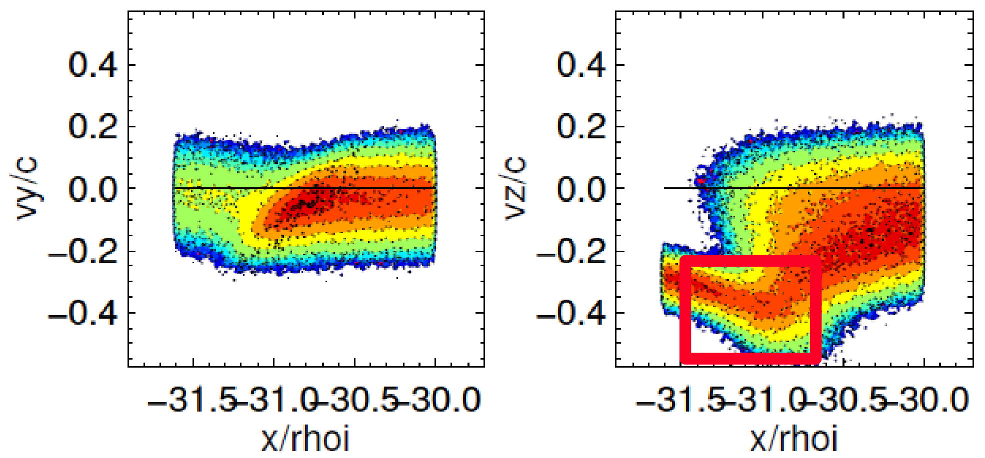

Plasmoid reconnection accelerates electrons up to almost 1 MeV electrons flat power law. Index: - 1.86

Self-consistent (PIC-code) simulations of finite Bg reconnection needed

Harris current sheets (CSs)

$$\vec{B}(x) = B_{\infty y}\left[\tanh\left(\frac{x - L_x/4}{L}\right) - \tanh\left(\frac{x - 3L_x/4}{L}\right) - 1\right]\hat{y} + B_z\hat{z}$$

Physical parameters

$b_g = B_z/B_{\infty y} = 0 \ldots 8$ … 50

$L/d_i = 0.5, M_i/m_e = 100$

$\omega_{pe}/\Omega_{ce} = 4.16, T_i/T_e = 1.0$

$n_b/n_0 = 0.2, d_{i/e} = c/\omega_{pi/pe}$

$v_{th,e}/c = 0.12$

Initial perturbation:

$$\delta A_z = \delta P B_{\infty y}\frac{L_y}{2\pi}\sin\left(\frac{2\pi\,(y + L_y/4)}{L_y}\right)\sin^2\left(\frac{2\pi x}{L_x}\right)$$

3D – force free CSs

200 ppc (e+i) everywhere

$L_x \times L_y \times L_z = (4 \times 8 \times 16) d_i^3$

512x512x1024 grid points

2 x 10^10 particles

2D-Harris CS for comparison

$L_x \times L_y = (20.9 \times 12.6) d_i^2$

2500×1500 grid points

$\Delta x = 0.7\lambda_{De}$

$\rho_{e,bg} = v_{th,e}/(b_g\Omega_{ce})$

$\Delta x/\rho_{e,bg} = 0.166 b_g$

$\Delta t = (1/23.9)\omega_{pe}^{-1}$

$CFL : c\Delta t/\Delta x = 0.5.$

Resulting turbulence (Bg=3)

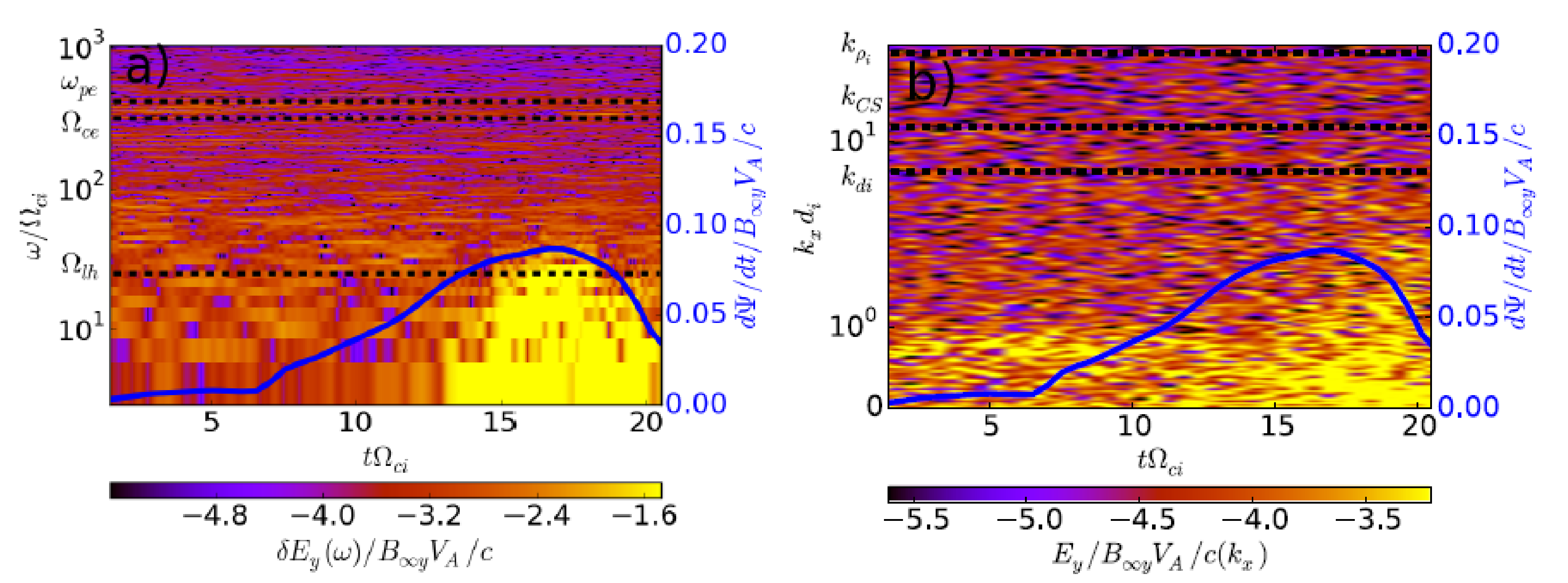

Ey: frequency spectrum: obliquely propagating, broadband, up to the lower hybrid frequency. Reason: countersteaming electron beams

Ey: kx-wave-number spectrum: broadband in 0.3< k di < 4; kx ~ kpar-> U ~ 6-81 Vthi -> resonance with electron beams

Solid line: evolution of the reconnection rate [Munoz&JB, 2018b]

Nonlinear stage of reconnection

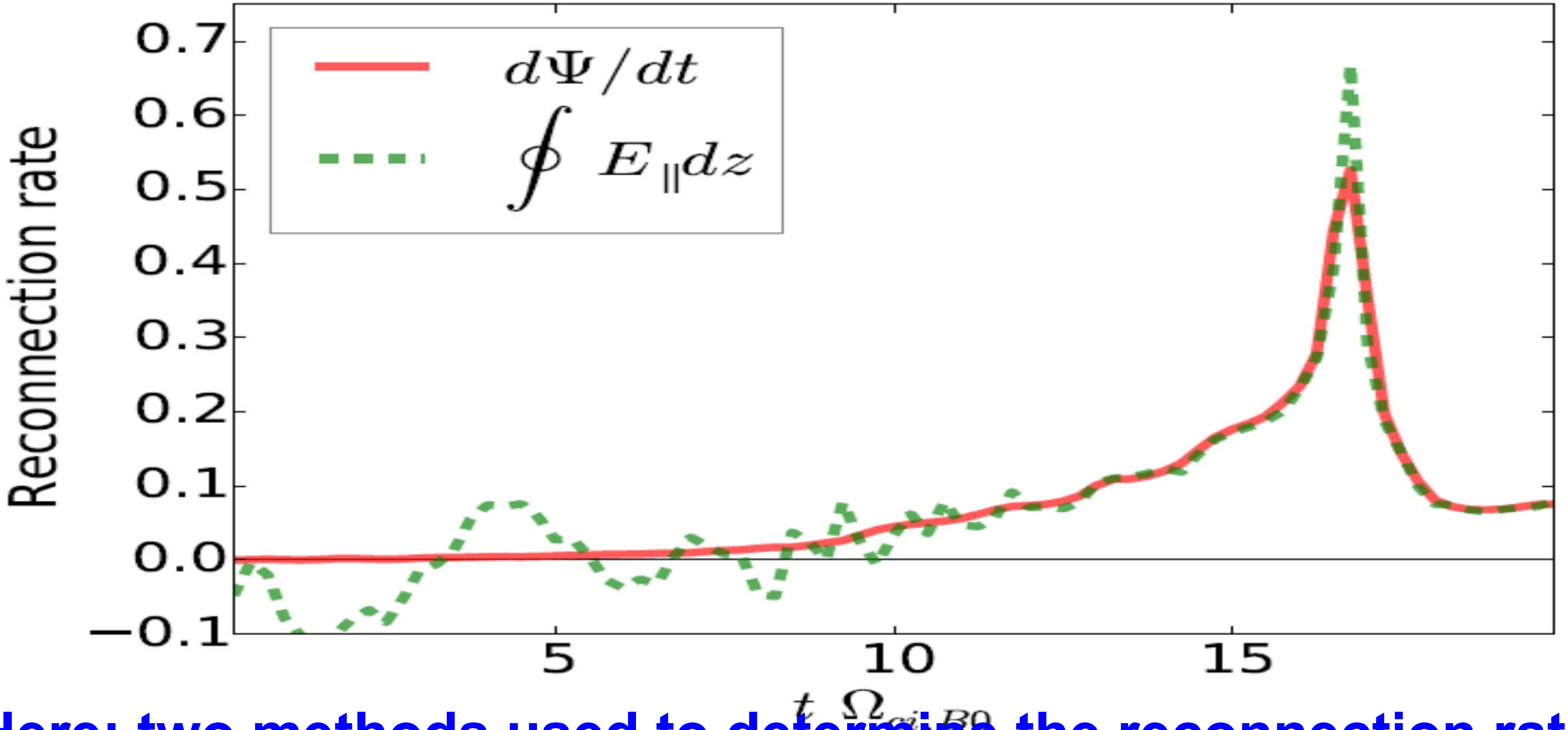

Here: two methods used to determine the reconnection rate.

Result: the reconnection rate is strongly enhanced during the non-linear evolution of reconnection – permitted by self-generated turbulence ! [from Munoz& JB, 2018a]

Free energy that causes the turbulence

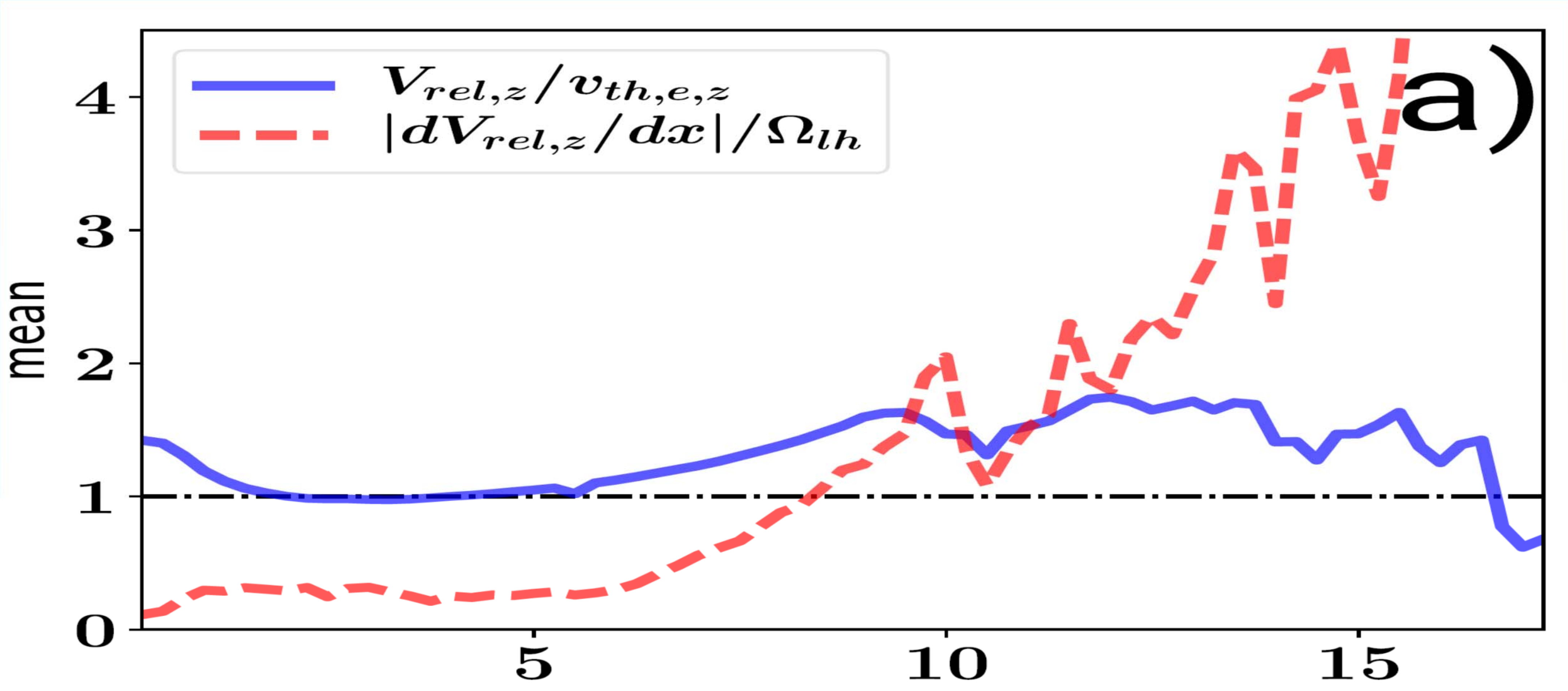

Mean values along the X-line of reconnection, averaged along z-direction of streaming Vrel,z (solid line) & shear flow |dVrel,z/dx| (red dashed line) - Horizontal dash-dotted line: threshold of the Buneman instability [from Munoz& JB, 2018a].

3D evolution (case Bg=3)

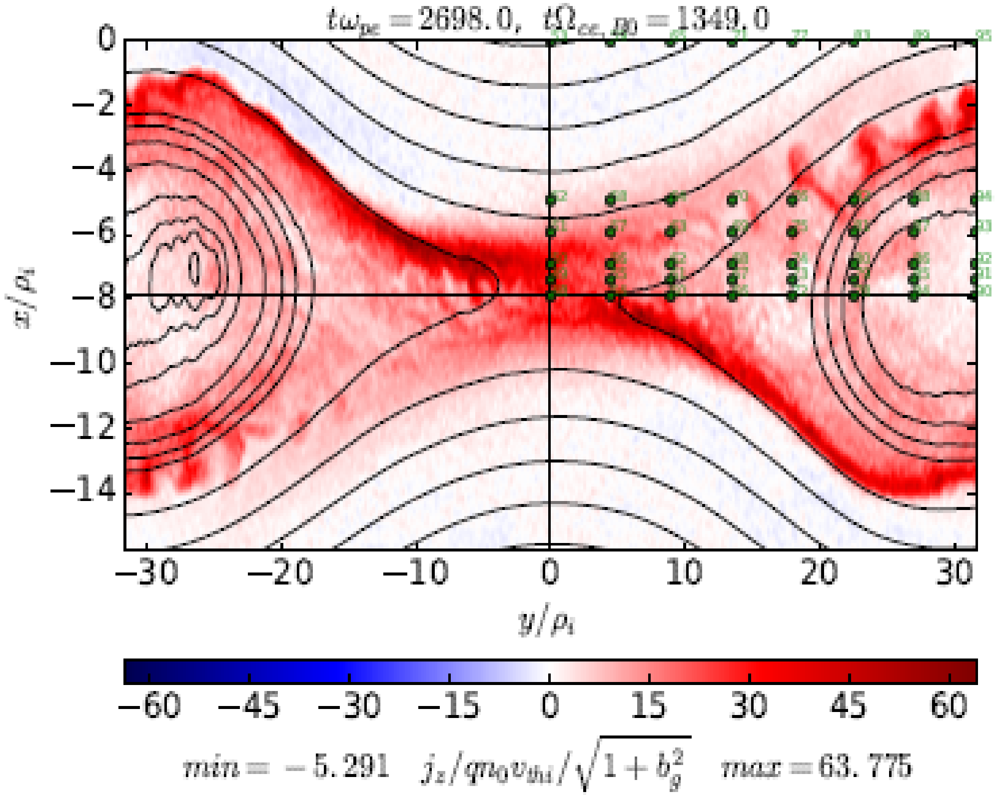

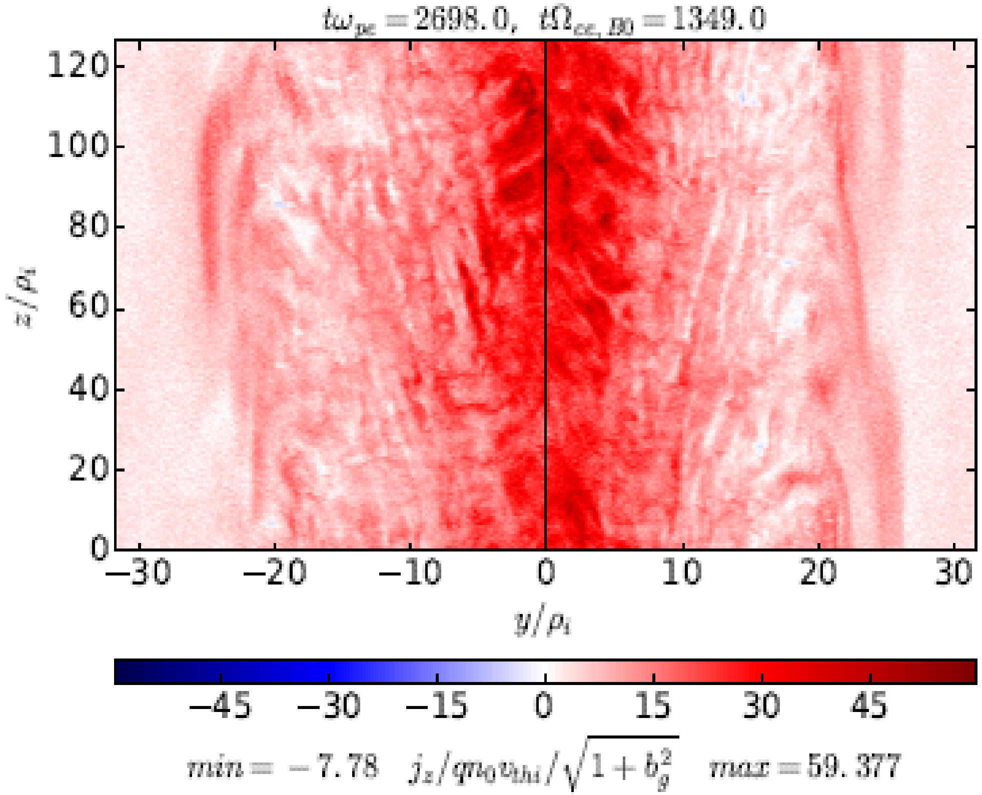

Reconnection plane (perp)　　**Central plane (par)**

(red structures: current density) : filamentation, formation of structures propagating in the direction perpendicular to the reconnection-plane: reconnection wave

Epar at the nonlinear stage: structure formation out of the turbulence!

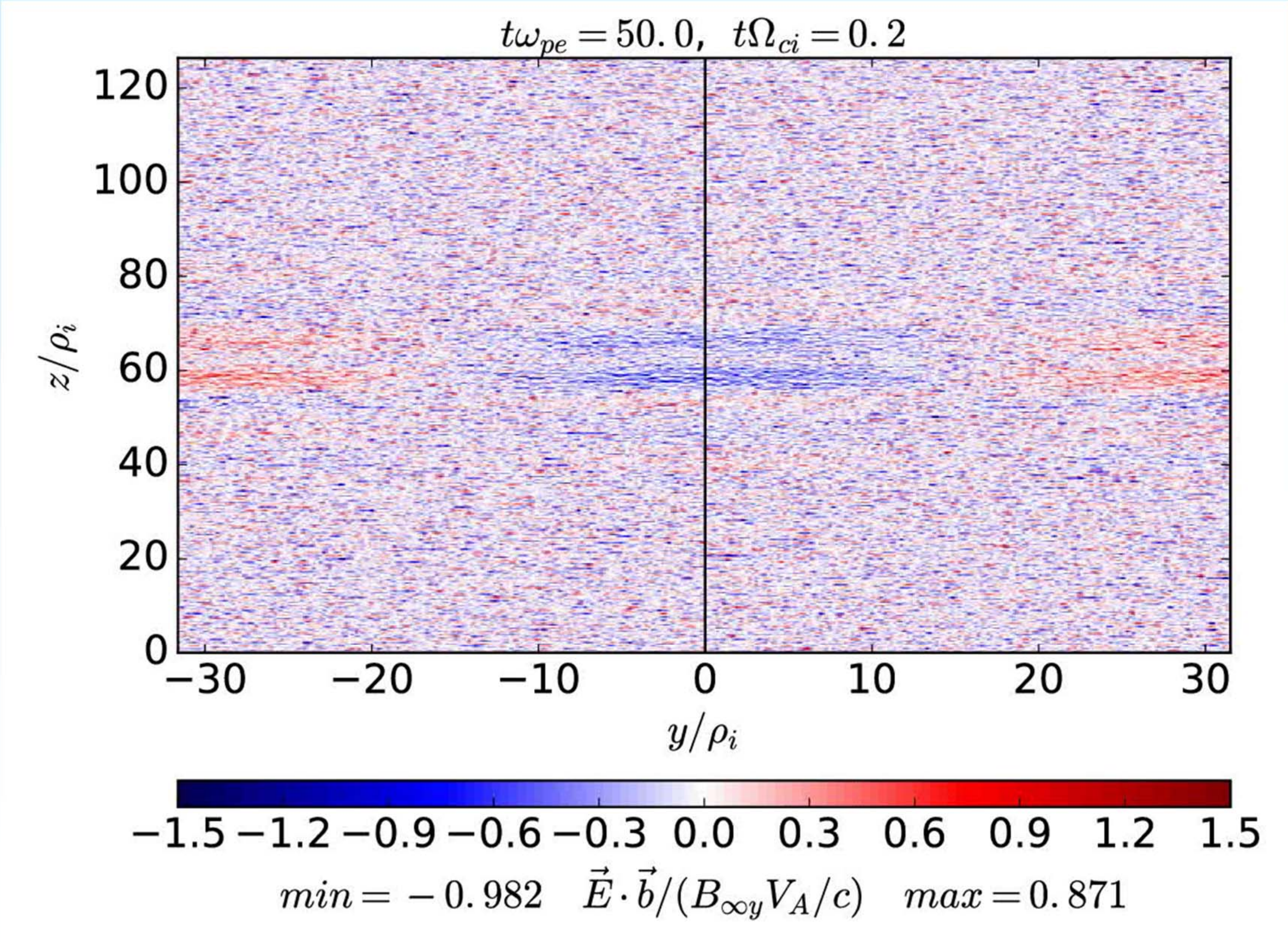

Hence: Epar gets filamented & travels

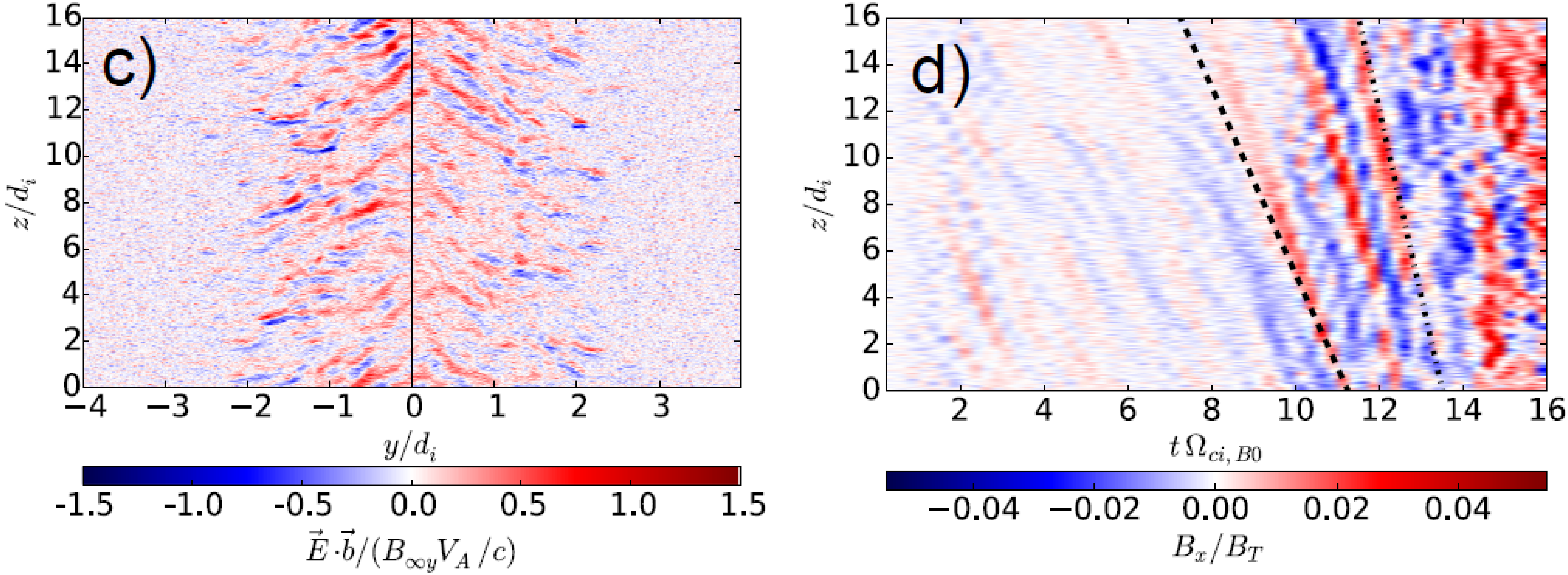

C) Spatial distribution of Epar(x,z) in the central plane at the nonlinear stage D) temporal evolution of the perpendicular (Bx) fluctuations. Black lines: initial electron drift speed Vte (dashed line) enhanced to 2 Vte, valid at later times (dotted)

Electron energization

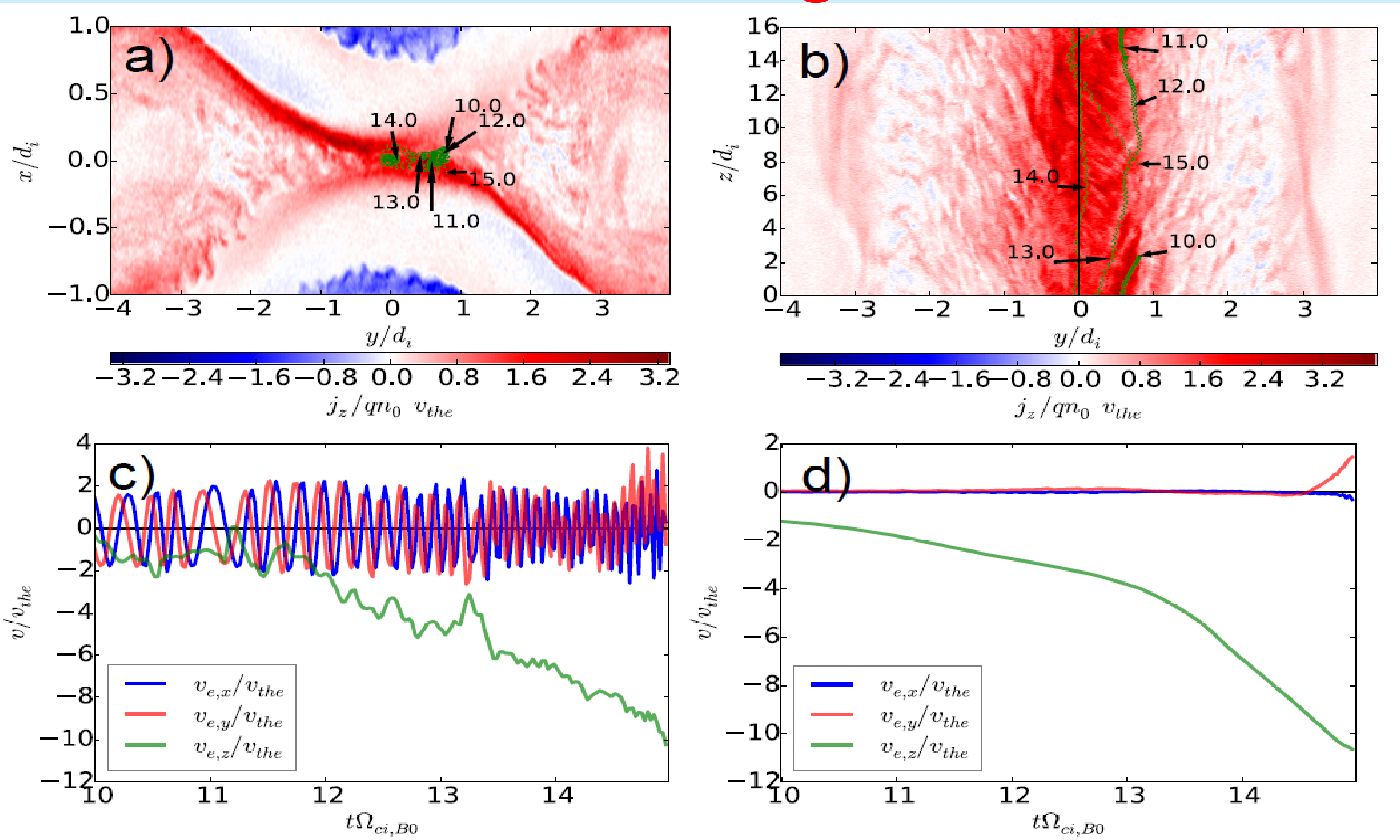

a) and b): trajectory of a strongly accelerated electron (green); red/blue: jz in the two planes at times of the nonlinear stage c) Velocity components of a typical strongly accelerated electron d) Temporary evolution of the average (four-) velocity components of the 10^4 most energized electrons [from Munoz& JB, 2018b]

Epar = Erec: traveling filaments

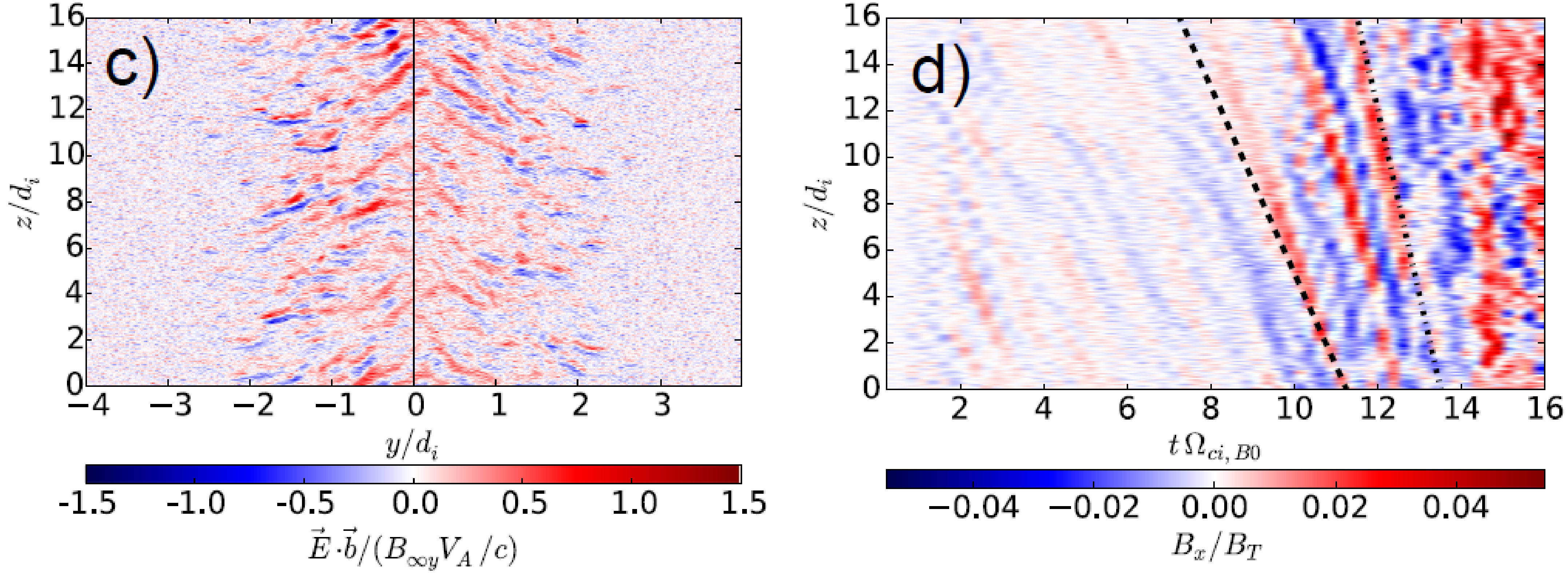

C) Spatial distribution of Epar(x,z) in the central plane at the nonlinear stage D) temporal evolution of the perpendicular (Bx) fluctuations. Black lines: initial electron drift speed Vte (dashed line) enhanced to 2 Vte, valid at later times (dotted)

Magnitized electron acceleration by 3D nonlinear guide field reconnection

$$\frac{dU}{dt} = E_{\parallel} J_{\parallel} + \left(p_{e,\parallel} + m_e n_e u_{e,\parallel}^2\right) \vec{u}_{\vec{E}} \cdot \vec{\kappa} \quad + \frac{p_{e,\perp}}{B} \left(\frac{\partial B}{\partial t} + \vec{u}_{\vec{E}} \cdot \vec{\nabla} B \right)$$

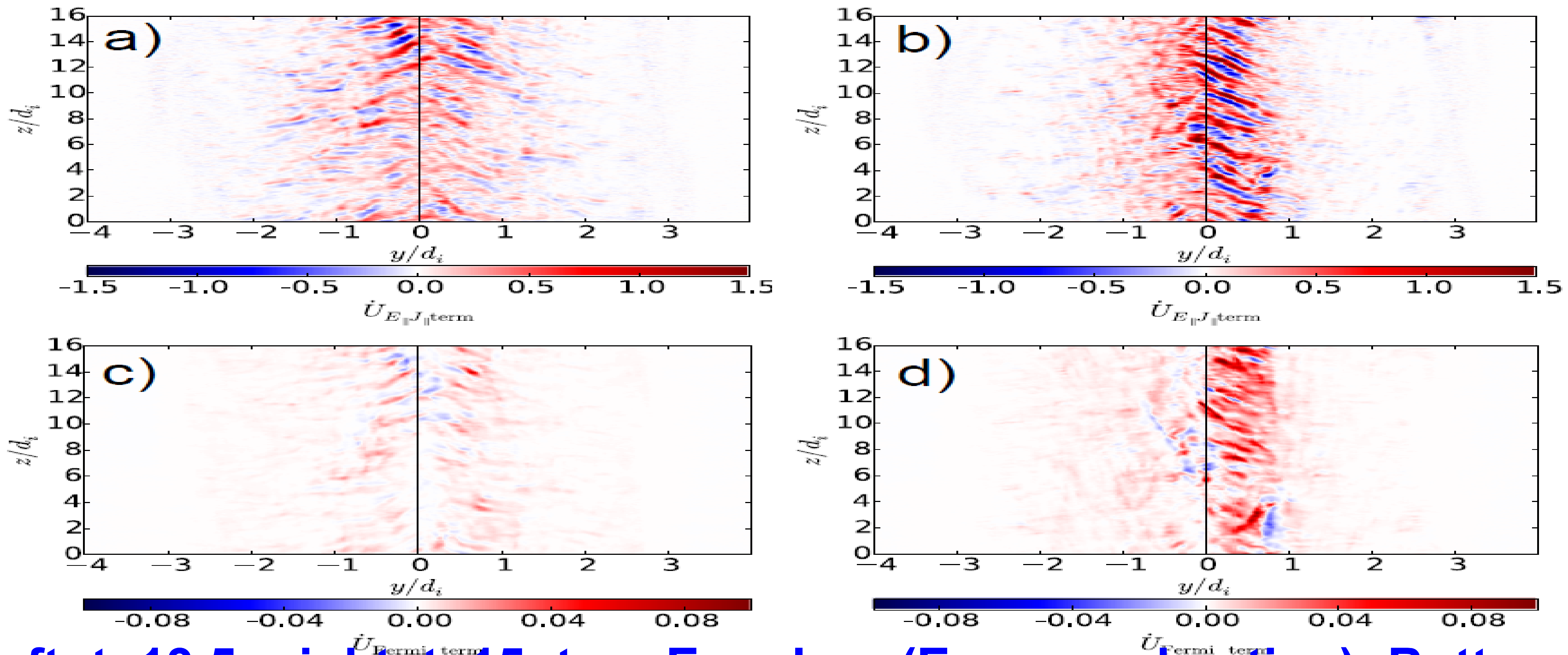

left: t=13,5 , right: t=15; top: EparJpar (Epar acceleration); Bottom: Fermi-type acceleration due to bouncing at curved magnetic fields

Curvature–induced acceleration

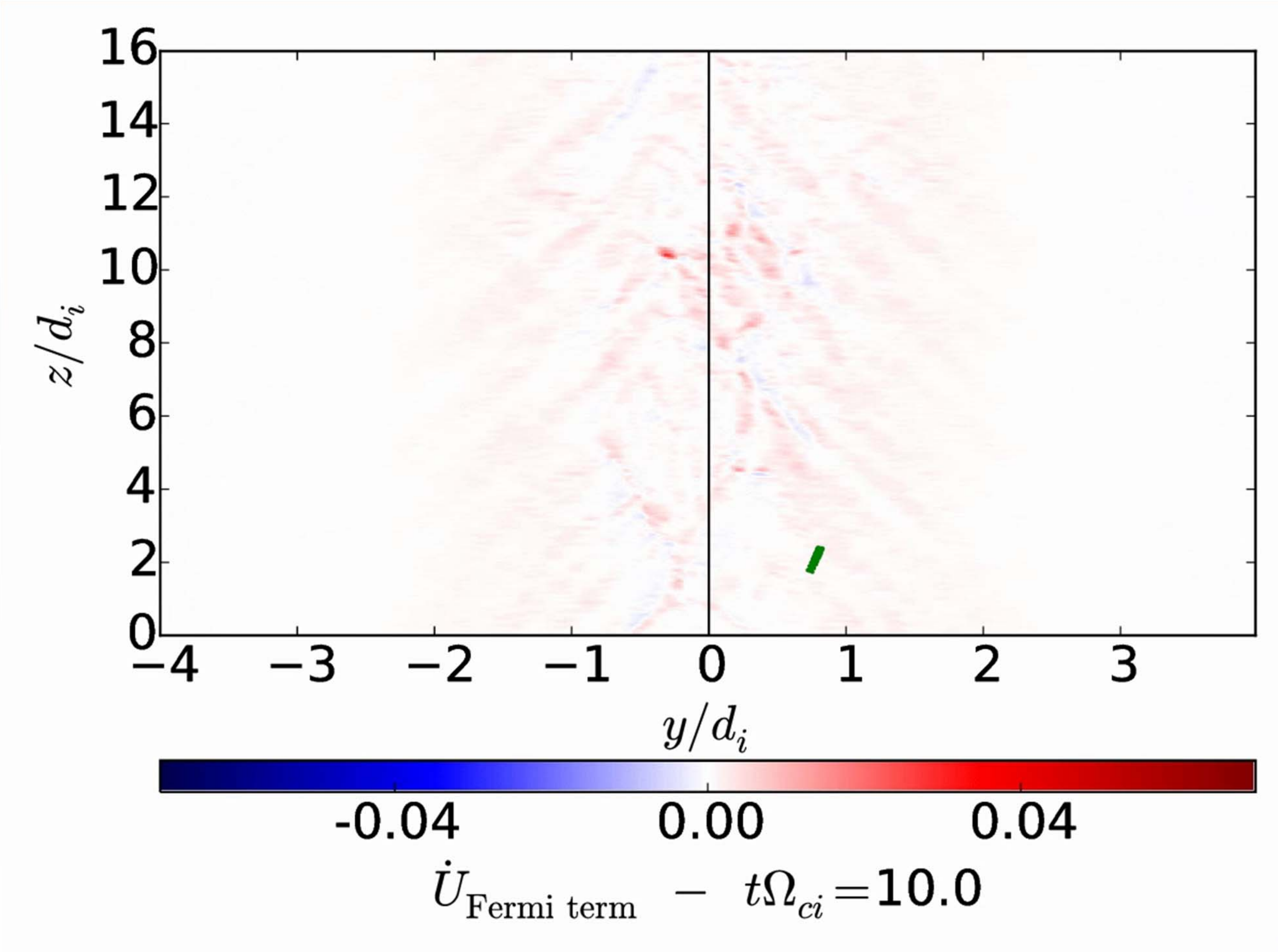

Green dots: Projection of a typical strongly energized electron trajectory in the Y-Z-plane

Red-blue: Fermi acceleration term at the electron location

Heating & energetic electrons' power law

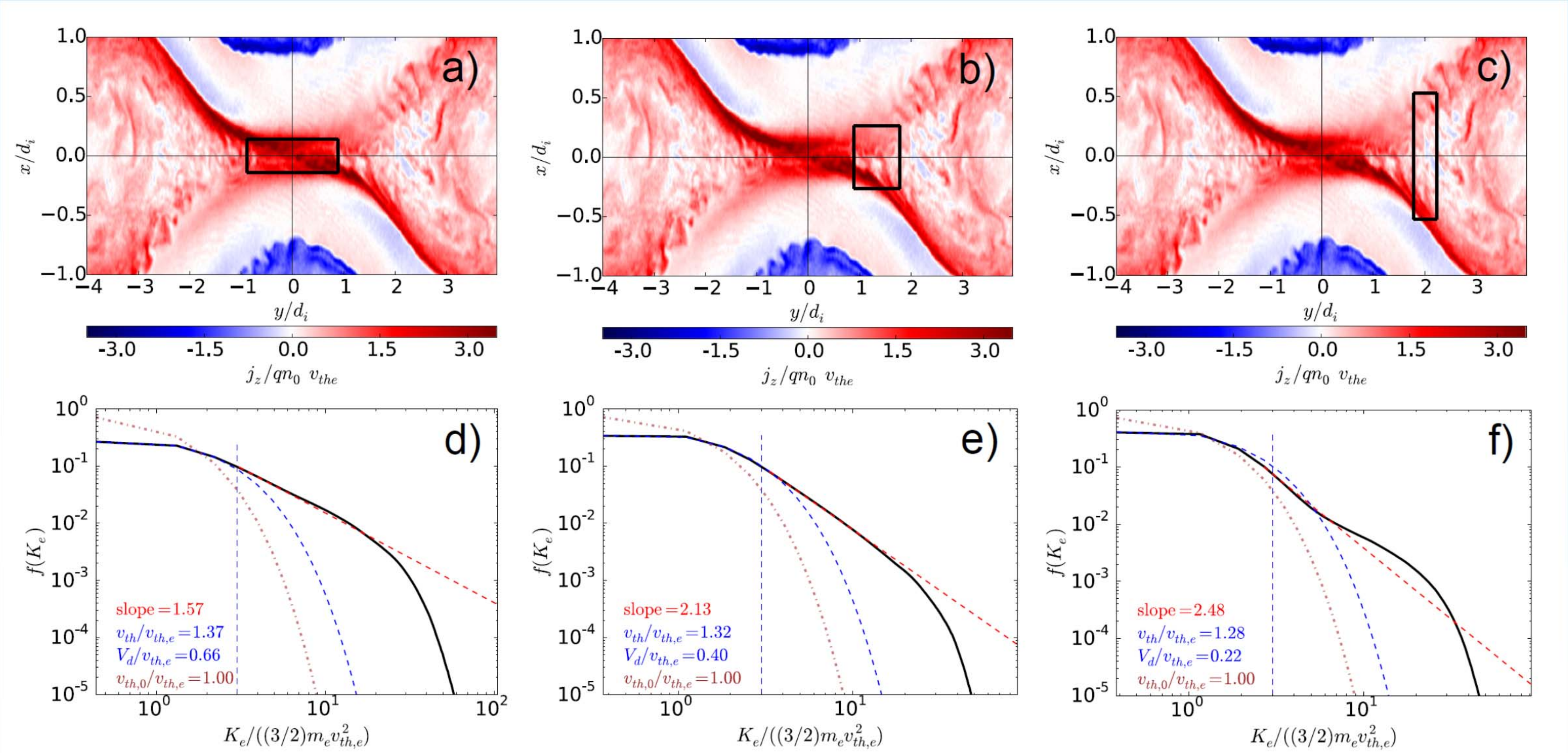

t=t_f = 15.1 Omega_ci (bottom row) for the black boxes in the top rows. (a)-(c) show the current density Jz in the plane x - y at z = center. Dashed-dotted line: initial thermal distribution, blue dashed line: Maxwellian fit to the distribution, red dashed lines: power law fit [from Munoz& JB, 2018b]

Summary 1: Parker Solar Probe (NASA)

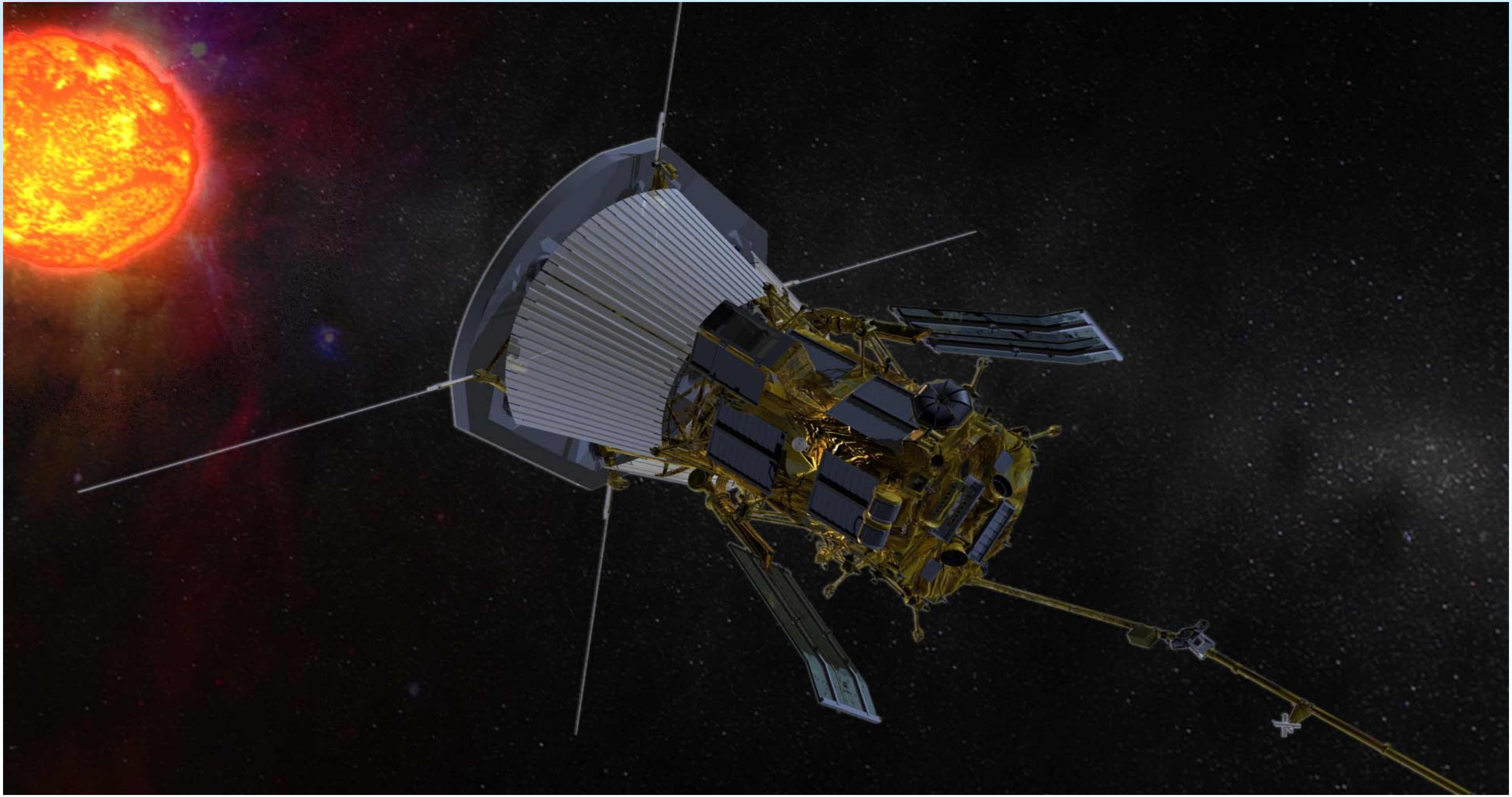

To be launched during the next few days ….

Summary 2: Solar Orbiter

To be launched in 2020, as the first ESA M-class mission (M1)